Electronic Supplementary Information

Solid-State Temperature-Dependent Luminescence of *C*,*C*′-Diaryl-*o*-Carboranes Based on Restriction of Excited-State Structural Relaxation

Kazuhiro Yuhara[a], Kazuo Tanaka*[a,b]

[a] Department of Polymer Chemistry, Graduate School of Engineering, Kyoto University, Katsura, Nishikyo-ku, Kyoto 615–8510, Japan

[b] Department of Technology and Ecology, Graduate School of Global Environmental Studies, Kyoto University, Katsura, Nishikyo-ku, Kyoto 615–8510, Japan

E-mail: tanaka@poly.synchem.kyoto-u.ac.jp

Index

Materials

Commercially available reagents used without purification

Decaborane ($B_{10}H_{14}$) (Toronto Research Chemicals)

$AgNO_3$ (Fujifilm Wako Pure Chemical Corporation)

2-Thiopheneboronic acid (Tokyo Chemical Industry Co., Ltd.)

Tetrakis(triphenylphosphine)palladium ($Pd(PPh_3)_4$) (Tokyo Chemical Industry Co., Ltd.)

CuI (Fujifilm Wako Pure Chemical Corporation)

Celite® (No. 535, Fujifilm Wako Pure Chemical Corporation)

9-Bromoanthracene (Fujifilm Wako Pure Chemical Corporation)

9-Anthracenecarbaldehyde (Tokyo Chemical Industry Co., Ltd.)

2,7-Dibromo-9,9-didodecyl-9*H*-fluorene (BLDpharm)

2-Bromo-3-dodecylthiophene (Tokyo Chemical Industry Co., Ltd.)

Bromine (Br_2) (Fujifilm Wako Pure Chemical Corporation)

Na_2CO_3 (Fujifilm Wako Pure Chemical Corporation)

$NaHSO_3$ (Fujifilm Wako Pure Chemical Corporation)

$MgSO_3$ (Fujifilm Wako Pure Chemical Corporation)

Commercially available solvents used after purification

Tetrahydrofuran (THF) (Super deoxidized, stabilizer free, Fujifilm Wako Pure Chemical Corporation) and triethylamine (Et_3N) (Guaranteed reagent, KANTO CHEMICAL CO., INC.) were purified using a two-column solid-state purification system (Glasscontour System, Joerg Meyer, Irvine, CA).

Commercially available solvents used without purification

Toluene (Deoxidized, Fujifilm Wako Pure Chemical Corporation)

Acetonitrile (MeCN) (Deoxidized, Fujifilm Wako Pure Chemical Corporation)

Dichloromethane (CH_2Cl_2) (Deoxidized, Fujifilm Wako Pure Chemical Corporation)

Ethyl acetate (EtOAc) (Fujifilm Wako Pure Chemical Corporation)

n-hexane (Fujifilm Wako Pure Chemical Corporation)

$CHCl_3$ (Fujifilm Wako Pure Chemical Corporation)

Methanol (MeOH) (Fujifilm Wako Pure Chemical Corporation)

2-Methyltetrahydrofuran (2-MeTHF) (BioRenewable, anhydrous, ≥99%, Inhibitor-free)

$CDCl_3$ (Eurisotop)

CD_2Cl_2 (Eurisotop)

Compounds prepared as described in the literatures

H-H[1] (2steps, 20% overall yield from 9-bromoanthracene)

9-Bromo-10-(4-bromophenylethynyl)anthracene[2] (2steps, 18% overall yield from 9-anthracenecarbaldehyde)

9,9-Didodecyl-2,7-diethynyl-9*H*-fluorene[3] (2steps, 80% overall yield from 2.7-dibromo-9,9-didodecyl 9*H*-fluorene)

3,3'-Didodecyl-5,5'-diethynyl-2,2'-bithiophene[4] (4steps, 2% overall yield from 2-bromo-3-dodecylthiophene)

Synthetic Experiments

Synthetic experiments were performed under dry N_2 atmosphere with typical Schlenk technique unless otherwise noted. ^{1}H, ^{13}C{^{1}H}, and ^{11}B{^{1}H} NMR spectra were recorded on a JEOL JNM-ECZ400 and JNM-ECZ400S FT-NMR instrument at 400, 100, and 128 MHz, respectively. Some of ^{13}C{^{1}H} spectra were recorded on a JNM-ECZ600R FT-NMR instrument at 150 MHz for better resolution. The ^{1}H and ^{13}C chemical shift values were expressed relative to tetramethylsilane (TMS) (0.00 ppm) and non-deuterated solvent in CD_2Cl_2 (5.32 ppm for ^{1}H and 53.84 ppm for ^{13}C) as an internal standard. The ^{11}B chemical shift values were expressed relative to BF_3・Et_2O (0.00 ppm) as an external standard. Analytical thin-layer chromatography (TLC) was performed with silica gel 60 Merck F254 plates. Column chromatography was performed with Wakogel® C-300 silica gel. High-resolution mass spectrometry (HRMS) spectra were obtained on a Thermo Fisher Scientific Exactive Plus for atmospheric pressure chemical ionization (APCI, mass accuracy < 3ppm RMS) or a Bruker Daltonics ultrafleXtreme for matrix-assisted laser desorption ionization (MALDI, mass accuracy < 1ppm). Characterization of compounds by HRMS was based on the difference between simulated and measured data within 5ppm. Gel permeation chromatography (GPC) was carried out on a SHIMADZU Prominence system equipped with three consecutive polystyrene gel columns (TSK gels: G4000HXL, G3000HXL, G2500HXL) using chloroform as an eluent after calibration with standard polystyrene samples (1.0 mL/min) at 40 ºC. ^{13}C{^{1}H} NMR measurements on JNM-ECZ600R FT-NMR instrument and HRMS were performed at the Technical Support Office (Department of Synthetic Chemistry and Biological Chemistry, Graduate School of Engineering, Kyoto University).

Synthetic Procedure of Br-H

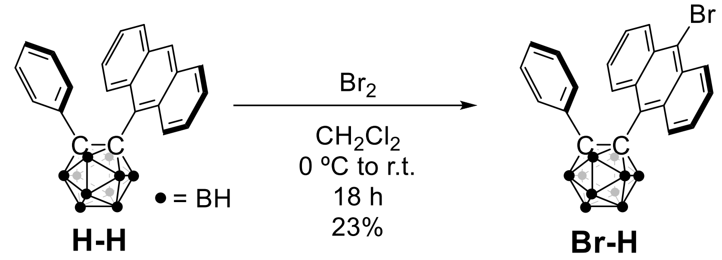

To the CH_2Cl_2 (10 mL) solution of **H-H** (77 mg, 0.19 mmol), CH_2Cl_2 (1.0 mL) solution of Br_2 (16 μL, 0.31 mmol) was added at 0 °C under ambient atmosphere. The reaction mixture was stirred by magnetic stirrer for 30 min at 0 °C, then the reaction temperature was raised to room temperature. After stirred for 18 h at room temperature, the mixture was quenched by aqueous $NaHSO_3$. Then the organic layer was washed with water and brine and dried over anhydrous $MgSO_4$. After filtration, the solvent was removed by a rotary evaporator to afford an orange solid. The crude product was purified by column chromatography (eluent: CH_2Cl_2/*n*-hexane 1/5 (v/v)) to give an orange solid. Recrystallization of the residual solid from MeOH/$CHCl_3$ ca. 10/1 (v/v) at 85 °C afforded **Br-H** as an orange crystal (21 mg, 44 μmol, 23%). ^{1}H NMR (400MHz, $CDCl_3$): δ (ppm) 8.98 (d, J = 8.8 Hz, 2H), 8.28 (dd, J = 8.7, 1.3 Hz, 2H), 7.52–7.44 (m, 4H), 6.92 (tt, J = 7.2, 1.2 Hz, 1H), 6.55 (dd, J = 8.0, 8.0 Hz, 2H), 6.39 (dd, J = 8.6, 1.0 Hz, 2H), 4.39–1.35 (m, 10H). ^{13}C{^{1}H} NMR (150 MHz, $CDCl_3$): 134.10, 130.39, 130.06, 129.85, 129.72, 128.71, 127.23, 127.22, 126.49, 126.43, 125.49, 119.41, 94.60, 89.79. ^{11}B{^{1}H} NMR (128 MHz, $CDCl_3$): δ (ppm) 0.17, –2.73, –9.34, –10.46. HRMS (n-APCI): calcd. for $C_{22}H_{23}B_{10}Br^{\cdot+}$ $[M]^{\cdot+}$ 476.1971, found 476.1965, error 1.3ppm.

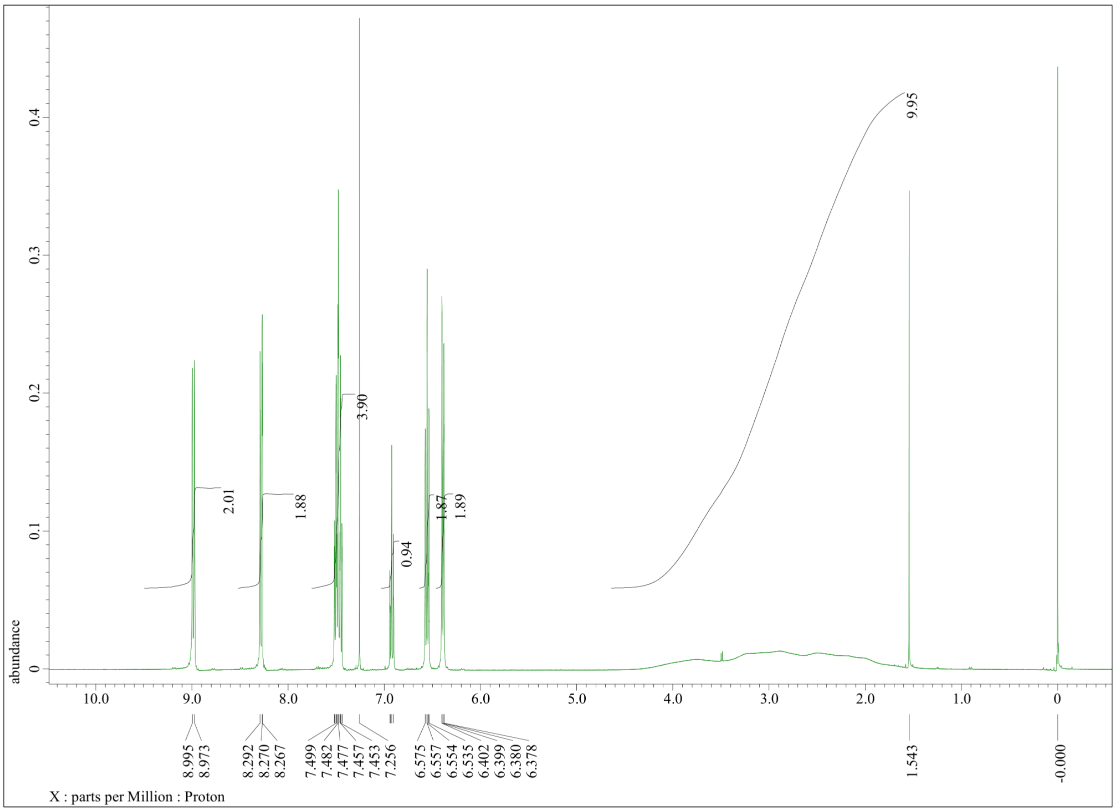

Chart S1. ^{1}H NMR spectrum of **Br-H** in $CDCl_3$.

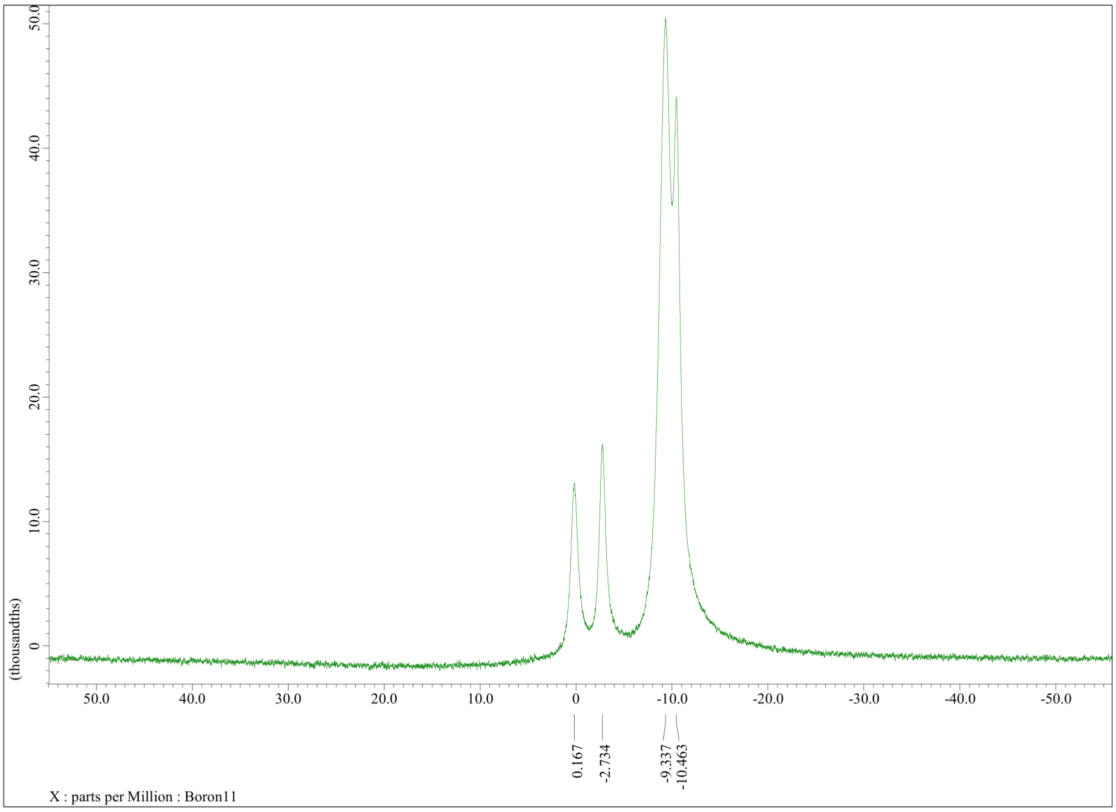

Chart S2. $^{11}B\{^{1}H\}$ NMR spectrum of **Br-H** in $CDCl_3$.

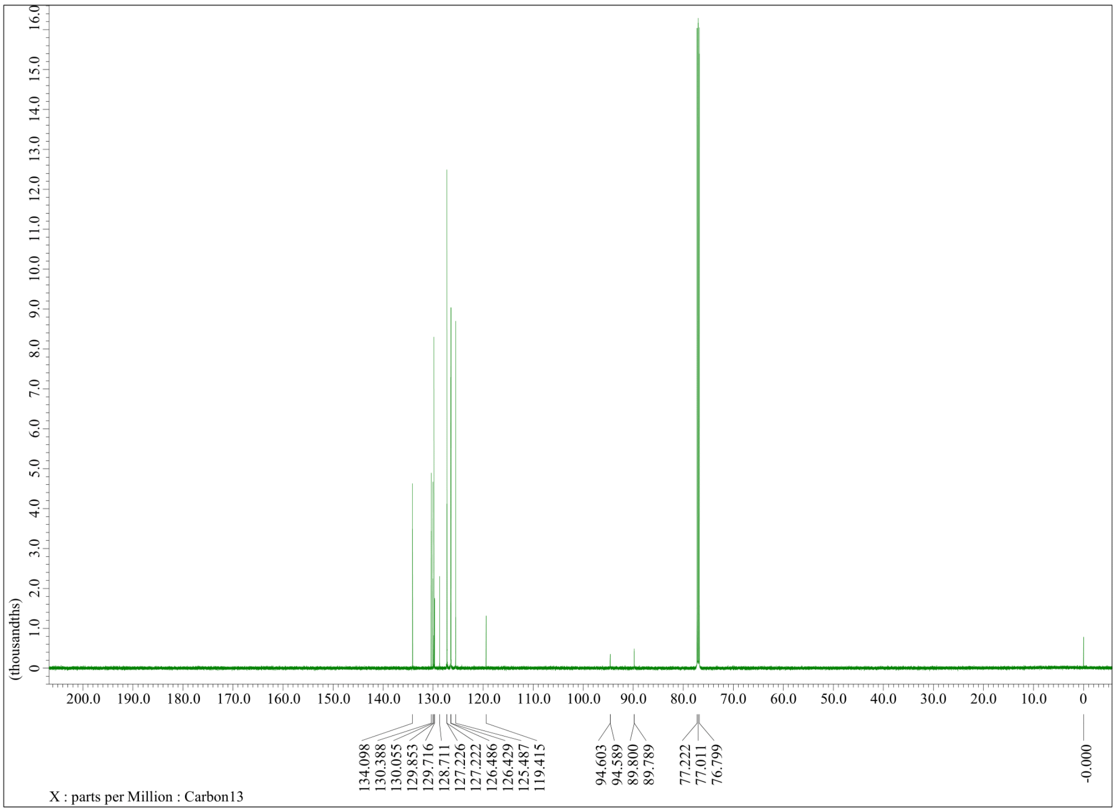

Chart S3. $^{13}C\{^{1}H\}$ NMR spectrum of **Br-H** in $CDCl_3$.

Synthetic Procedure of T-H

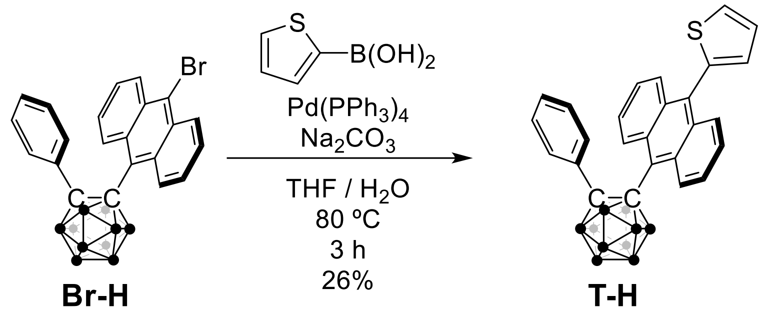

In the 2-necked test tube, **Br-H** (27 mg, 57 μmol), 2-thiopheneboronic acid (10 mg, 78 μmol), $Pd(PPh_3)_4$ (2 mg, 2 μmol) and Na_2CO_3 (15 mg, 0.14 mmol) were dissolved in THF (0.9 mL) and distilled water (0.1 mL, bubbling with dried N_2 for ca. 15 min was performed before use) under N_2 atmosphere. The reaction mixture was stirred by magnetic stirrer and heated at 80 ºC for 3 h. The black-red solution was diluted with EtOAc and H_2O, then the organic layer was washed with water and brine and dried over anhydrous $MgSO_4$. After filtration, the solvent was removed by a rotary evaporator to afford an orange solid. The crude product was purified by column chromatography (eluent: CH_2Cl_2/*n*-hexane 1/5 (v/v)) to give a red solid. Recrystallization of the residual solid from MeOH/$CHCl_3$ ca. 5/1 (v/v) at 85 °C afforded **T-H** as an orange crystal (7 mg, 15 μmol, 26%). ^{1}H NMR (400MHz, CD_2Cl_2): δ (ppm) 9.03 (d, J = 6.0 Hz, 2H), 7.60 (dd, J = 3.4, 0.6 Hz, 1H), 7.55 (dd, J = 6.0, 0.8 Hz, 2H), 7.50–7.47 (m, 2H), 7.32–7.29 (m, 2H), 7.24 (dd, J = 3.6, 2.4 Hz, 1H), 7.08 (tt, J = 5.0, 0.6 Hz, 1H), 6.91 (dd, J = 2.4, 0.8 Hz, 1H), 6.66–6.63 (m, 2H), 6.48 (dd, J = 6.0, 0.8 Hz, 2H) 4.23–1.56 (br, 10H). ^{13}C{^{1}H} NMR (100 MHz, CD_2Cl_2): δ (ppm) 137.83, 135.04, 133.62, 132.03, 130.70, 130.41, 130.39, 130.35, 127.66, 127.53, 127.41, 126.61, 126.58, 125.54, 125.43, 120.25, 95.50, 91.19. ^{11}B{^{1}H} NMR (128 MHz, CD_2Cl_2): δ (ppm) –0.21, –3.01, –9.30, –10.60. HRMS (n-APCI): calcd. for $C_{26}H_{26}B_{10}S+Cl^-$ $[M+Cl]^-$ 515.2380, found 515.2403, error 4.5ppm.

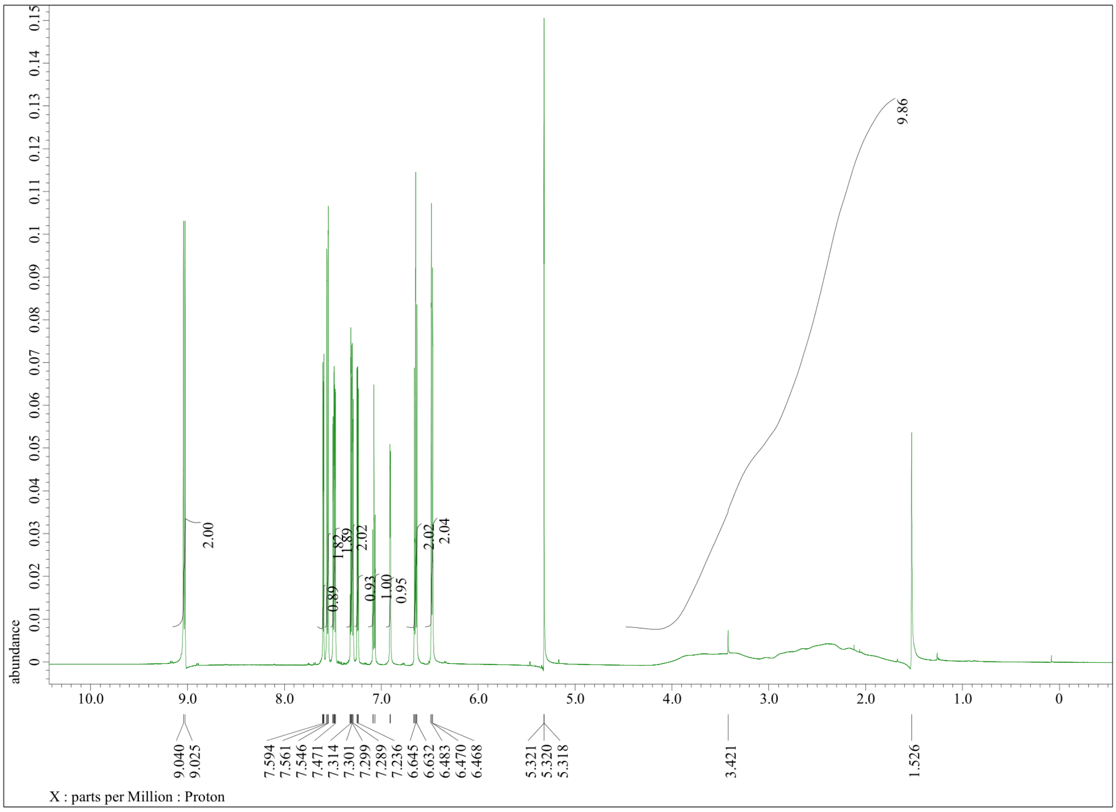

Chart S4. ^{1}H NMR spectrum of **T-H** in CD_2Cl_2.

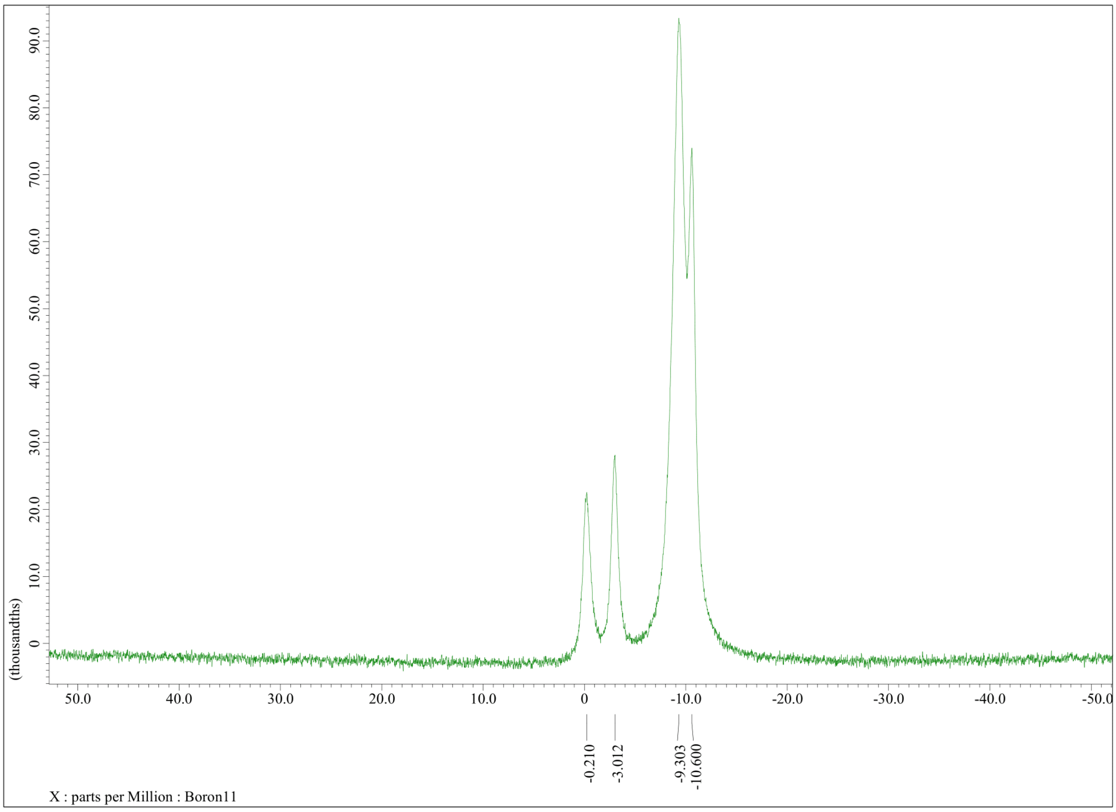

Chart S5. $^{11}B\{^{1}H\}$ NMR spectrum of **T-H** in CD_2Cl_2.

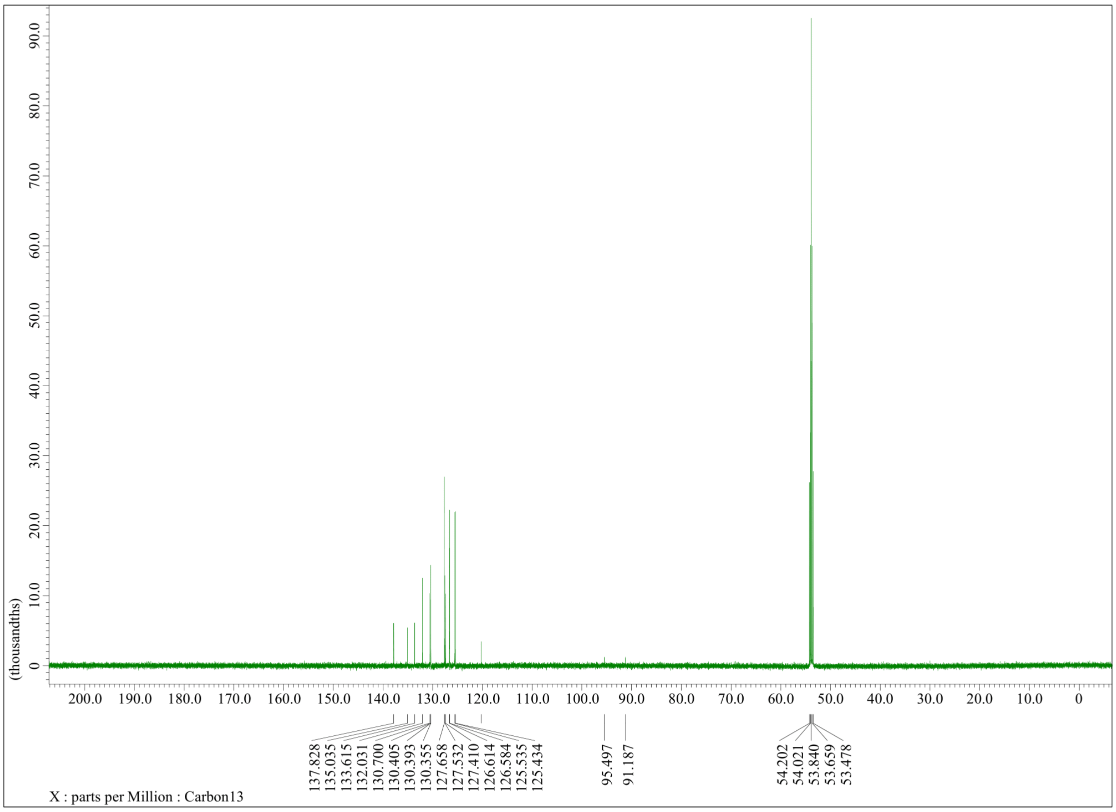

Chart S6. $^{13}C\{^{1}H\}$ NMR spectrum of **T-H** in CD_2Cl_2.

Synthetic Procedure of Br-Br

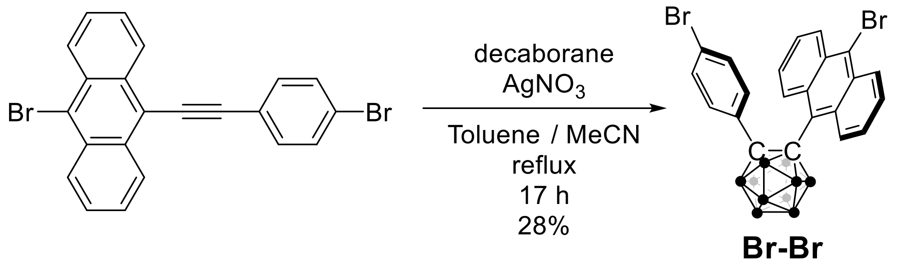

In the 30 mL 2-necked round bottom flask, 9-Bromo-10-(4-bromophenylethynyl)anthracene (438 mg, 1.00 mmol), decaborane (277 mg, 2.27 mmol) and $AgNO_3$ (37 mg, 0.22 mmol) were dissolved in toluene (5.0 mL) and MeCN (0.63 mL) under N_2 atmosphere. The reaction mixture was stirred by magnetic stirrer and refluxed at 110 °C for 3 h. After additional amount of toluene (2.5 mL) and MeCN (0.3 mL) were added, the reaction mixture was refluxed for 14 h. After filtration to remove any insoluble impurities, the solvent was removed by a rotary evaporator. The crude product was purified by column chromatography (eluent: CH_2Cl_2/*n*-hexane 1/20 (v/v)) to give an orange solid. Recrystallization of the residual solid from MeOH/$CHCl_3$ ca. 2/1 (v/v) at 90 °C afforded **Br-Br** as an orange crystal (156 mg, 0.17 mmol, 28%). ^{1}H NMR (400MHz, $CDCl_3$): δ (ppm) 8.95 (dd, J = 8.0, 2.0 Hz, 2H), 8.34 (dd, J = 7.4, 2.2 Hz, 2H), 7.54–7.47 (m, 4H), 6.70 (d, J = 8.8 Hz, 2H), 6.22 (d, J = 9.2 Hz, 2H), 4.38–1.65 (br, 10H). ^{13}C{^{1}H} NMR (150 MHz, $CDCl_3$): δ (ppm) 134.13, 131.38, 130.46, 130.39, 128.81, 128.78, 127.30, 126.55, 126.38, 125.70, 125.16, 118.85, 93.45, 90.09. ^{11}B{^{1}H} NMR (128 MHz, $CDCl_3$): δ (ppm) 0.29, −2.48, −9.32, −10.28. HRMS (n-APCI): calcd. for $C_{22}H_{22}B_{10}Br_2^-$ $[M]^-$ 554.1076, found 554.1079, error 0.5ppm.

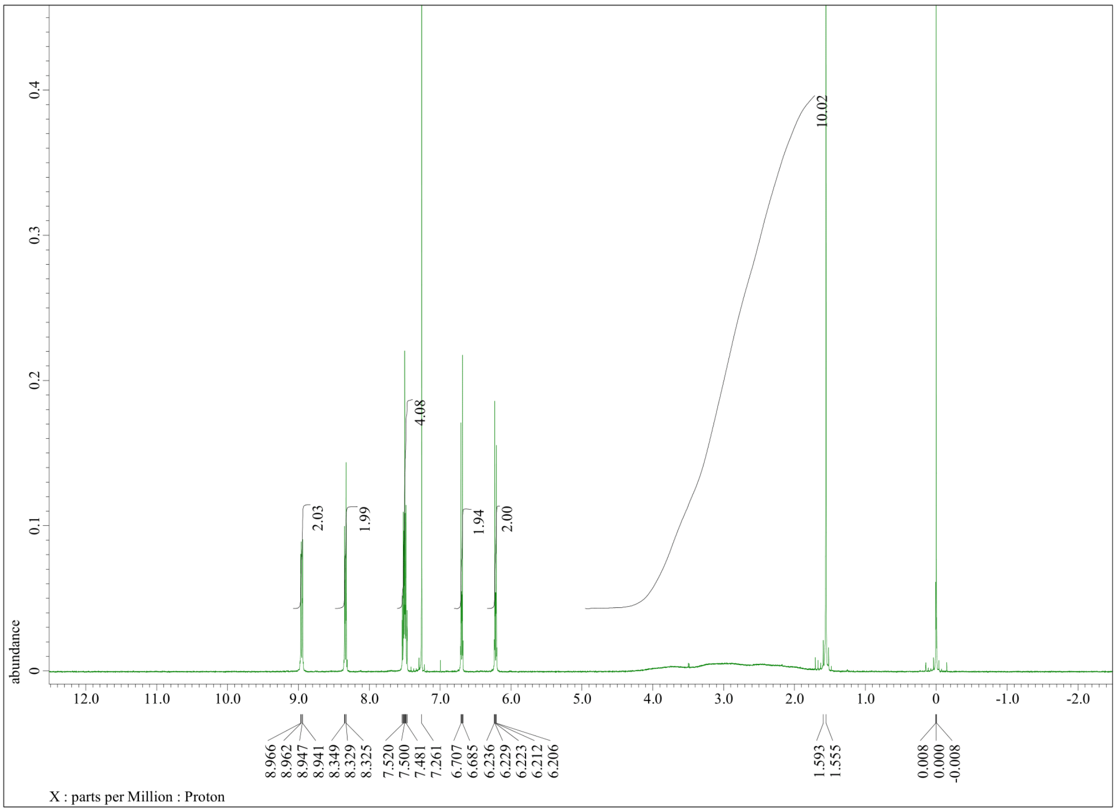

Chart S7. ^{1}H NMR spectrum of **Br-Br** in $CDCl_3$.

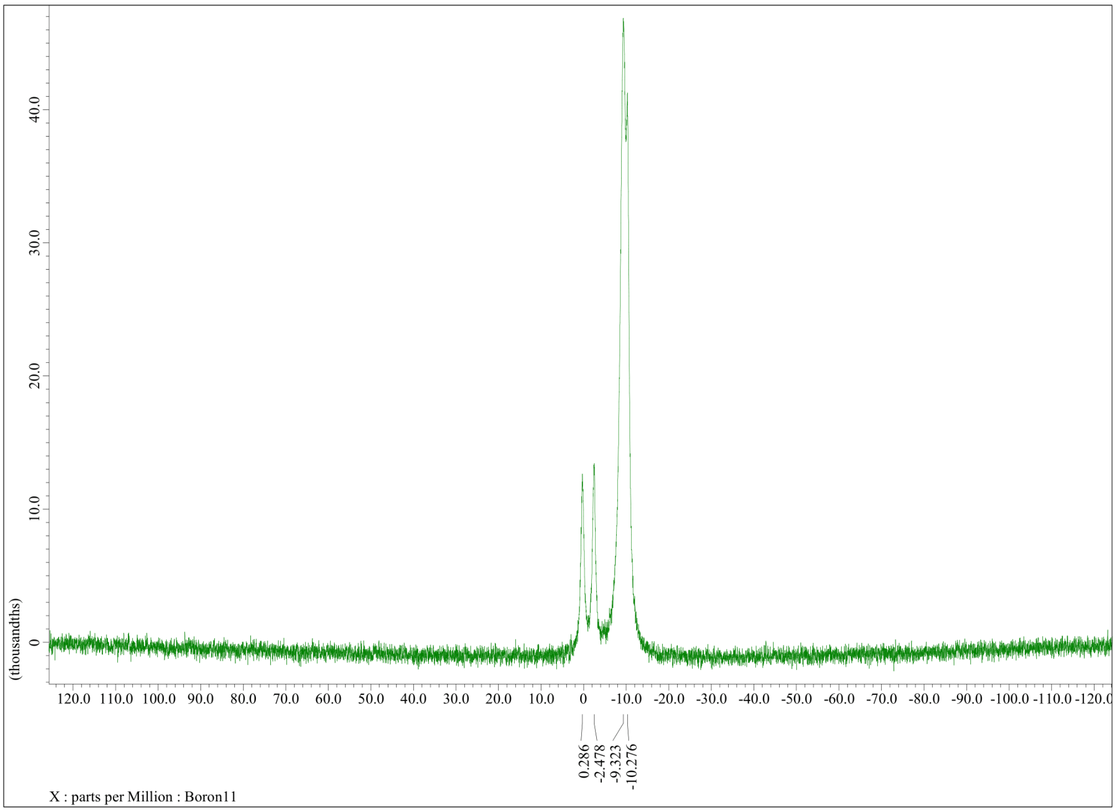

Chart S8. ^{11}B{^{1}H} NMR spectrum of **Br-Br** in $CDCl_3$.

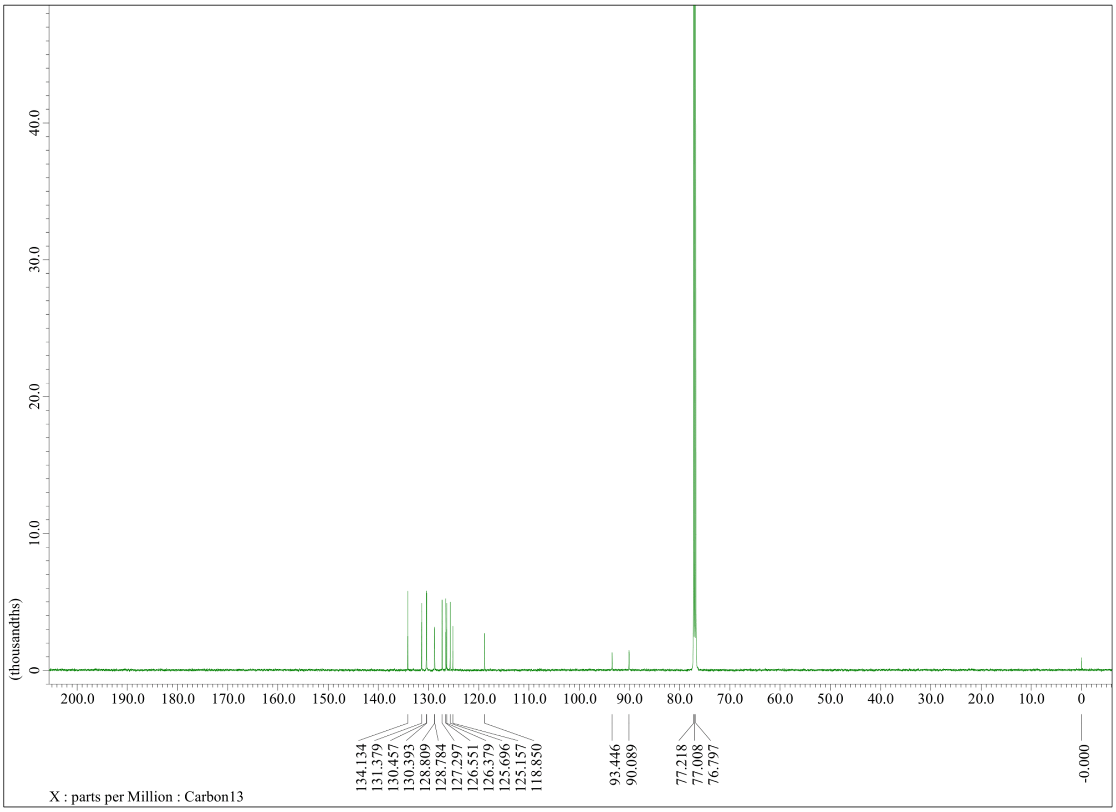

Chart S9. $^{13}C\{^{1}H\}$ NMR spectrum of **Br-Br** in $CDCl_3$.

Synthetic Procedure of T-T

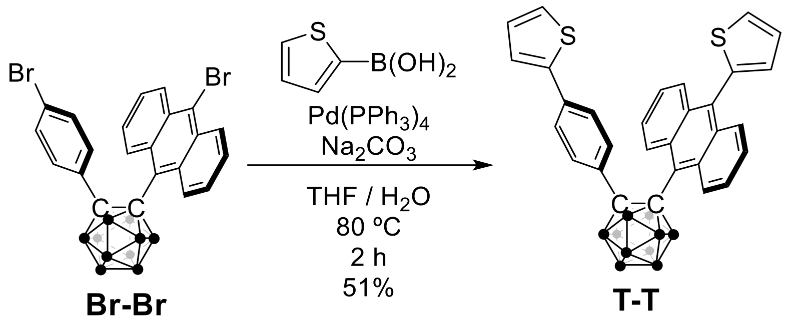

In the 2-necked test tube, **Br-Br** (56 mg, 0.10 mmol), 2-thiopheneboronic acid (30 mg, 0.23 mmol), $Pd(PPh_3)_4$ (3 mg, 3 μmol) and Na_2CO_3 (27 mg, 0.25 mmol) were dissolved in THF (1.6 mL) and distilled water (0.3 mL, bubbling with dried N_2 for ca. 15 min was performed before use) under N_2 atmosphere. The reaction mixture was stirred by magnetic stirrer and heated at 80 °C for 2 h. The black-red solution was diluted with EtOAc and water, then the organic layer was washed with water and brine and dried over anhydrous $MgSO_4$. After filtration, the solvent was removed by a rotary evaporator to afford a red solid. The crude product was purified by column chromatography (eluent: CH_2Cl_2/*n*-hexane 1/5 (v/v)) to give a red solid. Recrystallization of the residual solid from MeOH/$CHCl_3$ ca. 5/1 (v/v) at 80 °C afforded **T-T** as a red crystal (29 mg, 52 µmol, 51%). ^{1}H NMR (400MHz, CD_2Cl_2): δ (ppm) 9.05 (d, J = 8.4 Hz, 2H), 7.56 (d, J = 8.8 Hz, 2H), 7.50 (dd, J = 8.2, 7,0 Hz, 2H), 7.42 (d, J = 5.2 Hz, 1H), 7.34–7.29 (m, 3H), 7.20 (d, J = 4.0 Hz, 1H), 7.07 (dd, J = 3.1, 1.6 Hz, 1H), 7.03 (dd, J = 5.4, 3.4 Hz, 1H), 6.88 (d, J = 8.4 Hz, 2H), 6.70 (d, J = 3.2 Hz, 1H), 6.48 (d, J = 8.4 Hz, 2H), 4.64–1.60 (br, 10H). ^{13}C{^{1}H} NMR (100 MHz, CD_2Cl_2): δ (ppm) 142.62, 137.71, 136.35, 135.24, 133.63, 132.07, 130.95, 130.20, 129.48, 128.56, 127.37, 127.23, 126.69, 126.56, 126.50, 125.63, 125.47, 124.81, 125.57, 120.28, 95.64, 91.83. ^{11}B{^{1}H} NMR (128 MHz, CD_2Cl_2): δ (ppm) –0.19, –2.94, –9.27, –10.49. HRMS (n-APCI): calcd. for $C_{30}H_{28}B_{10}S_2+H^+$ $[M+H]^+$ 563.2636, found 563.2660, error 4.3ppm.

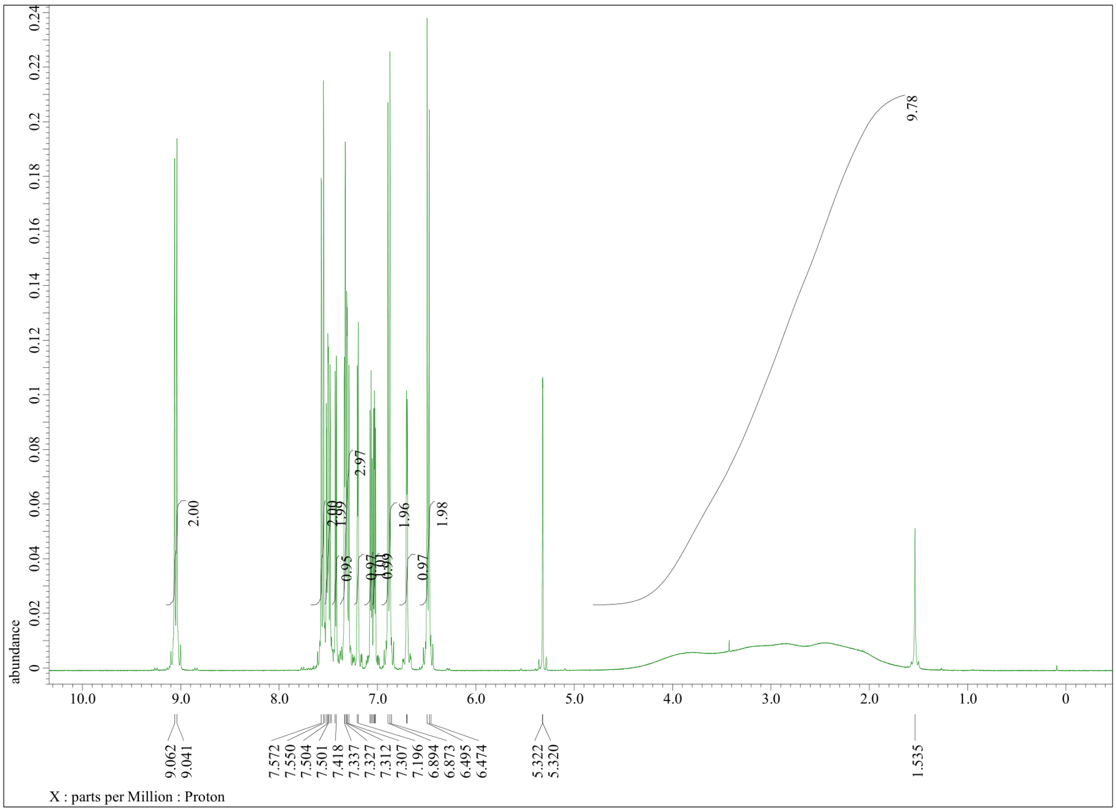

Chart S10. ^{1}H NMR spectrum of **T-T** in CD_2Cl_2.

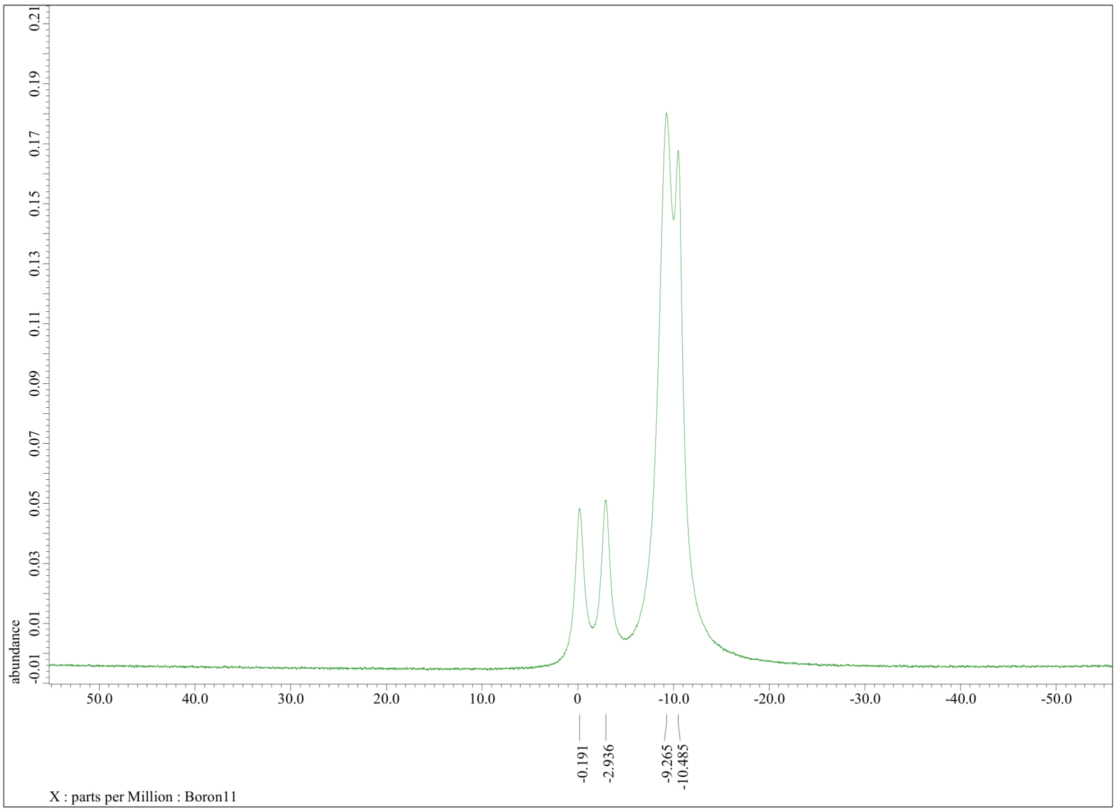

Chart S11. $^{11}B\{^{1}H\}$ NMR spectrum of **T-T** in CD_2Cl_2.

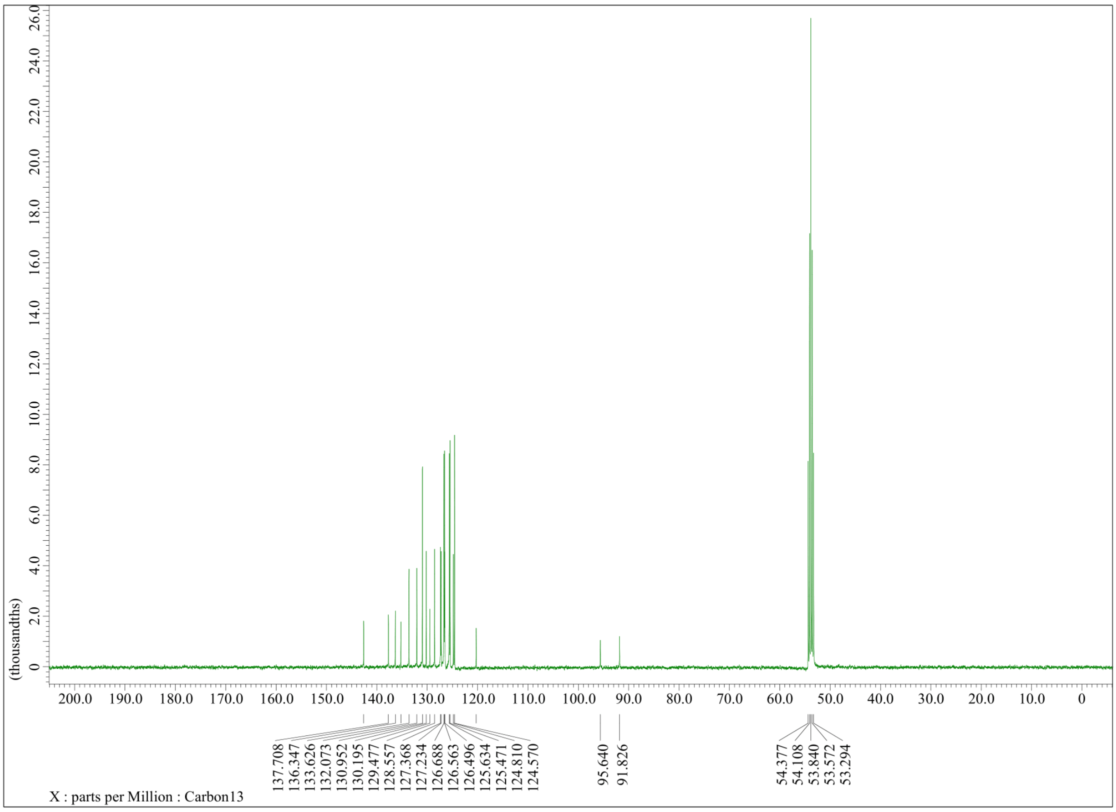

Chart S12. $^{13}C\{^{1}H\}$ NMR spectrum of **T-T** in CD_2Cl_2.

Synthetic Procedure of o-FL

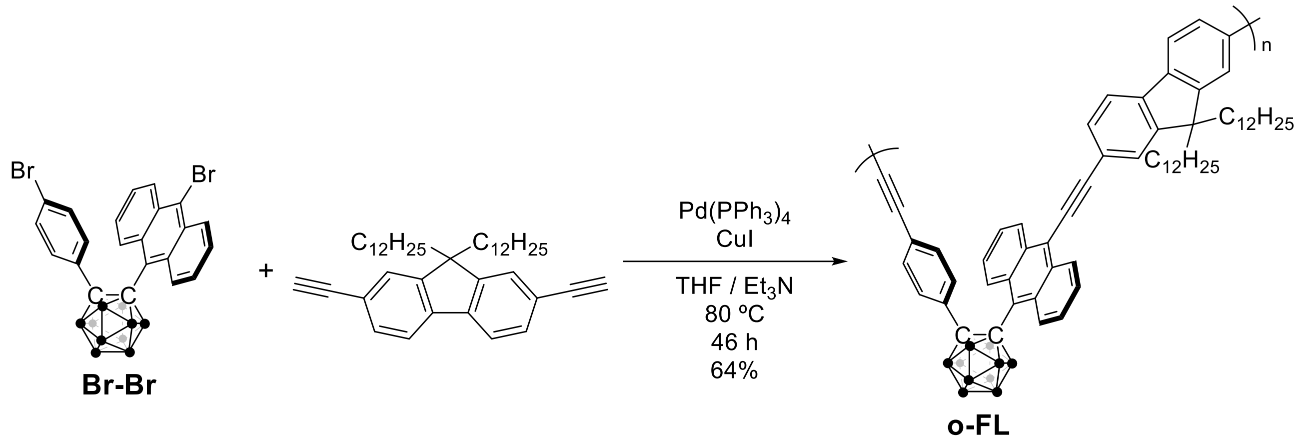

In the 2-necked test tube, **Br-Br** (150 mg, 0.27 mmol), 9,9-didodecyl-1,7-diethynyl-9*H*-fluorene (148 mg, 0.27 mmol), $Pd(PPh_3)_4$ (6 mg, 5 μmol) and CuI (1 mg, 5 μmol) were dissolved in THF (1.2 mL) and Et_3N (0.5 mL) under N_2 atmosphere. The reaction mixture was stirred by magnetic stirrer and reflexed at 80 °C for 46 h. The black-red solution was diluted with $CHCl_3$ and filtrated with Celite®, then the $CHCl_3$ solution was reprecipitated into MeOH. After filtration under reduced pressure, a reddish orange solid (231 mg) was obtained. The small molecules were extracted by Soxhlet extractor with MeOH at 110 °C for 7 h and *n*-hexane at 90 °C for 13.5 h, then the residual solid was dissolved in hot $CHCl_3$ at 105 °C. After the solvent was removed by rotary evaporator, the $CHCl_3$ solution of the red solid was reprecipitated into MeOH. After filtration under reduced pressure, **o-FL** was obtained as a reddish orange solid (163 mg, 64%). M_n = 3,200, M_w = 4,200, M_w/M_n = 1.31. ^{1}H NMR (400MHz, $CDCl_3$): δ (ppm) 9.20–8.88 (br, 8H), 8.64–8.38 (m, 8H), 7.92–6.94 (m, 40H), 6.92–6.64 (m, 8H), 6.34–6.40 (br, 5H), 6.32–6.14 (m, 3H), 4.79–1.65 (br, 49H), 1.37–0.24 (br, 177H). $^{13}C\{^1H\}$ NMR (100 MHz, $CDCl_3$): δ (ppm) 151.49, 151.40, 151.32, 151.13, 141.18, 141.06, 140.62, 140.50, 133.50, 132.49, 132.23, 132.07, 131.43, 131.26, 131.11, 130.34, 130.12, 130.00, 129.88, 129.07, 127.14, 126.79, 126.67, 126.45, 126.36, 126.16, 125.81, 125.70, 125.33, 125.27, 123.44, 123.36, 123.03, 121.92, 121.77, 121.57, 120.47, 120.33, 120.23, 119.66, 119.19, 105.67, 105.59, 105.40, 94.83, 93.97, 92.71, 91.35, 90.86, 88.68, 86.42, 86.26, 77.77, 77.63, 77.33, 77.22, 77.02, 76.70, 55.46, 55.34, 55.24, 40.52, 40.32, 40.23, 40.04, 31.87, 31.72, 30.18, 30.03, 29.96, 29.61, 29.31, 28.86, 28.71, 23.94, 23.79, 22.64, 14.10. $^{11}B\{^1H\}$ NMR (128 MHz, $CDCl_3$): δ (ppm) –4.50, –10.70.

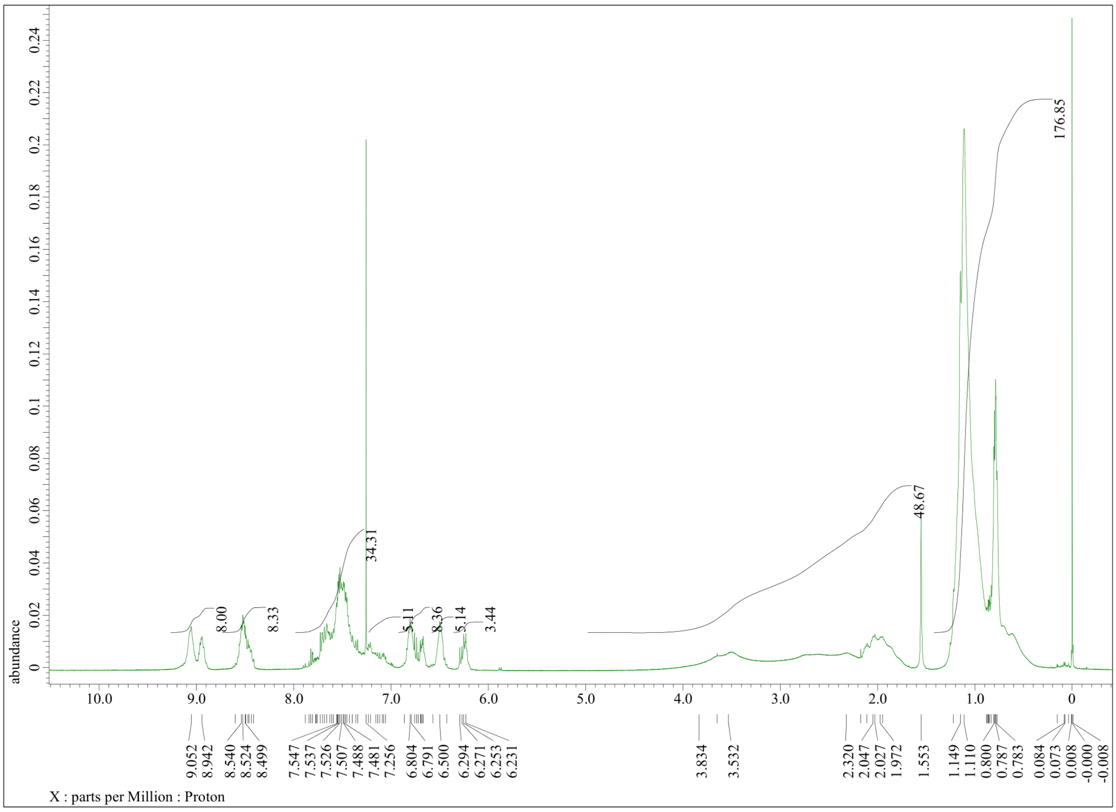

Chart S13. ^{1}H NMR spectrum of **o-FL** in $CDCl_3$.

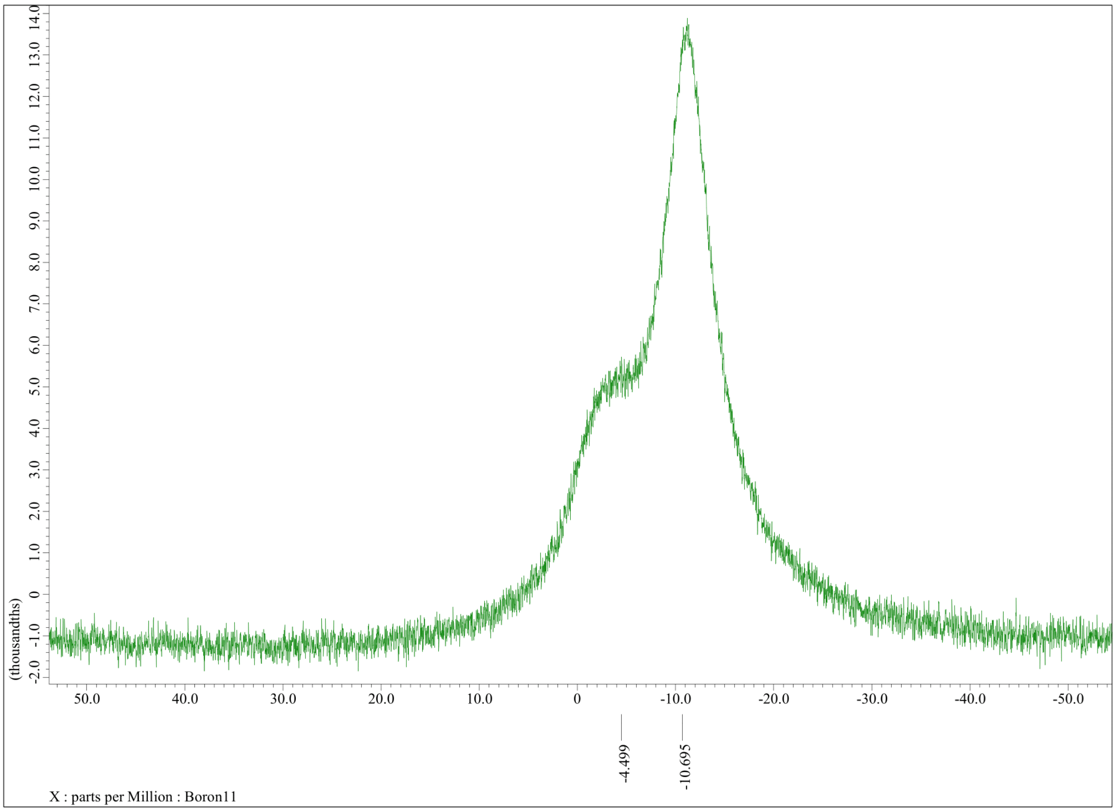

Chart S14. $^{11}B\{^{1}H\}$ NMR spectrum of **o-FL** in $CDCl_3$.

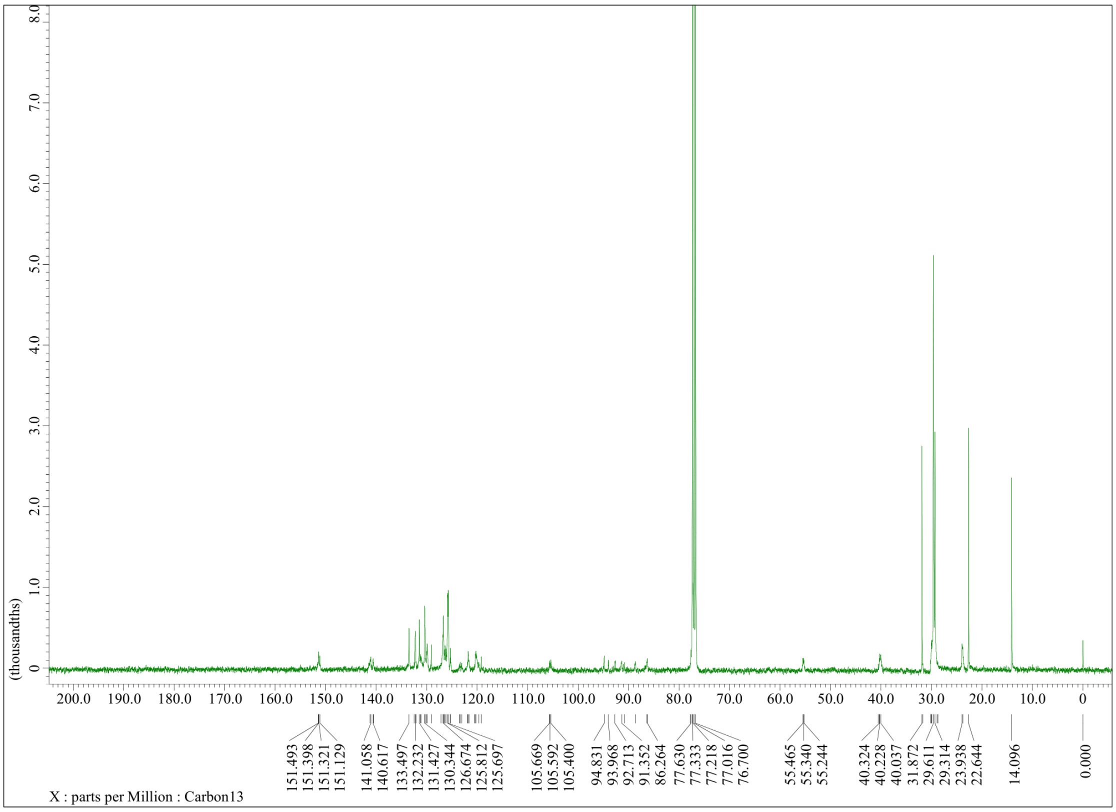

Chart S15. $^{13}C\{^1H\}$ NMR spectrum of **o-FL** in $CDCl_3$.

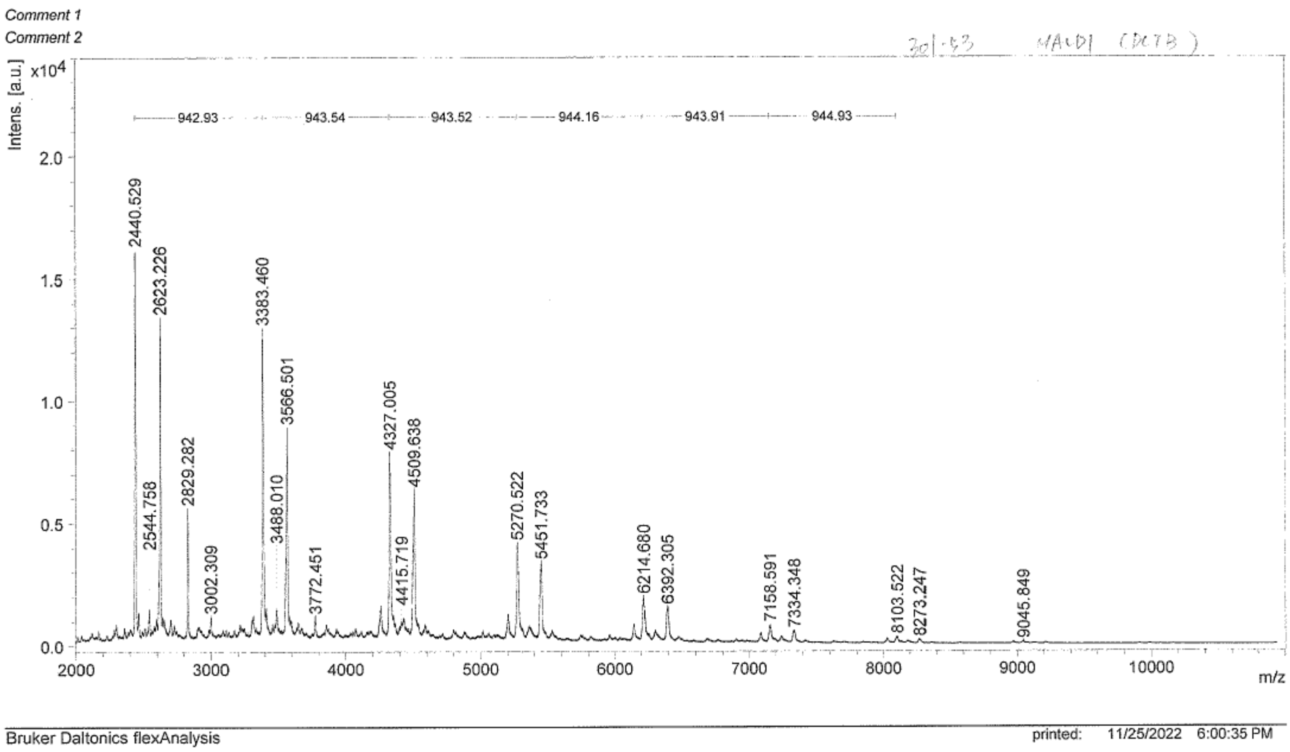

Chart S16. MALDI TOFMS spectrum of **o-FL**.

Synthetic Procedure of o-BT

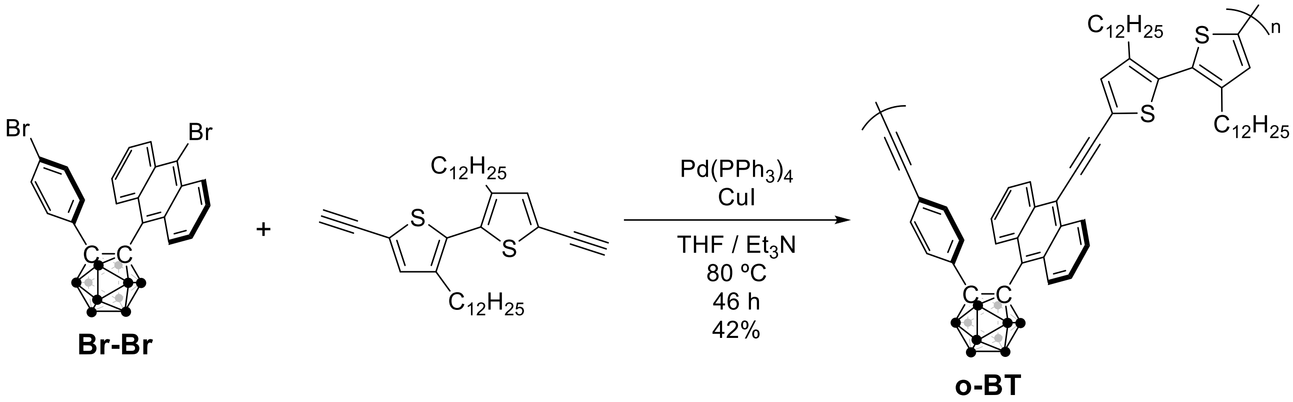

In the 2-necked test tube, **Br-Br** (168 mg, 0.30 mmol), 3,3'-didodecyl-5,5'-diethynyl-2,2'-bithiophene (168 mg, 0.30 mmol), $Pd(PPh_3)_4$ (7 mg, 6 μmol) and CuI (1 mg, 5 μmol) were dissolved in THF (1.3 mL) and Et_3N (0.6 mL) under N_2 atmosphere. The reaction mixture was stirred by magnetic stirrer and reflexed at 80 °C for 46 h. The black-red solution was diluted with $CHCl_3$ and filtrated with Celite®, then the $CHCl_3$ solution was reprecipitated into MeOH. After filtration under reduced pressure, a red solid (267 mg) was obtained. The small molecules were extracted by Soxhlet extractor with MeOH at 110 °C for 4.5 h and *n*-hexane at 95 °C for 13.5 h, then the residual solid was dissolved in hot $CHCl_3$ at 105 °C. After the solvent was removed by rotary evaporator, the $CHCl_3$ solution of the red solid was reprecipitated into MeOH. After filtration under reduced pressure, **o-BT** was obtained as a reddish orange solid (119 mg, 42%). M_n = 3,500, M_w = 5,700, M_w/M_n = 1.64. ^{1}H NMR (400MHz, $CDCl_3$): δ (ppm) 9.48–8.66 (m, 2H), 8.62–7.86 (m, 2H), 7.86–7.29 (m, 6H), 7.13–6.00 (m, 4H), 4.94–1.78 (br, 14H), 1.72–1.42 (br, 4H), 1.42–0.93 (br, 36H), 0.93–0.35 (br, 6H). ^{13}C{^{1}H} NMR (100 MHz, $CDCl_3$): δ (ppm) 143.41, 143.20, 135.12, 134.60, 134.05, 133.44, 133.13, 132.09, 131.79, 131.63, 131.43, 131.01, 130.93, 130.40, 130.26, 129.95, 129.86, 129.00, 126.68, 126.28, 126.16, 125.98, 125.72, 125.31, 122.82, 122.71, 122.47, 97.45, 94.00, 90.78, 77.62, 77.33, 77.22, 77.01, 76.69, 31.92, 30.71, 29.72, 29.48, 29.38, 28.98, 22.68, 22.50, 14.13. ^{11}B{^{1}H} NMR (128 MHz, $CDCl_3$): δ (ppm) –3.20, –10.31.

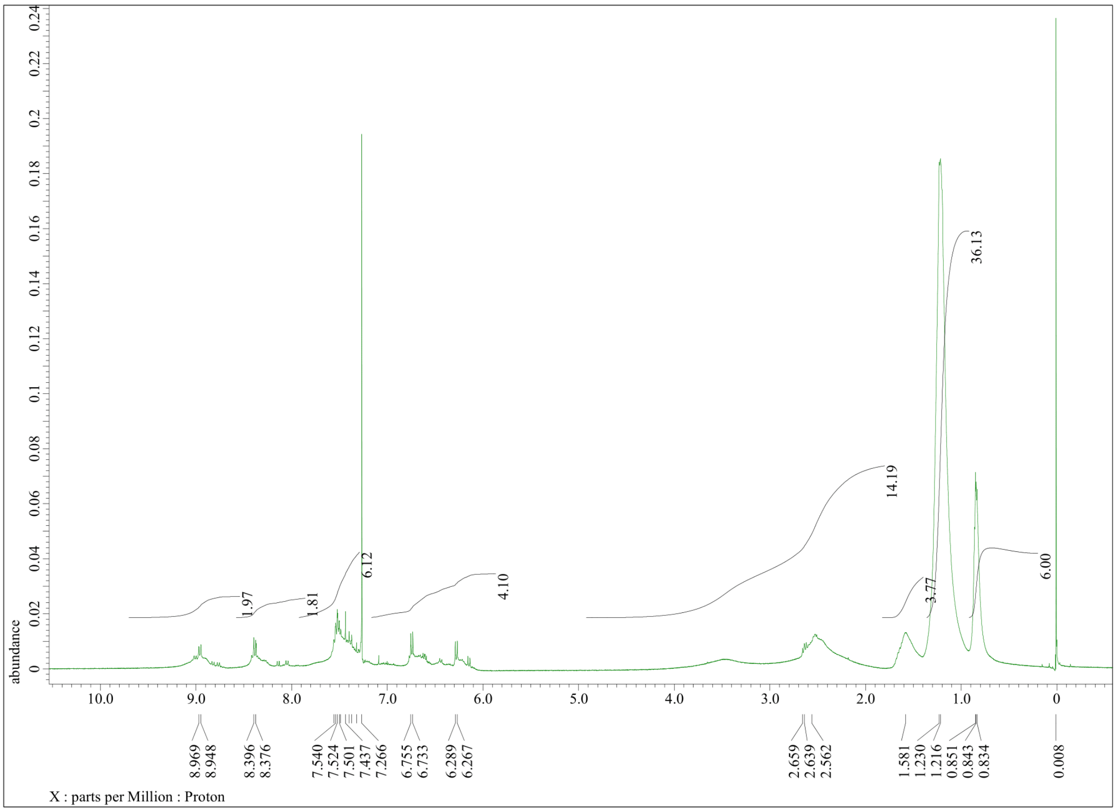

Chart S17. ^{1}H NMR spectrum of **o-BT** in $CDCl_3$.

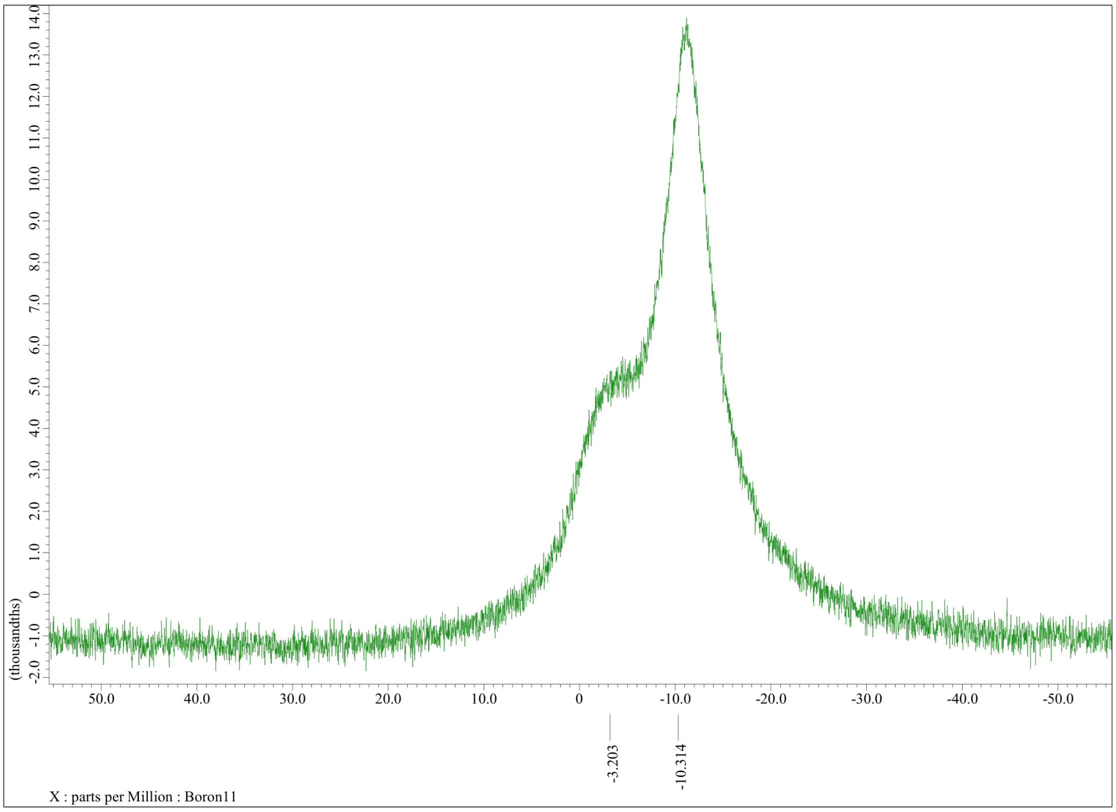

Chart S18. $^{11}B\{^{1}H\}$ NMR spectrum of **o-BT** in $CDCl_3$.

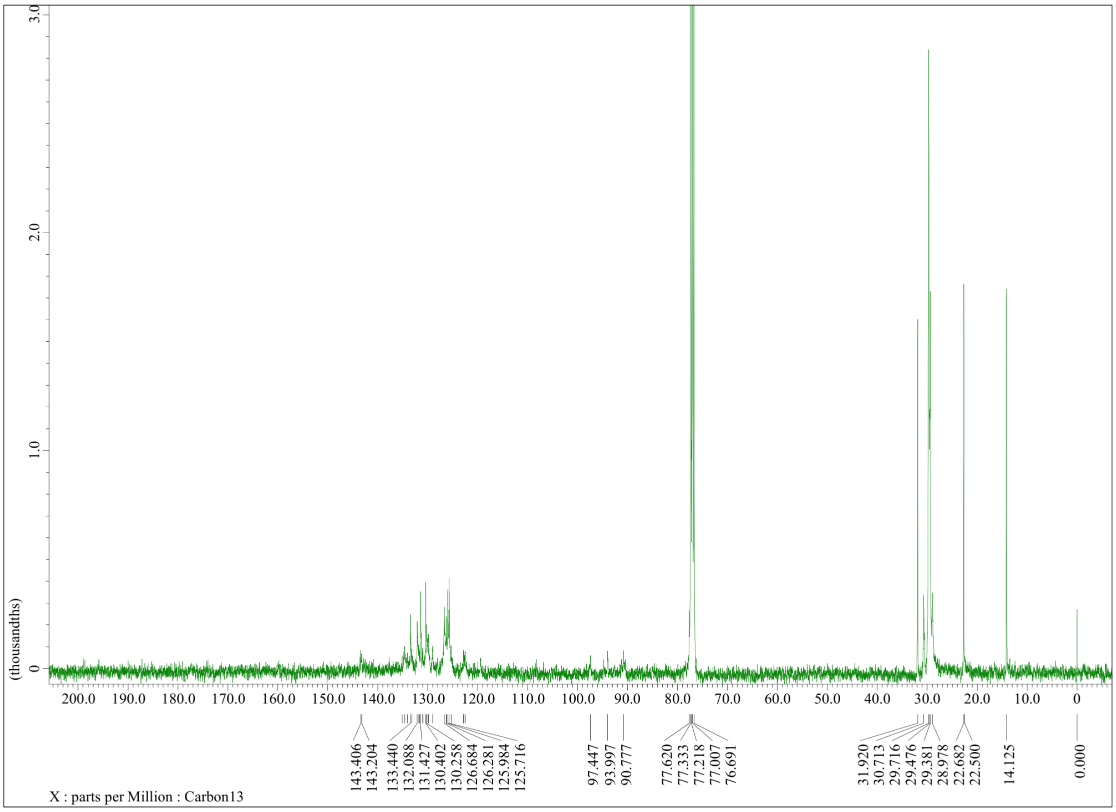

Chart S19. $^{13}C\{^{1}H\}$ NMR spectrum of **o-BT** in $CDCl_3$.

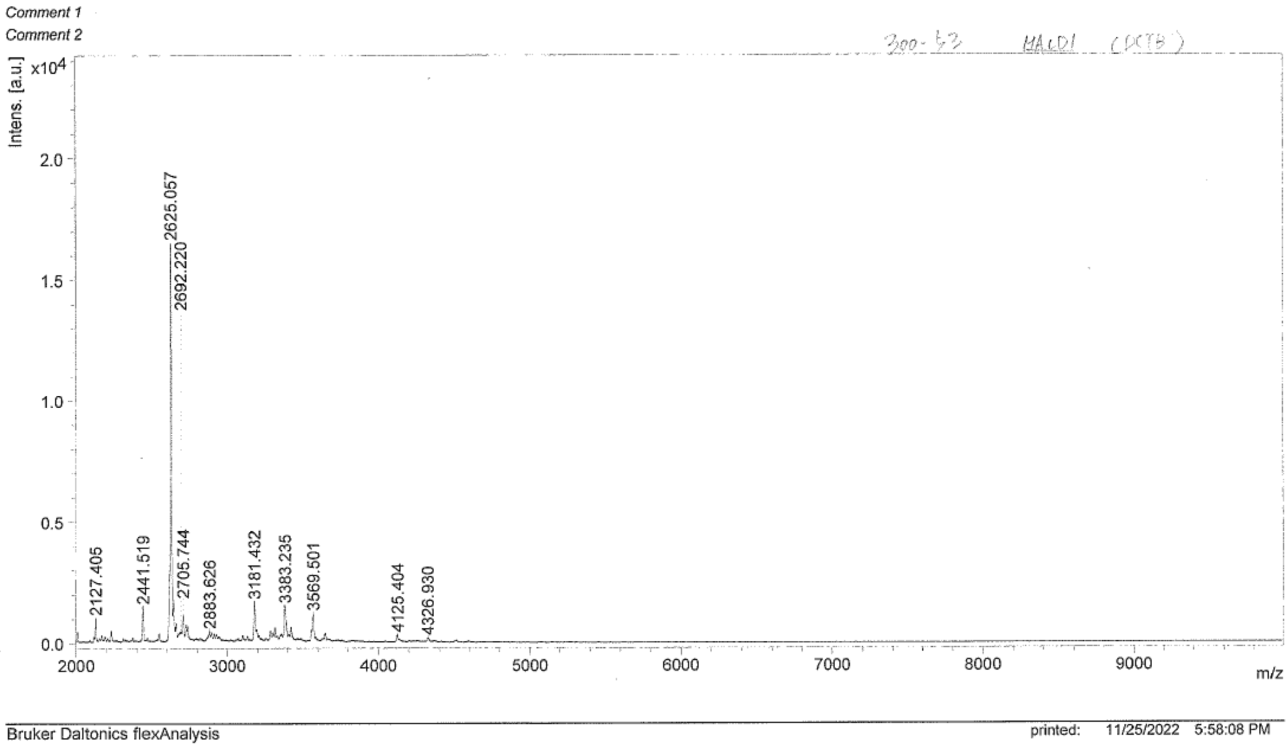

Chart S20. MALDI TOFMS spectrum of **o-BT**.

Single-Crystal X-ray Diffraction Analysis

The X-ray crystallographic analysis was carried out with a Rigaku Saturn 724+ with MicroMax-007 HF CCD diffractometer with Varimax Mo optics using graphite-monochromated Mo Kα radiation. Temperature control was performed by Rigaku nitrogen gas splaying cooler (temperature controller: CHINO KP 1000, gas generator: Iwatani gas GN-12). The structures were solved with SHELXT 2015[5] and refined on F^2 with SHELXL 2015[6] on Olex 2-1.2.[7] All hydrogen atoms were placed at calculated positions and refined using a riding model. The program *Mercury 2020.3.0*[8] and *ORTEP-3*[9] was used to generate the X-ray structural diagram. The volume of void in the crystal structure was calculated by the program *CrystalExplorer* 21.5.[10] Isovalue was set as 0.002 e・au^{-3}.

Table S1. Crystallographic data

Compound name	**H-H**	**Br-H**	**Br-Br**	**T-H**	**T-T**
CCDC number	2411824	2411825	2411826	2411827	2411828
Empirical formula	$C_{22}H_{24}B_{10}$	$C_{22}H_{23}B_{10}Br$	$C_{22}H_{22}B_{10}Br_2$	$C_{26}H_{26}B_{10}S$	$C_{30}H_{28}B_{10}S_2$
Formula weight	396.51	475.41	554.31	478.63	560.74
Temperature / K	143(2)	143(2)	143(2)	143(2)	143(2)
Wavelength / Å	0.71075	0.71075	0.71075	0.71075	0.71075
Crystal system	monoclinic	monoclinic	monoclinic	triclinic	monoclinic
Space group	$P2_1/n$ (No.14)	$C2/c$ (No.15)	$C2/c$ (No.15)	$P\bar{1}$ (No.2)	$P2_1/c$ (No.14)
a / Å	11.896(6)	30.080(8)	30.140(7)	9.459(4)	11.075(4)
b / Å	12.504(6)	10.105(3)	10.366(2)	11.316(5)	19.436(8)
c / Å	14.801(7)	17.857(5)	17.799(4)	12.775(6)	13.485(5)
α / °	90	90	90	109.650(5)	90
β / °	99.230(7)	124.970(3)	123.658(2)	100.826(3)	97.585(7)
γ / °	90	90	90	99.410(5)	90
V / Å^3	2172.9(19)	4448(2)	4629.1(18)	1226.3(9)	2877(2)
Z	4	8	8	2	4
ρ / g cm^{-3}	1.212	1.420	1.591	1.296	1.294
a / cm^{-1}	0.061	1.859	3.514	0.149	0.208
F(000)	824	1920	2192	496	1160
θ range / °	3.230–27.486	3.140–27.490	3.100–27.485	3.057–27.488	3.048−27.527
Limiting indices	$-15\leq h\leq 12$, $-16\leq k\leq 16$, $-18\leq l\leq 19$	$-38\leq h\leq 37$ $-13\leq k\leq 12$ $-22\leq l\leq 23$	$-34\leq h\leq 39$ $-13\leq k\leq 13$ $-21\leq l\leq 23$	$-11\leq h\leq 12$ $-13\leq k\leq 14$ $-16\leq l\leq 16$	$-14\leq h\leq 13$ $-25\leq k\leq 25$ $-17\leq l\leq 13$
Collected unique reflections	17387/4974	17643/5079	18383/5309	10041/5379	23165/6496
R_{int}[a]	0.1491	0.0410	0.0631	0.0486	0.0847
S (Goodness-of-fit on F^2)[b]	1.130	0.777	0.824	0.872	1.092
R_1 [$I > 2\sigma(I)$][c]	0.1187	0.0370	0.0281	0.0416	0.0742
wR_2 (all data)[d]	0.2188	0.1153	0.0631	0.0990	0.1864

[a] $R_{int} = \Sigma||F_0|^2 - <|F_o|^2>|/\Sigma|F_o|^2$ [b] $S = [\{\Sigma w(|F_0|^2-|F_c|^2)^2\}/(N_o - N_p)]^{1/2}$ [c] $R_1 = [\Sigma(|F_0|^2-|F_c|^2)^2/\Sigma(|F_0|^2)^2]^{1/2}$

[d] $wR_2 = [\Sigma w(|F_0|^2-|F_c|^2)^2/\Sigma w(|F_0|^2)^2]^{1/2}$. $w = 1/[\sigma^2(|F_0|^2)+[(ap)^2+bp]]$, where $p = [|F_0|^2, +2|F_c|^2]/3$

Table S2. Geometrical data of crystal structures

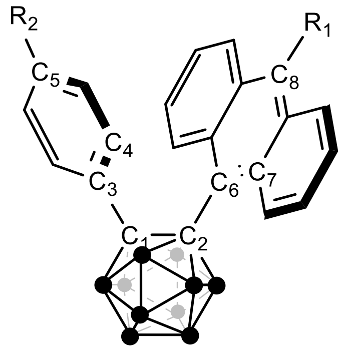

H-H ($R_1 = R_2 = H$)
Br-H (R_1 = Br, R_2 = H)
Br-Br ($R_1 = R_2$ = Br)
T-H (R_1 = 2-thienyl, R_2 = H)
T-T ($R_1 = R_2$ = 2-thienyl)

	$d(C_1–C_2)$ / Å	$d(C_3–C_6)$ / Å	$d(C_5–C_8)$ / Å	$\varphi(C_2–C_1–C_3–C_4)$ / º	$\varphi(C_1–C_2–C_6–C_7)$ / º	d(Ph-Ant) / Å[a]
H-H	1.830(5)	3.077(5)	4.318(6)	−95.2(4)	83.6(4)	3.808
Br-H	1.821(3)	3.192(3)	5.109(4)	−63.0(3)	89.7(3)	4.232
Br-Br	1.820(4)	3.177(4)	5.069(4)	–113.9(3)	87.7(3)	4.198
T-H	1.830(3)	3.153(3)	4.756(3)	−111.3(2)	94.2(2)	4.069
T-T	1.827(4)	3.108(4)	4.412(4)	–86.2(3)	84.1(3)	3.895

[a] Distance between centroids of phenyl group and central benzene ring of anthryl group.

Table S3. Crystallographic data of **H-H** measured in different temperature

Temperature / K	143(2)	208(2)	243(2)
CCDC number	2411824	2425738	2425739
Empirical formula	$C_{22}H_{24}B_{10}$	$C_{22}H_{24}B_{10}$	$C_{22}H_{24}B_{10}$
Formula weight	396.51	396.51	396.51
Wavelength / Å	0.71075	0.71075	0.71075
Crystal system	monoclinic	monoclinic	monoclinic
Space group	$P2_1$/n (No.14)	$P2_1$/n (No.14)	$P2_1$/n (No.14)
a / Å	11.896(6)	11.912(2)	11.910(3)
b / Å	12.504(6)	12.511(2)	12.514(3)
c / Å	14.801(7)	14.825(3)	14.838(3)
α / º	90	90	90
β / º	99.230(7)	99.261(3)	99.142(3)
γ / º	90	90	90
V / Å^3	2172.9(19)	2180.6(7)	2183.5(8)
Z	4	4	4
ρ / g cm^{-3}	1.212	1.208	1.206
a / cm^{-1}	0.061	0.061	0.061
F(000)	824	824	824
θ range / º	3.230–27.486	3.257–27.487	3.223–27.478
Limiting indices	$-15\leq h\leq 12$, $-16\leq k\leq 16$, $-18\leq l\leq 19$	$-11\leq h\leq 15$ $-16\leq k\leq 15$ $-19\leq l\leq 19$	$-15\leq h\leq 13$ $-15\leq k\leq 14$ $-19\leq l\leq 19$
Collected unique reflections	17387/4974	17321/4980	17258/4922
R_{int}[a]	0.1491	0.0328	0.0488
S (Goodness-of-fit on F^2)[b]	1.130	1.083	0.962
R_1 [$I > 2\sigma(I)$][c]	0.1187	0.0462	0.0488
wR_2 (all data)[d]	0.2188	0.1294	0.1381

[a] $R_{int} = \Sigma||F_0|^2 – <|F_o|^2>|/\Sigma|F_o|^2$ [b] $S = [\{\Sigma w(|F_0|^2–|F_c|^2)^2\}/(N_o – N_p)]^{1/2}$ [c] $R_1 = [\Sigma(|F_0|^2–|F_c|^2)^2/\Sigma(|F_0|^2)^2]^{1/2}$
[d] $wR_2 = [\Sigma w(|F_0|^2–|F_c|^2)^2/\Sigma w(|F_0|^2)^2]^{1/2}$. $w = 1/[\sigma^2(|F_0|^2)+[(ap)^2+bp]]$, where $p =[|F_0|^2,+2|F_c|^2]/3$

Table S4. Variable temperature crystallographic data of **H-H**

Temperature / K	V_{cell} / Å^3 [a]	V_{void} / Å^3 [b]	$V_{molecule}$ / Å^3 [c]
143(2)	2172.9(19)	253	480
208(2)	2180.6(7)	262	480
243(2)	2183.5(8)	267	479

[a] Unit cell volume determined by single-crystal X-ray diffraction. [b] Void volume in the unit cell calculated by *CrystalExplorer* 21.5. [c] Averaged volume occupied by each molecule in the unit cell calculated by the equation: $(V_{cell} - V_{void})/Z$, where Z denotes number of molecules contained in the unit cell.

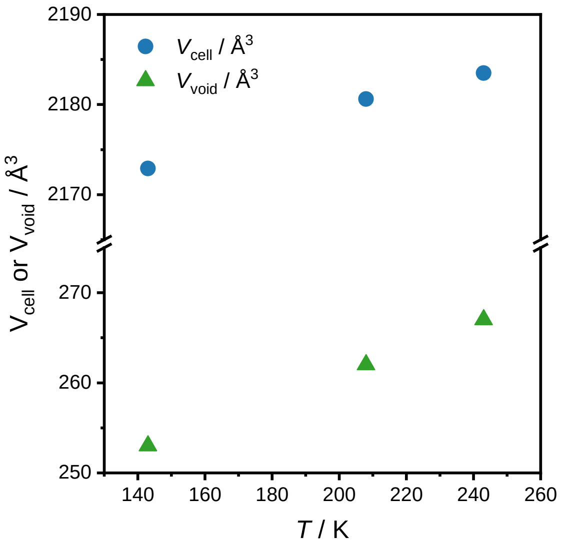

Figure S1. Temperature-dependence of unit cell volume and crystal void volume of **H-H**.

Table S5. Crystalline geometrical data of **H-H** in variable temperature

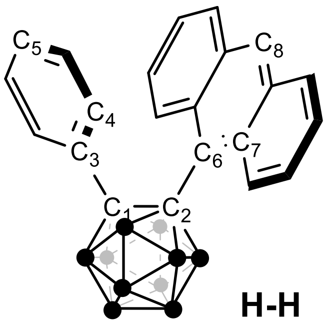

H-H

T / K	*d*(C_1–C_2) / Å	*d*(C_3–C_6) / Å	*d*(C_5–C_8) / Å	*φ*(C_2–C_1–C_3–C_4) / °	*φ*(C_1–C_2–C_6–C_7) / °	*d*(Ph-Ant) / Å[a]
143	1.830(5)	3.077(5)	4.318(6)	−95.2(4)	83.6(4)	3.808
208	1.819(2)	3.074(2)	4.326(2)	−84.6(1)	86.7(1)	3.804
243	1.817(2)	3.076(2)	4.328(2)	–84.5(2)	86.7(1)	3.806

[a] Distance between centroids of phenyl group and central benzene ring of anthryl group.

Powder X-ray Diffraction Analysis

Powder X-ray diffraction (PXRD) data were collected with a Rigaku SmartLab Diffractometer (sealed tube (50 kV, 40 mA); Cu Kα, 1.542 Å; Bragg–Brentano geometry). PXRD samples were placed on a single-crystal silicon substrate.

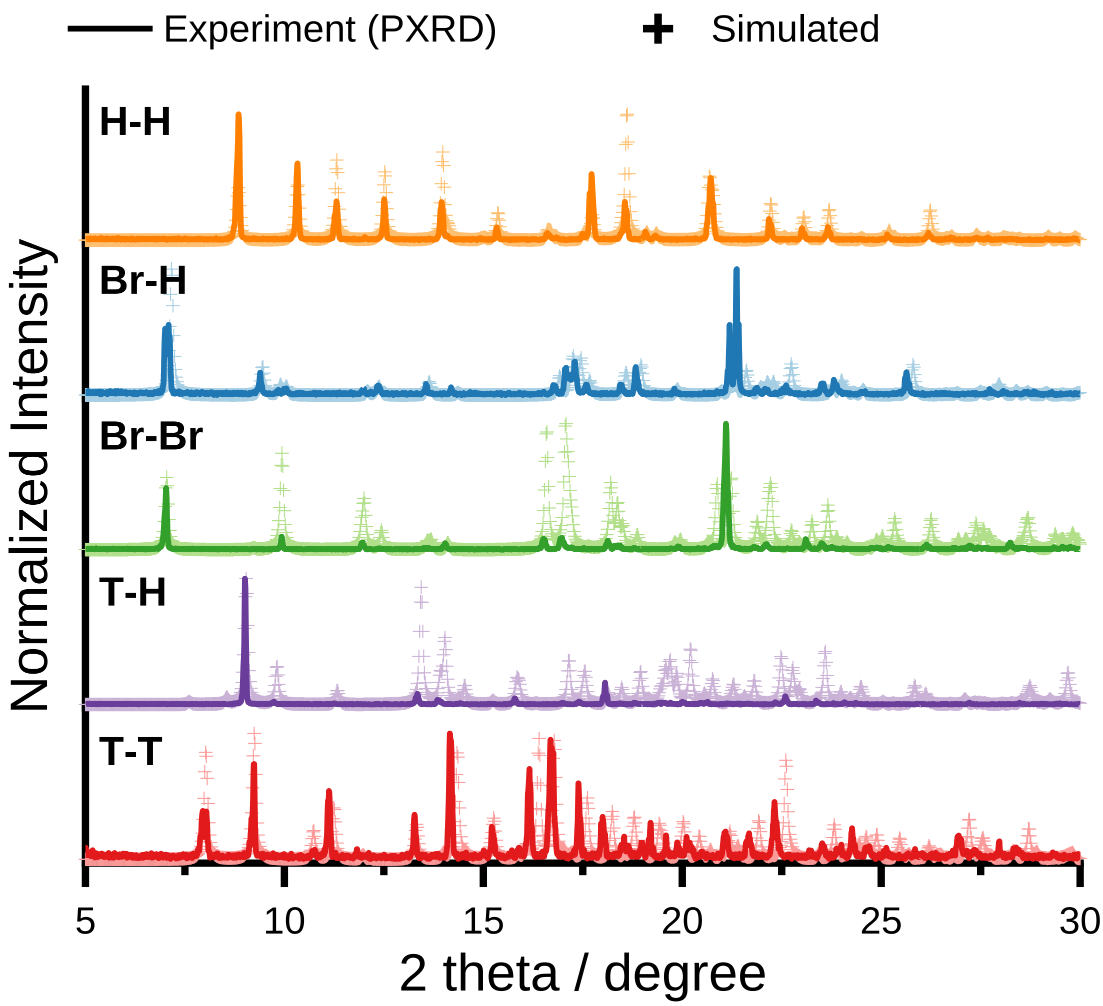

Figure S2. PXRD patterns and simulated diffraction patterns of *C*,*C*′-diaryl-*o*-carborane derivatives.

Optical Properties

UV–vis absorption and diffusion reflectance spectra were obtained on a SHIMADZU UV3600i plus spectrophotometer. Photoluminescence (PL) spectra were measured with a HORIBA JOBIN YVON Fluorolog-3 spectrofluorometer and an Oxford Optistat DN for temperature control. The fluorescence quantum yield (QY) was recorded on a HAMAMATSU Quantaurus-QY Plus C13534-01 model. The PL lifetime measurement was performed on a HORIBA FluoroCube spectrofluorometer system with a UV diode laser (NanoLED 369 nm) or a HORIBA Deltaflex spectrofluorometer system with a UV diode laser (DeltaDiode 375 nm).

Preparation of samples

The solution for optical measurements was prepared by following procedure. First, measured solid samples were dissolved in each solvent using whole pipette to afford 1.0×10^{-3} M solution. Then, 100 μL of 1.0×10^{-3} M solution was placed in 10 mL volumetric flask. Finally, the same solvent was added up to the marked line to obtain 10 mL of 1.0×10^{-5} M solution.

Crystalline samples were prepared by recrystallization. Samples were dissolved in boiling MeOH/$CHCl_3$. After allowed to room temperature, the solution was placed at −20 °C refrigerator. Precipitated crystals were collected by membrane filter and then dried in vacuo to remove any residual solvent.

Films were prepared by spin-coating method from 1 mg / 300 mL (per repeating unit) $CHCl_3$ solution. (1000 rpm, 30 sec) and then dried in vacuo for 1.5 h.

Calculation method for the relative PL quantum yield

In this paper, relative PL quantum yield was used for discussion in temperature dependence. Integration of PL spectra (absolute PL intensity (cps unit) vs wavelength (nm)) was performed to obtain integrated PL intensity. Then, data at 290 K was used as a standard of PL data with absolute quantum yield measured at room temperature. Relative PL quantum yield was calculated according to the following equation.

$$\phi_{\mathrm{T}}^{\mathrm{rel}} = \frac{I_T}{I_{290}} \times \phi_{\mathrm{rt}}^{\mathrm{abs}}$$

,where ϕ_T^{rel} was relative PL quantum yield at T K, I_T was integrated PL intensity at T K, and $\phi_{\mathrm{rt}}^{\mathrm{abs}}$ was absolute PL quantum yield. *Origin 2020* software was used for integration of PL spectra. If calculated ϕ_T^{rel} values exceeded 1.0, virtual value of 0.999 was used instead for k_{r} and k_{nr}

calculation. This excess can be because the calculation was performed under approximation of temperature-independency in absorption.

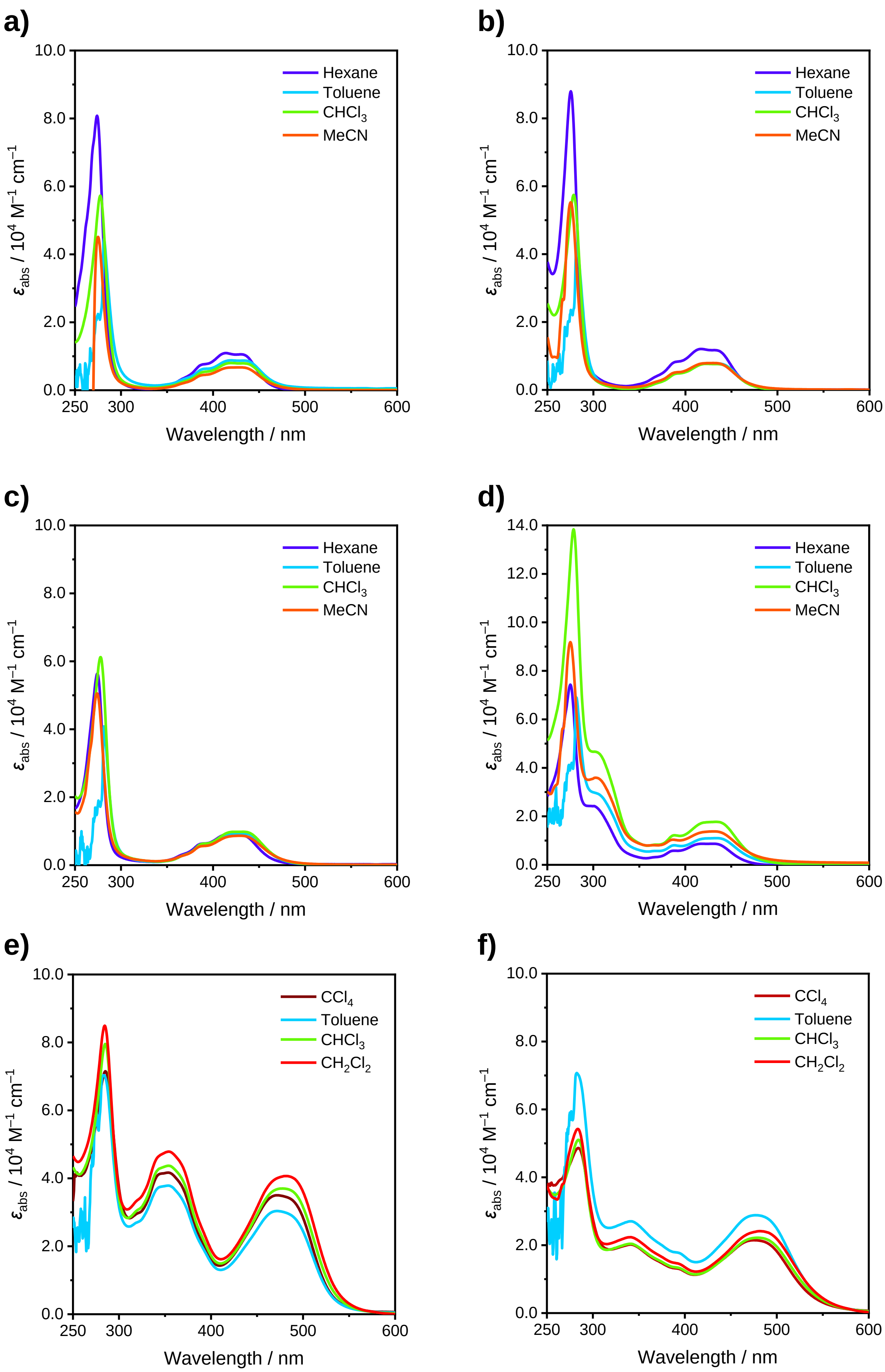

Figure S3. Solution-state UV–vis absorption spectra of a) **Br-H**, b) **Br-Br**, c) **T-H**, d) **T-T**, e) **o-FL** and f) **o-BT**.

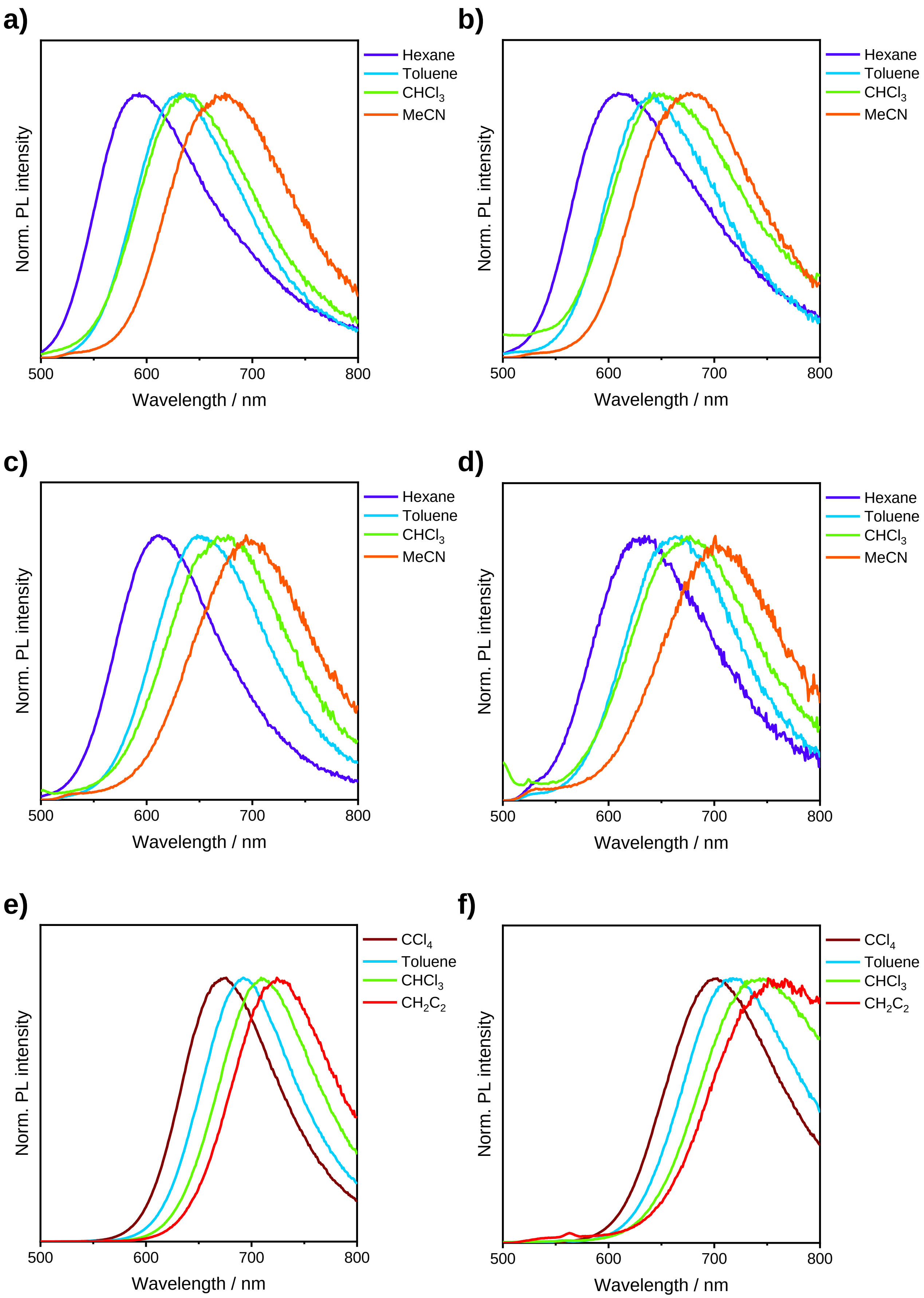

Figure S4. Solution-state PL spectra of a) **Br-H**, b) **Br-Br**, c) **T-H**, d) **T-T**, e) **o-FL** and f) **o-BT**.

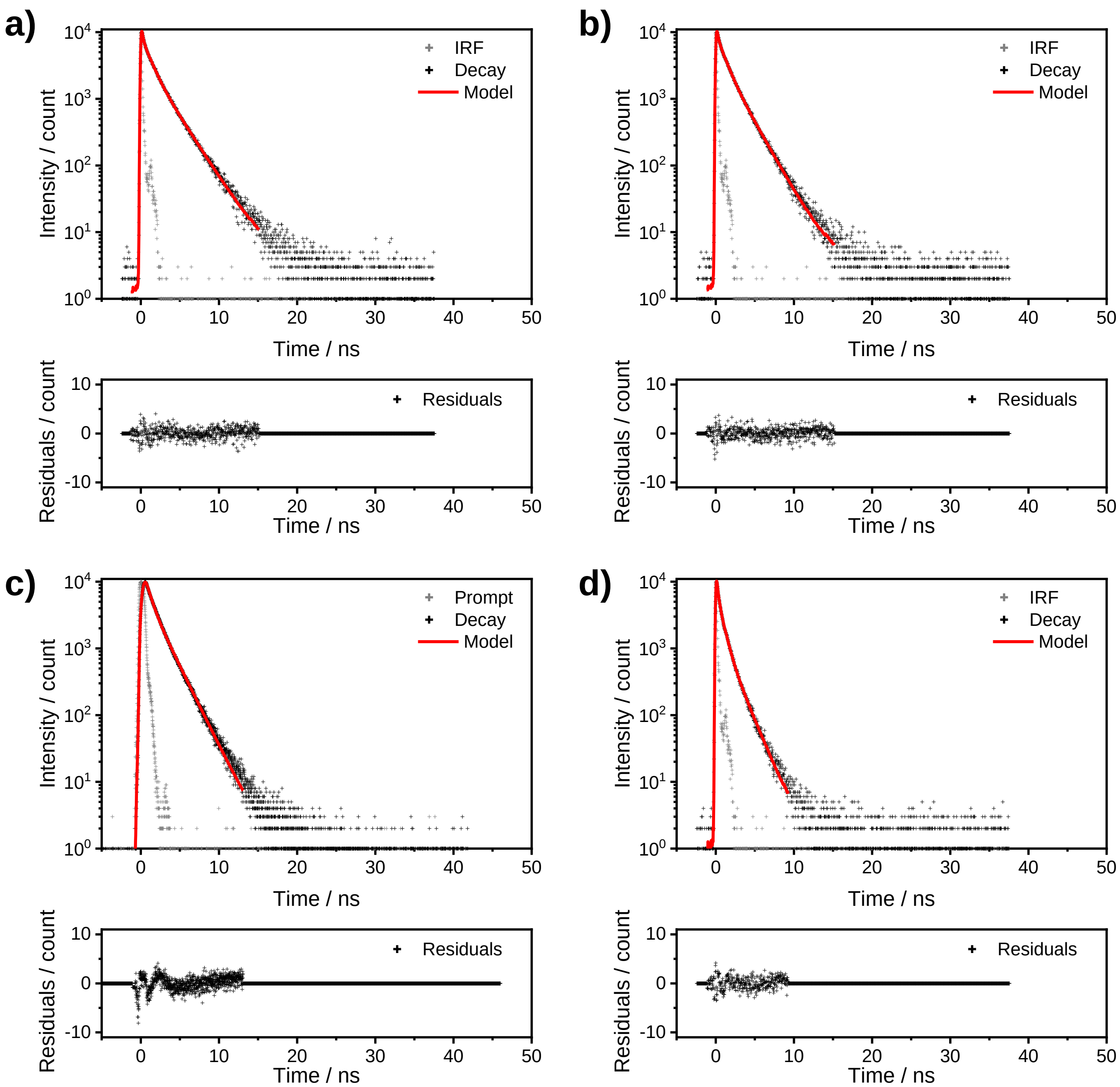

Figure S5. Photoluminescence decay profiles of **o-FL** in a) CCl_4, b) toluene, c) $CHCl_3$, and d) CH_2Cl_2 solution state.

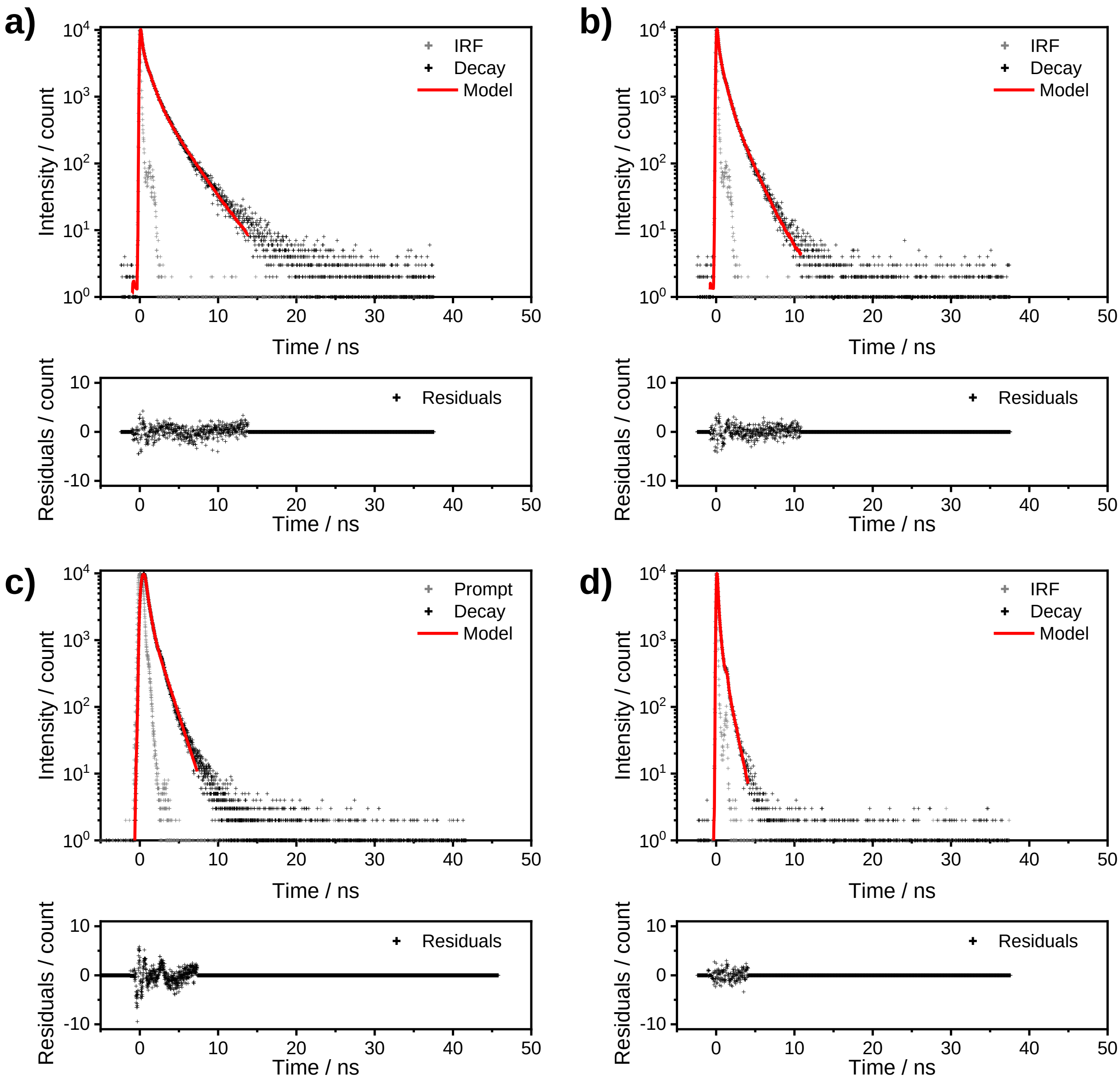

Figure S6. Photoluminescence decay profiles of **o-BT** in a) CCl_4, b) toluene, c) $CHCl_3$, and d) CH_2Cl_2 solution state.

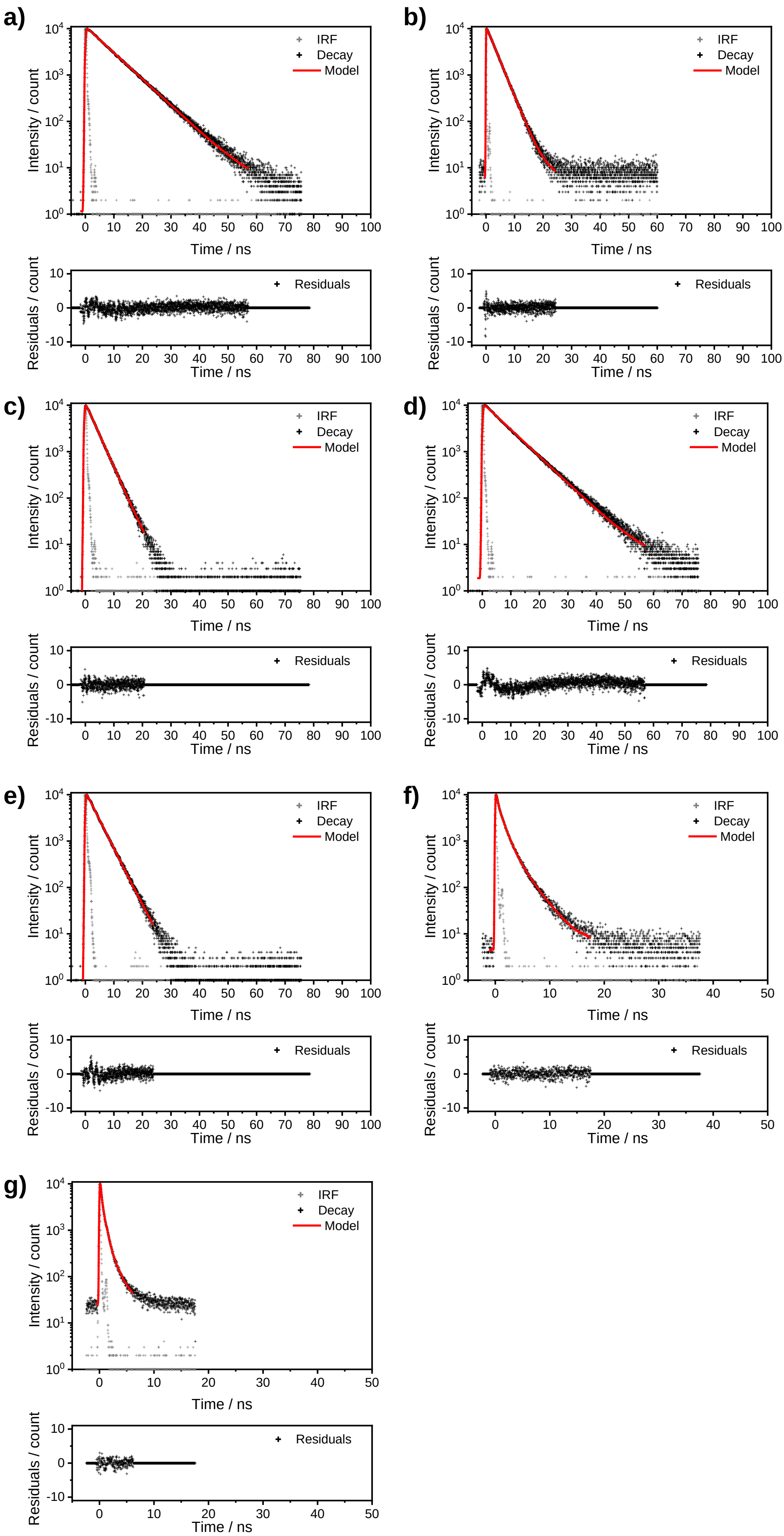

Figure S7. Photoluminescence decay profiles of a) **H-H**, b) **Br-H**, c) **Br-Br**, d) **T-H**, e) **T-T**, f) **o-FL** and g) **o-BT** in solid.

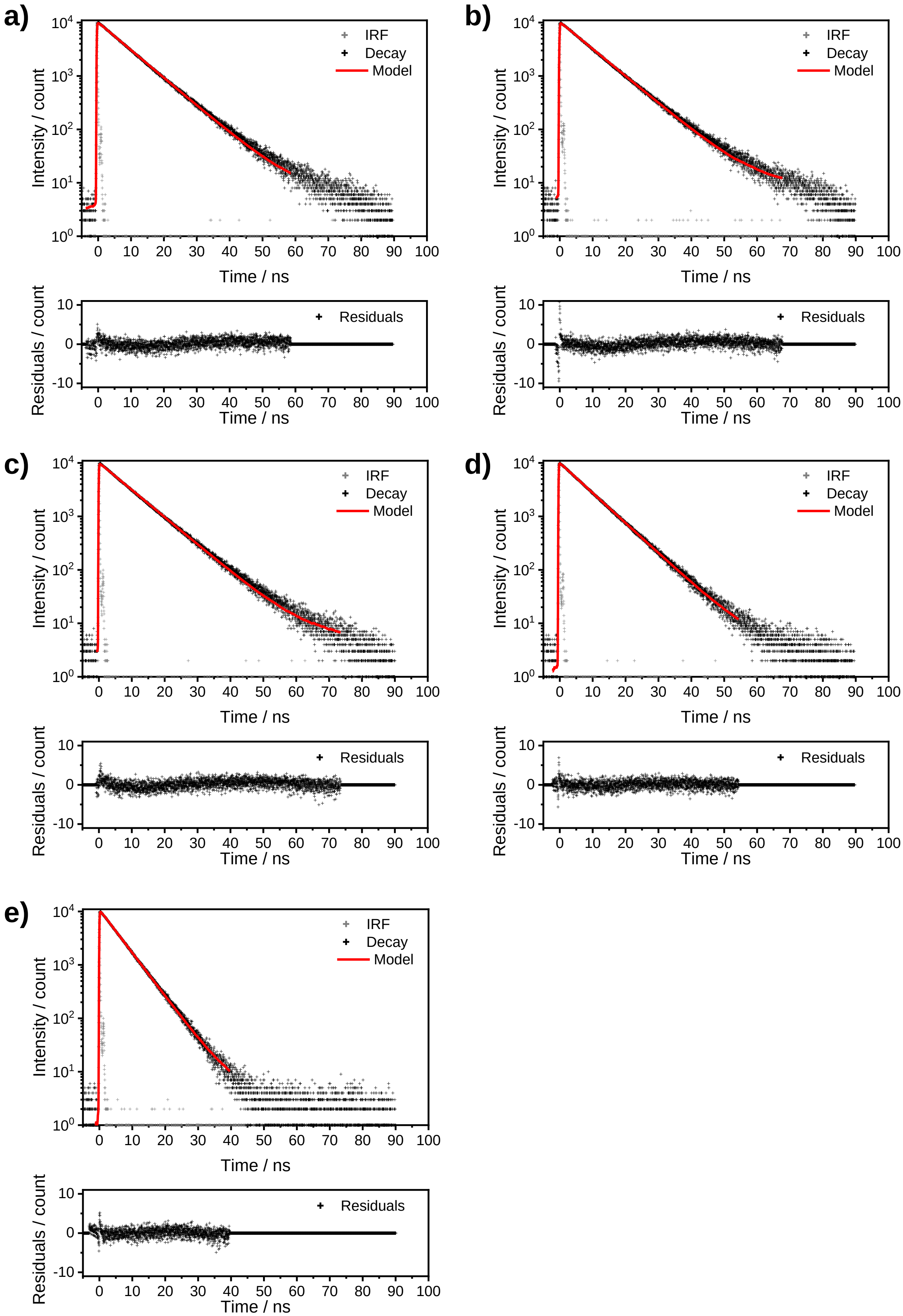

Figure S8. Photoluminescence decay profiles of **H-H** at a) 80 K, b) 170 K, c) 260 K, d) 350 K, and e) 410 K in the crystalline state.

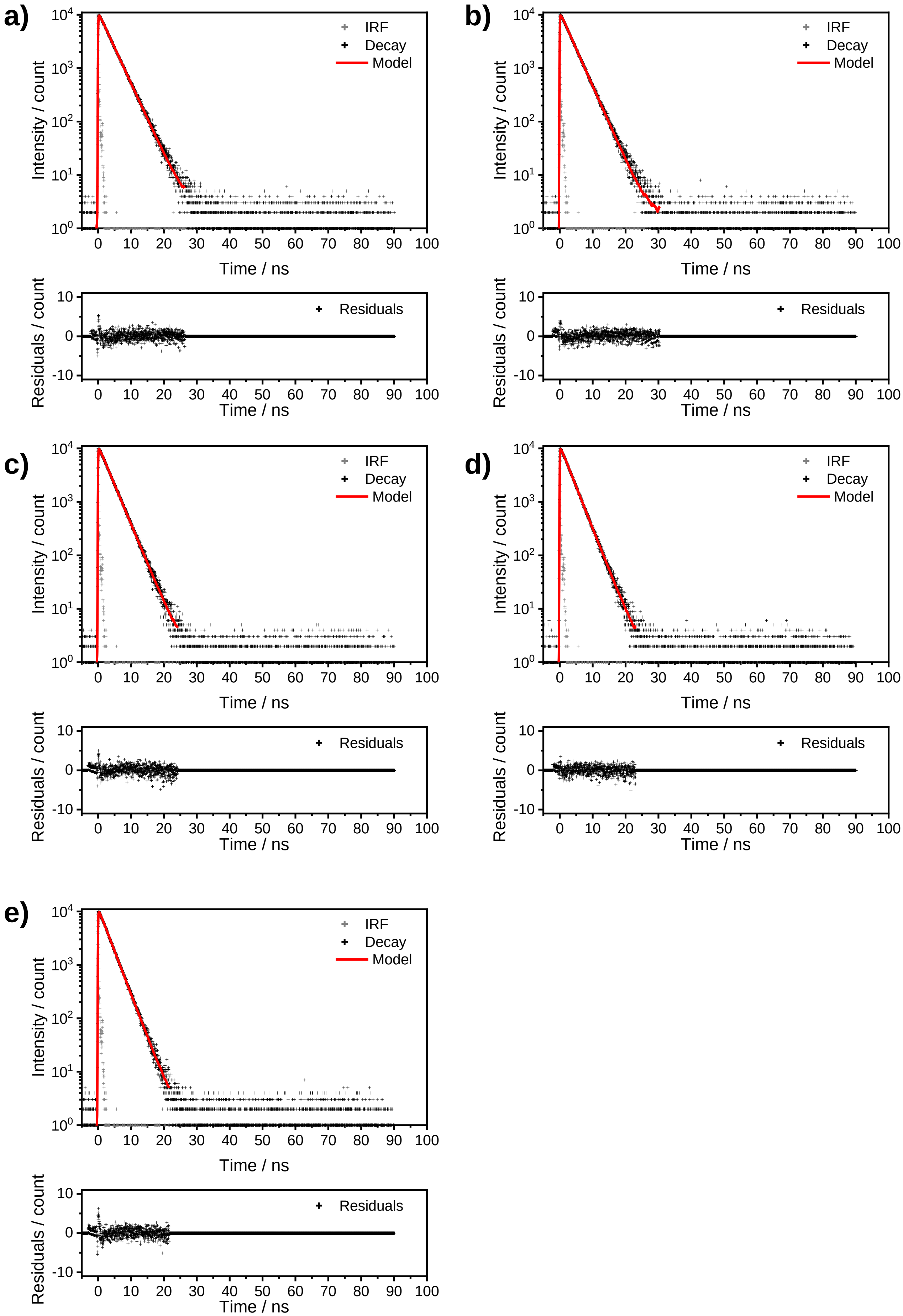

Figure S9. Photoluminescence decay profiles of **Br-H** at a) 80 K, b) 170 K, c) 260 K, d) 350 K, and e) 410 K in the crystalline state.

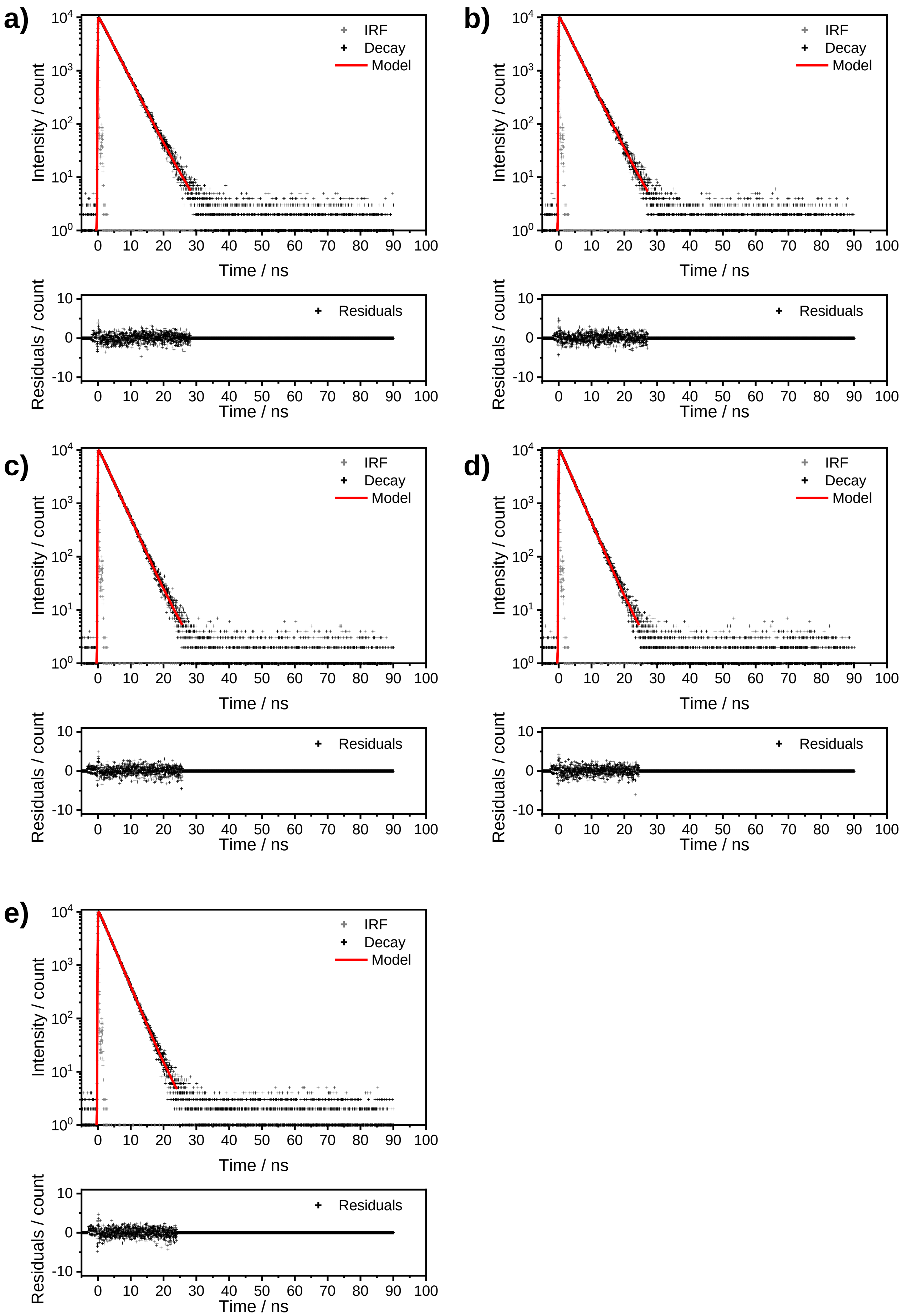

Figure S10. Photoluminescence decay profiles of **Br-Br** at a) 80 K, b) 170 K, c) 260 K, d) 350 K, and e) 410 K in the crystalline state.

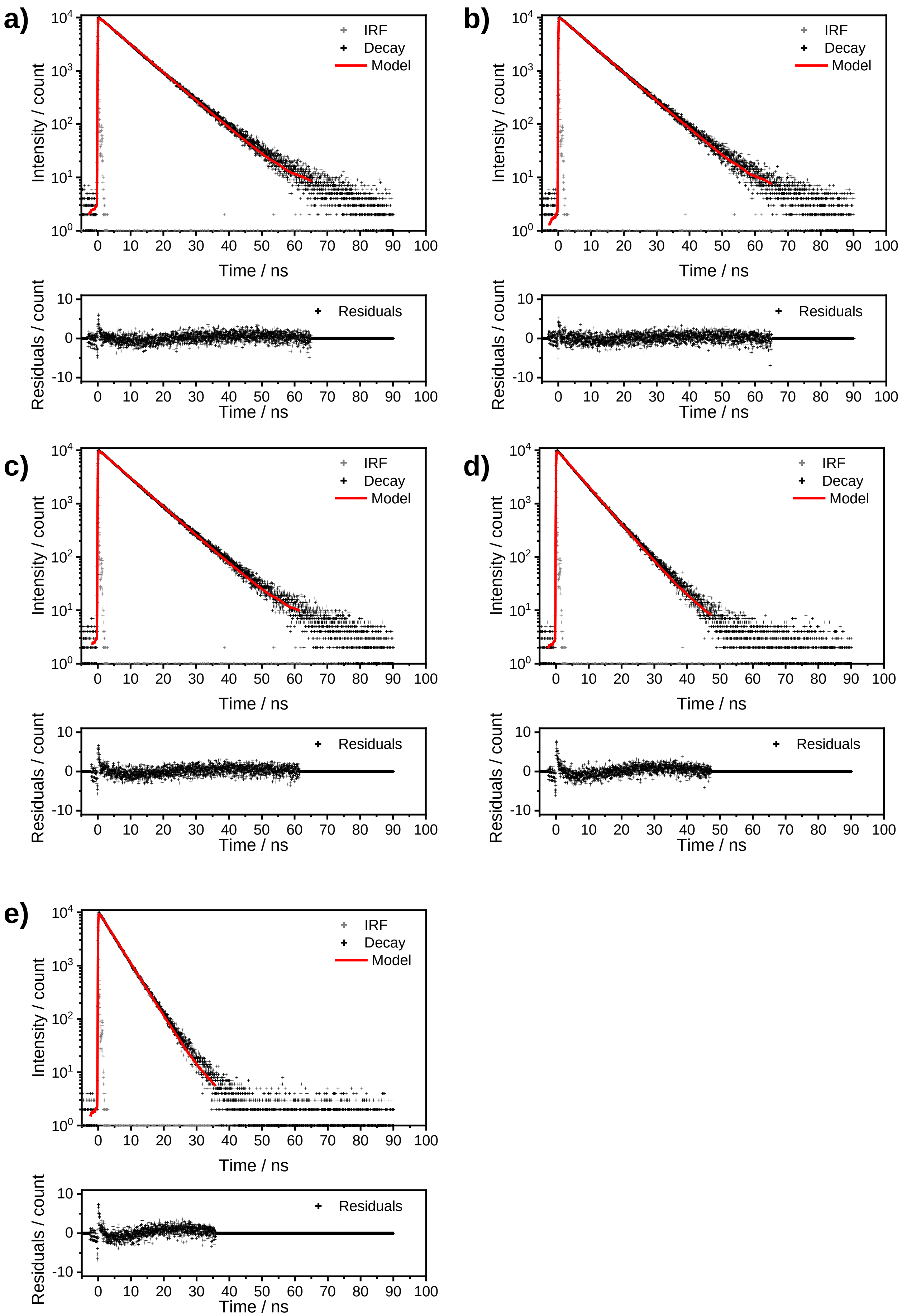

Figure S11. Photoluminescence decay profiles of **T-H** at a) 80 K, b) 170 K, c) 260 K, d) 350 K, and e) 410 K in the crystalline state.

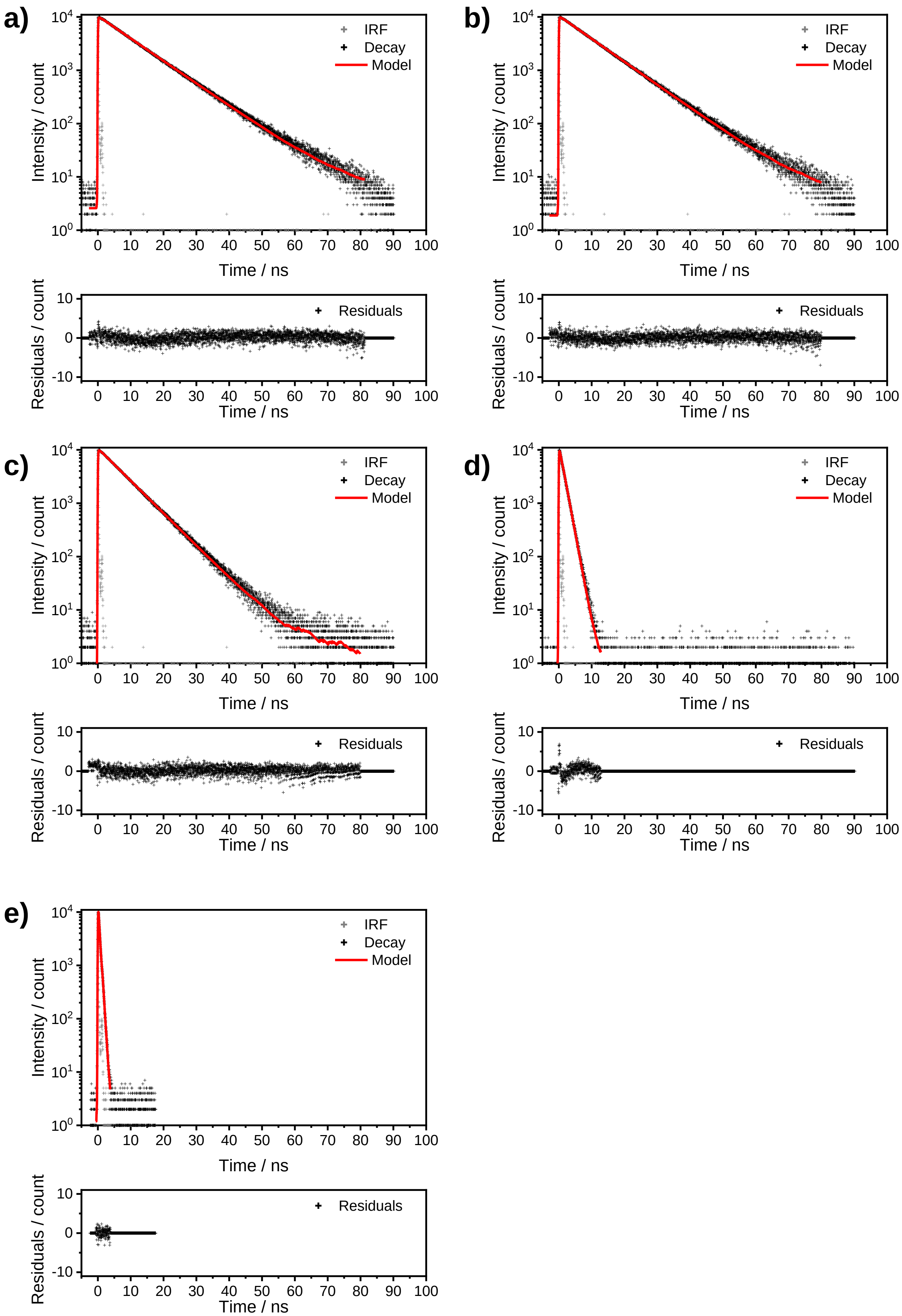

Figure S12. Photoluminescence decay profiles of **T-T** at a) 80 K, b) 170 K, c) 260 K, d) 350 K and e) 410 K in the crystalline state.

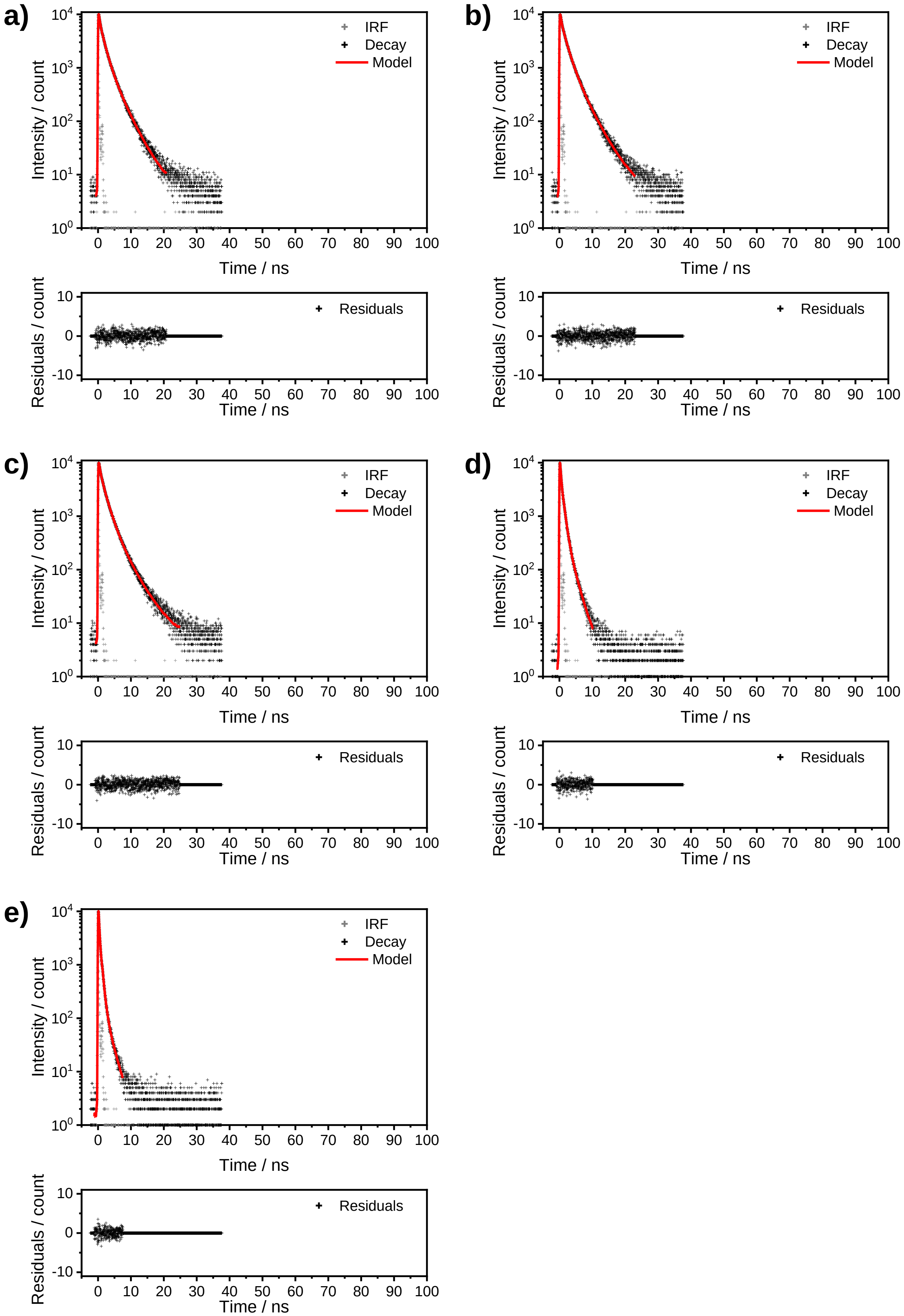

Figure S13. Photoluminescence decay profiles of **o-FL** at a) 80 K, b) 170 K, c) 260 K, d) 350 K, and e) 410 K in film.

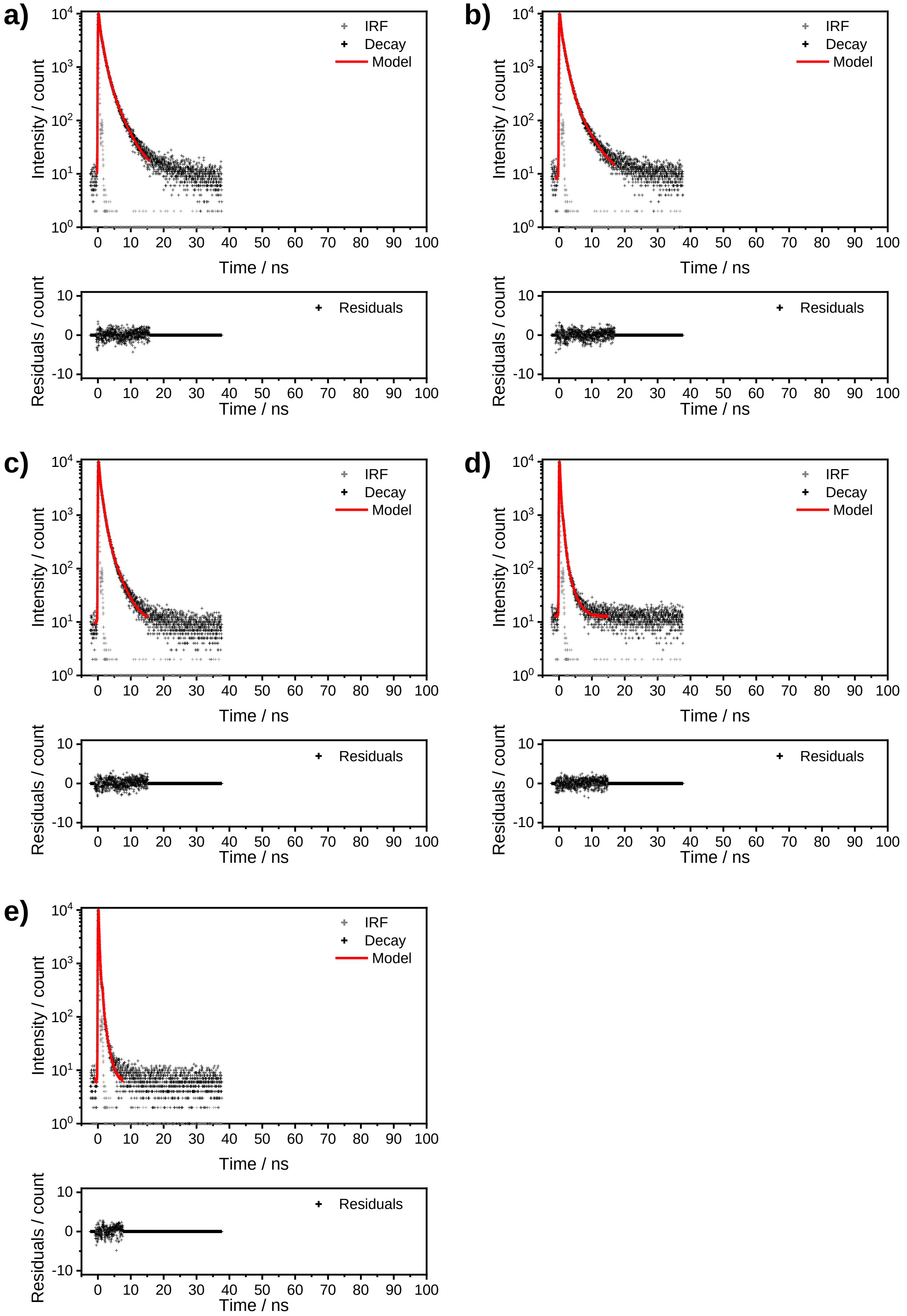

Figure S14. Photoluminescence decay profiles of **o-BT** at a) 80 K, b) 170 K, c) 260 K, d) 350 K, and e) 410 K in film.

Table S6. Summary of photophysical properties

Name	State[a, b]	λ_{abs} / nm	λ_{PL} / nm[c]	Stokes shift / 10^3 cm^{-1}[d]	Φ_{PL}[c,e]	τ_{PL} / ns	τ_{PL}^{ave} / ns[f]	χ^2
H-H	in $CHCl_3$	408, 272	643	8.96	0.01	n.d.	n.d.	n.d.
	in THF	410, 270	645	8.89	0.01	n.d.	n.d.	n.d.
	Crystal	–	592	–	0.70	7.7 (100%)	7.7	1.32
Br-H	in Hexane	414, 274	593	7.29	< 0.01	n.d.	n.d.	n.d.
	in Toluene	420	630	7.94	< 0.01	n.d.	n.d.	n.d.
	in $CHCl_3$	419, 277	637	8.17	< 0.01	n.d.	n.d.	n.d.
	in MeCN	429, 275	674	8.47	< 0.01	n.d.	n.d.	n.d.
	Crystal	–	619	–	0.26	2.9 (100%)	2.9	1.07
Br-Br	in Hexane	417, 275	609	7.56	< 0.01	n.d.	n.d.	n.d.
	in Toluene	423	639	7.99	< 0.01	n.d.	n.d.	n.d.
	in $CHCl_3$	422, 278	643	8.15	< 0.01	n.d.	n.d.	n.d.
	in MeCN	430, 275	678	8.51	< 0.01	n.d.	n.d.	n.d.
	Crystal	–	625	–	0.26	3.2 (100%)	3.2	1.22
T-H	in Hexane	415, 274	610	7.70	< 0.01	n.d.	n.d.	n.d.
	in Toluene	432	648	7.72	< 0.01	n.d.	n.d.	n.d.
	in $CHCl_3$	432, 278	676	8.36	< 0.01	n.d.	n.d.	n.d.
	in MeCN	430, 274	694	8.85	< 0.01	n.d.	n.d.	n.d.
	Crystal	–	637	–	0.66	7.5 (100%)	7.5	1.87
T-T	in Hexane	431, 275	634	7.43	< 0.01	n.d.	n.d.	n.d.
	in Toluene	433	663	8.01	< 0.01	n.d.	n.d.	n.d.
	in $CHCl_3$	434, 278	677	8.27	< 0.01	n.d.	n.d.	n.d.
	in MeCN	431, 275	701	8.94	< 0.01	n.d.	n.d.	n.d.
	Crystal	–	671	–	0.22	3.5 (100%)	3.5	1.61
o-FL	in CCl_4	472, 353, 285	676	6.39	0.06	n.d.	n.d.	n.d.
	in Toluene	471, 353, 283	692	6.78	0.06	n.d.	n.d.	n.d.
	in $CHCl_3$	478, 354, 285	709	6.82	0.05	n.d.	n.d.	n.d.
	in CH_2Cl_2	481, 354, 284	724	6.98	0.02	n.d.	n.d.	n.d.
	Film	491, 353, 289	700	6.08	0.06	1.0 (56%), 0.23 (15%), 2.8 (29%)	1.4	1.18
o-BT	in CCl_4	475,341, 284	703	6.83	0.02	n.d.	n.d.	n.d.
	in Toluene	476, 341, 282	718	7.08	0.02	n.d.	n.d.	n.d.
	in $CHCl_3$	479, 341, 284	743	7.42	0.01	n.d.	n.d.	n.d.
	in CH_2Cl_2	481, 341, 283	767	7.75	< 0.01	n.d.	n.d.	n.d.
	Film	494, 341, 289	729	6.53	0.02	n.d.	n.d.	n.d.

[a] Solutions were prepared for 1.0×10^{-5} M concentration (per repeating units for oligomers). [b] Films were prepared by spin-coating method. [c] Excited at longest λ_{abs} wavelength (longest λ_{abs} wavelength in $CHCl_3$ were used for solid-state samples). [d] Stokes shift = $1/\lambda_{abs} - 1/\lambda_{PL}$, where the longest wavelength values were used in λ_{abs}. [e] Absolute quantum yield determined by integrating sphere method. [f] $\tau_{PL}^{ave} = \Sigma_i\tau_i f_i$, where f_i : relative amplitude of ith component (%), τ_i: luminescent decay lifetime of ith component (s). –: not measured. n.d.: cannot be determined reliably due to weak luminescence.

Suggestion from luminescent properties of oligomers

In contrast to the small compounds, oligomers (**o-FL** and **o-BT**) show weak emission enhancement upon aggregation. We interpret this result with two effects.

One is that the molecular motion leading to non-radiative decay might be partially suppressed by oligomerization. The molecular motion of the diaryl-*o*-carborane units can be restricted by the neighboring sterically hindered comonomer units.

The other reason is that both oligomers showed luminescence in the NIR region, and therefore the two polymers potentially have more non-radiative decay channels than other small molecules (energy gap law), which leads to the suppression of luminescence.

o-BT showed slight but consistent luminescent efficiency in both solution and solid states. This is probably because more red-shifted PL of **o-BT** than **o-FL** might result in dominant effect of the energy gap law in PL properties.

In contrast, **o-FL** showed almost identical efficiency in the solid state to that in the solution state and the solution-state efficiency was quite higher than those of small molecules. From these results, we suggest here that the compound should be affected by the smaller contribution of the energy gap law and strong luminescence was realized by the suppression of quenching by sterically restraint *o*-carborane units in the oligomer chain.

Table S7. Temperature dependency on photophysical properties of crystalline samples

Compounds	T / K	λ_{PL} / nm[a]	Φ^{rel} [b]	τ_{PL} / ns	τ_{PL}^{ave} / ns[c]	χ^2	k_r / 10^8 s^{-1}[d]	k_{nr} / 10^8 s^{-1}[e]
H-H	80	576	1.09	8.6 (100%)	8.6	1.68	1.2	0.0012
	110	576	1.07	–	–	–	–	–
	140	580	1.03	–	–	–	–	–
	170	583	0.99	8.4 (100%)	8.5	1.91	1.2	0.0078
	200	583	0.94	–	–	–	–	–
	230	587	0.87	–	–	–	–	–
	260	585	0.79	8.5 (100%)	8.5	1.36	0.93	0.24
	290	592	0.70	–	–	–	–	–
	320	593	0.59	–	–	–	–	–
	350	596	0.47	7.7 (100%)	7.7	1.17	0.61	0.68
	380	600	0.36	–	–	–	–	–
	410	607	0.26	5.4 (100%)	5.4	1.26	0.48	1.4
Br-H	80	609	0.29	3.2 (100%)	3.2	1.32	0.91	2.2
	110	609	0.30	–	–	–	–	–
	140	611	0.30	–	–	–	–	–
	170	612	0.30	3.1 (100%)	3.1	1.24	0.96	2.3
	200	613	0.30	–	–	–	–	–
	230	616	0.29	–	–	–	–	–
	260	618	0.27	2.9 (100%)	2.9	1.32	0.94	2.5
	290	618	0.26	–	–	–	–	–
	320	620	0.25	–	–	–	–	–
	350	624	0.23	2.8 (100%)	2.8	1.11	0.83	2.7
	380	626	0.22	–	–	–	–	–
	410	628	0.20	2.7 (100%)	2.7	1.51	0.73	3.0
Br-Br	80	617	0.30	3.6 (100%)	3.6	1.12	0.82	2.0
	110	619	0.30	–	–	–	–	–
	140	618	0.29	–	–	–	–	–
	170	620	0.29	3.4 (100%)	3.4	1.15	0.84	2.1
	200	621	0.28	–	–	–	–	–
	230	622	0.28	–	–	–	–	–
	260	623	0.27	3.2 (100%)	3.2	1.13	0.83	2.3
	290	623	0.26	–	–	–	–	–
	320	628	0.25	–	–	–	–	–
	350	634	0.24	3.1 (100%)	3.1	1.17	0.76	2.5
	380	633	0.22	–	–	–	–	–
	410	640	0.20	3.0 (100%)	3.0	1.20	0.68	2.7
T-H	80	623	1.03	8.2 (100%)	8.2	1.34	1.2	0.0012
	110	624	1.01	–	–	–	–	–
	140	626	0.97	–	–	–	–	–
	170	626	0.94	8.2 (100%)	8.2	1.28	1.1	0.077

	200	629	0.88	–	–	–	–	–
	230	634	0.82	–	–	–	–	–
	260	633	0.75	8.1 (100%)	8.1	1.41	0.92	0.31
	290	634	0.66	–	–	–	–	–
	320	637	0.56	–	–	–	–	–
	350	642	0.45	6.2 (100%)	6.2	1.79	0.72	0.89
	380	642	0.34	–	–	–	–	–
	410	645	0.24	4.4 (100%)	4.4	2.11	0.55	1.7
T-T	80	654	0.79	10 (100%)	10	1.24	0.79	0.21
	110	658	0.80	–	–	–	–	–
	140	659	0.82	–	–	–	–	–
	170	663	0.79	10 (100%)	10	1.13	0.79	0.21
	200	661	0.75	–	–	–	–	–
	230	668	0.66	–	–	–	–	–
	260	665	0.46	7.1 (100%)	7.1	1.16	0.65	0.75
	290	666	0.22	–	–	–	–	–
	320	668	0.11	–	–	–	–	–
	350	671	0.06	1.3 (100%)	1.3	2.13	0.44	7.3
	380	671	0.03	–	–	–	–	–
	410	693	0.02	0.44 (80%), 0.20 (20%)	0.39	1.11	0.46	25
o-FL	80	674	0.16	1.4 (52%), 0.30 (10%), 3.5 (38%)	2.1	1.12	0.77	4.0
	110	682	0.16	–	–	–	–	–
	140	679	0.12	–	–	–	–	–
	170	688	0.11	1.6 (53%), 0.40 (10%), 3.8 (37%)	2.3	1.07	0.50	3.8
	200	689	0.10	–	–	–	–	–
	230	697	0.09	–	–	–	–	–
	260	698	0.08	0.46 (13%), 1.7 (59%), 4.1 (28%)	2.2	1.04	0.35	4.2
	290	699	0.06	–	–	–	–	–
	320	699	0.04	–	–	–	–	–
	350	705	0.03	0.21 (23%), 2.1 (18%), 0.74 (58%)	0.86	1.10	0.38	11
	410	703	0.01	0.15 (38%)[f], 0.55 (51%), 1.8 (10%)	0.52	1.05	0.27	19
o-BT	80	703	0.04	1.0 (56%), 3.1 (28%), 0.14 (16%)[f]	1.4	1.32	0.28	6.7
	110	704	0.04	–	–	–	–	–
	140	708	0.04	–	–	–	–	–
	170	712	0.03	1.1 (60%), 0.19	1.4	1.26	0.24	6.9

			(20%)[f], 3.6 (20%)				
200	722	0.03	–	–	–	–	–
230	728	0.03	–	–	–	–	–
260	726	0.03	0.83 (57%), 0.15 (22%)[f], 2.6 (21%)	1.0	1.26	0.25	9.4
290	735	0.02	–	–	–	–	–
320	729	0.02	–	–	–	–	–
350	737	0.01	0.52 (42%), 0.10 (48%)[f], 1.8 (10%)	0.44	1.04	0.27	23
410	731	0.01	0.32 (26%), 0.06 (65%)[f], 1.1 (9%)	0.22	1.52	0.29	46

[a] Excited at longest λ_{abs} wavelength in $CHCl_3$. [b] Relative quantum yield calculated with integration of luminescent spectra (*vide supra*). [c] $\tau_{PL}^{ave} = \Sigma_i \tau_i f_i$, f_i : relative amplitude of ith component (%), τ_i: luminescent decay lifetime of ith component (s). [d] Radiative decay constant calculated by following equation: $k_r = \Phi^{rel}{}_{PL}/\tau_{PL}^{ave}$. [e] Non-radiative decay constant calculated by following equation: $k_{nr} = (1-\Phi^{rel}{}_{PL})/\tau_{PL}^{ave}$ [f] Reference value because luminescent lifetime of this component is below limit of detection of our apparatus (0.2 ns). –: not measured.

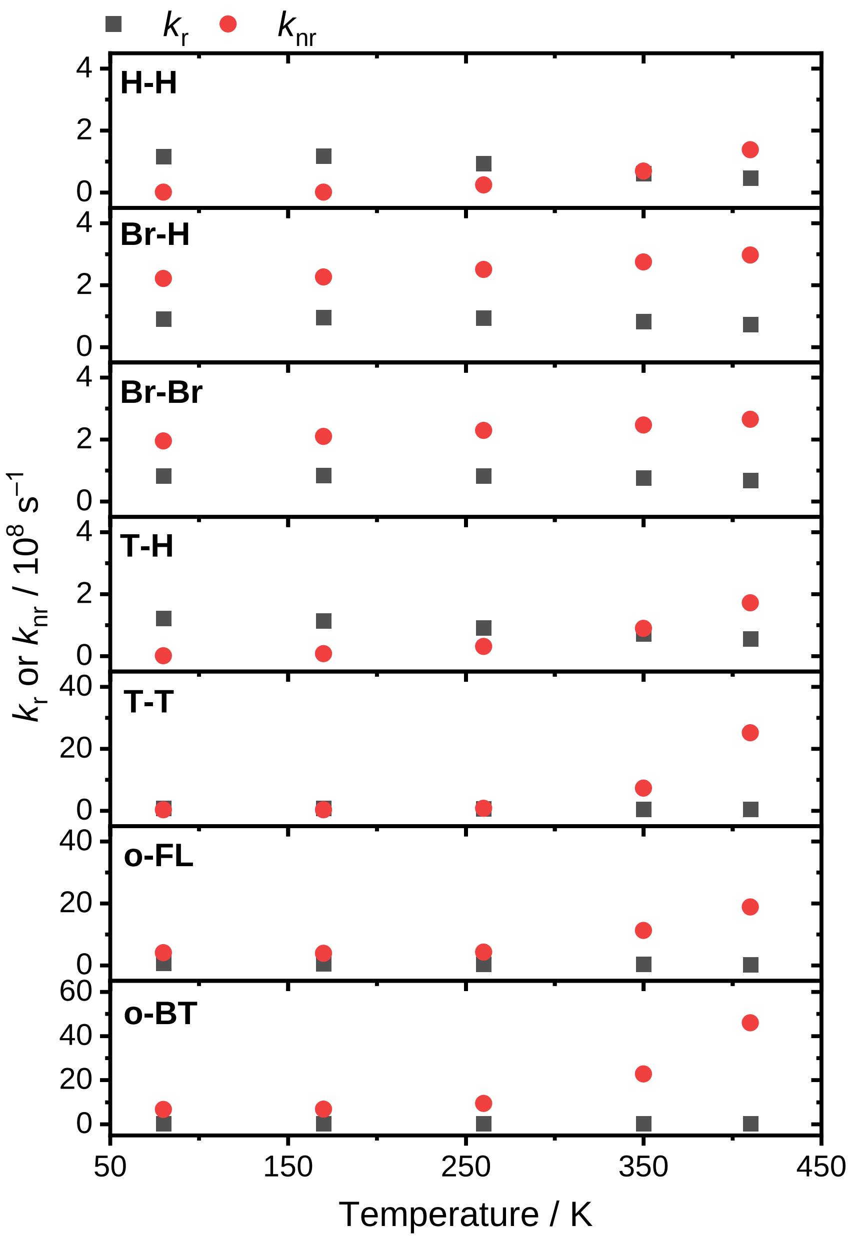

Figure S15. Temperature dependencies of radiative rate constant (k_r) and non-radiative rate constant (k_{nr}) in the solid state.

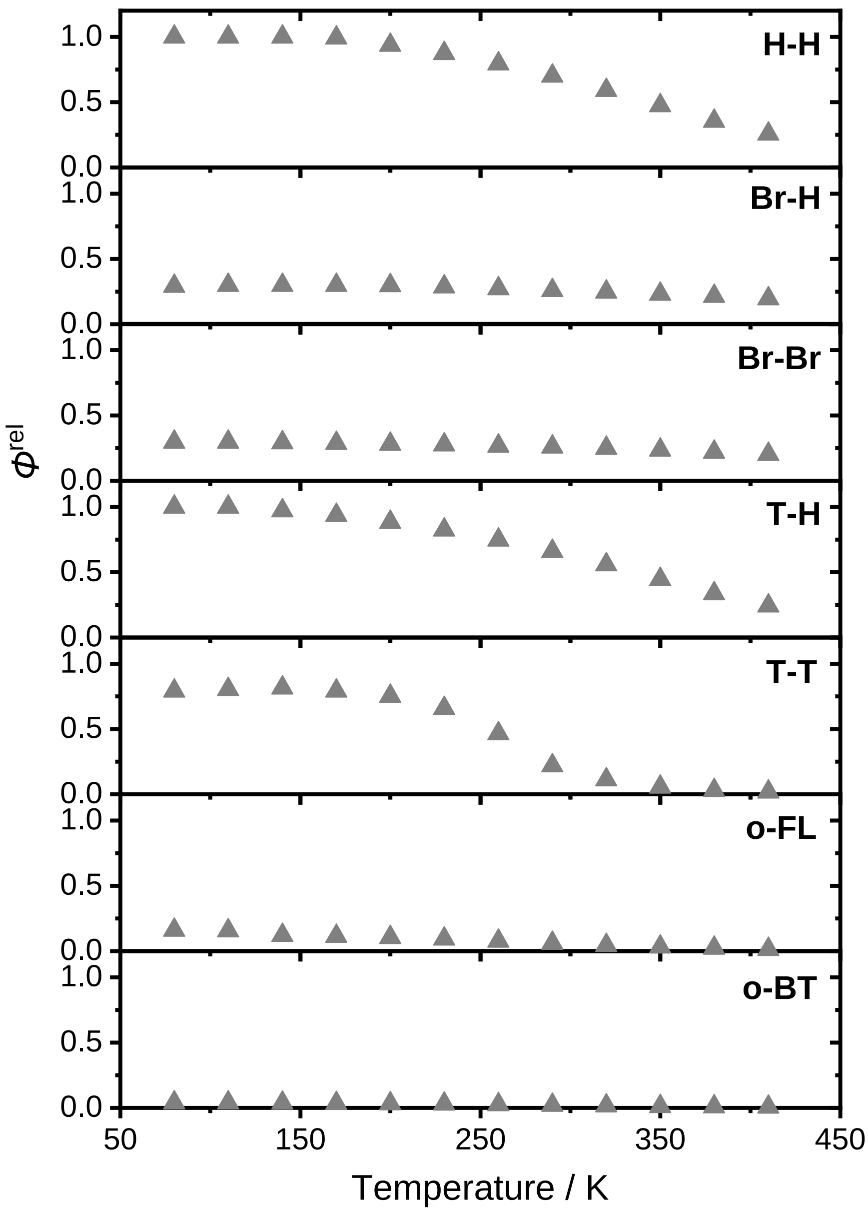

Figure S16. Temperature dependencies of relative PL quantum yield in the solid state.

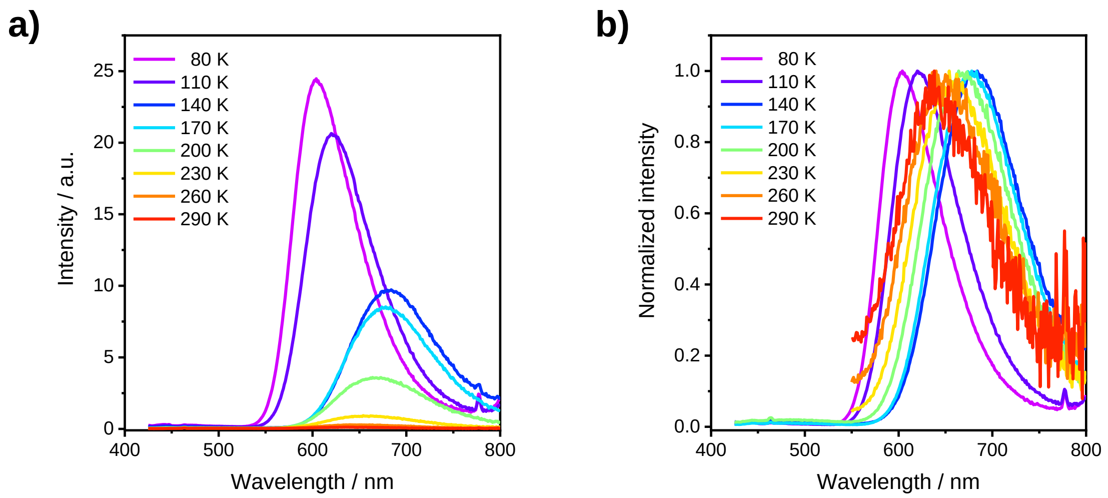

Figure S17. Solution-state temperature-dependent luminescent spectra of **H-H** in 2-MeTHF solution (1.0×10^{-5} M). While the solution was in the glass state below 140 K (glass transition temperature of 2-MeTHF: 137 K), the spectra showed bathochromic shift as observed in the solid state. This suggests that the excited-state relaxation processes should be accelerated by temperature rise. Over 140 K at which solution is in the fluid state, the spectra showed hypsochromic shift. This shift should be a consequence of the decrease in the dielectric constant of the solvent, resulting in lower polarity in higher temperature regions. The temperature-dependent property of 2-MeTHF solvent was according to the literature.[11]

Cyclic Voltammetry

Cyclic voltammetry (CV) was carried out on a BASALS-Electrochemical-Analyzer Model 600D with a glassy carbon working electrode, a Pt counter electrode, an Ag/AgCl reference electrode, and the ferrocene/ferrocenium (Fc/Fc^+) external reference at a scan rate of 0.1 V s^{-1}. Cyclic voltammograms were measured in CH_2Cl_2 (1.0×10^{-3} M, per repeating units for the oligomers) containing NBu_4PF_6 (0.10 M). Energy levels of frontier orbitals were calculated by the following equation: E_{LUMO} (eV) = −4.8 − E_{onset}^{red} (V) and E_{HOMO} (eV) = −4.8 − E_{onset}^{ox} (V), where E_x is energy of x orbital and $E_{onset}^{red/ox}$ is onset value of the first reduction or oxidation waves.

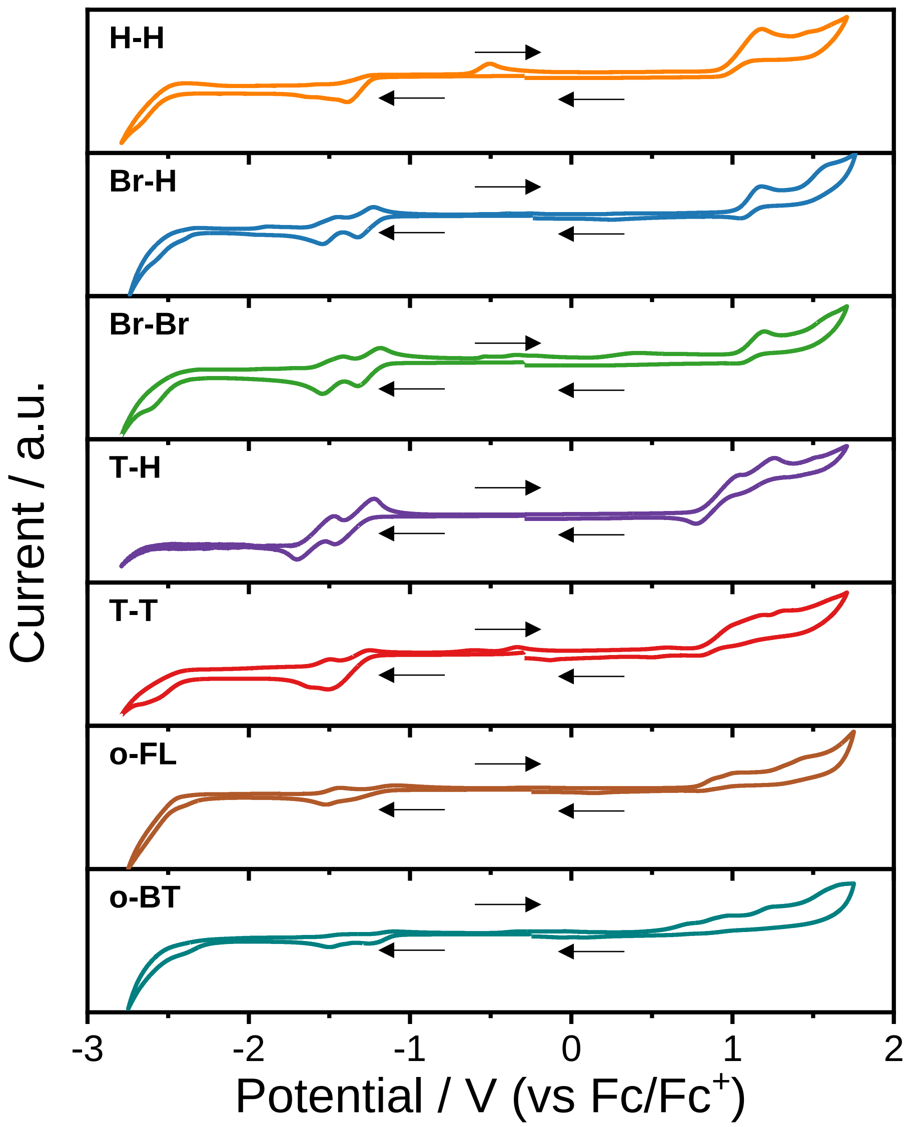

Figure S18. Cyclic voltammograms of *C*,*C*′-diaryl-*o*-carborane derivatives.

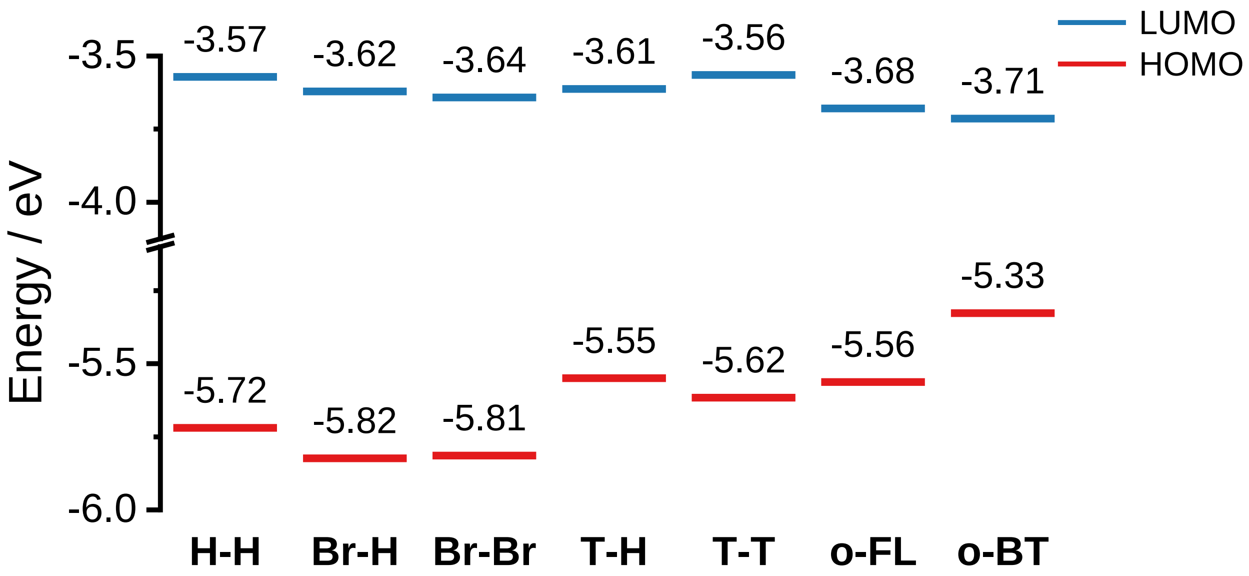

Figure S19. Energy levels of frontier orbitals of *C*,*C*′-diaryl-*o*-carborane derivatives.

Thermal analysis

Thermogravimetric analyses (TGA) were performed by a HITACHI STA 7200RV instrument with the aluminum pan and the heating rate of 10 °C/min. up to 500 °C under nitrogen flow (200 mL/min). Differential scanning calorimetry (DSC) measurements were carried out on a HITACHI DSC 7020 instrument with the aluminum pan and the heating rate of 10 °C/min under nitrogen flow (50 mL/min).TGA measurements were conducted up to 500 K. DSC measurements were conducted under 20 K lower than the temperature where decomposition started.

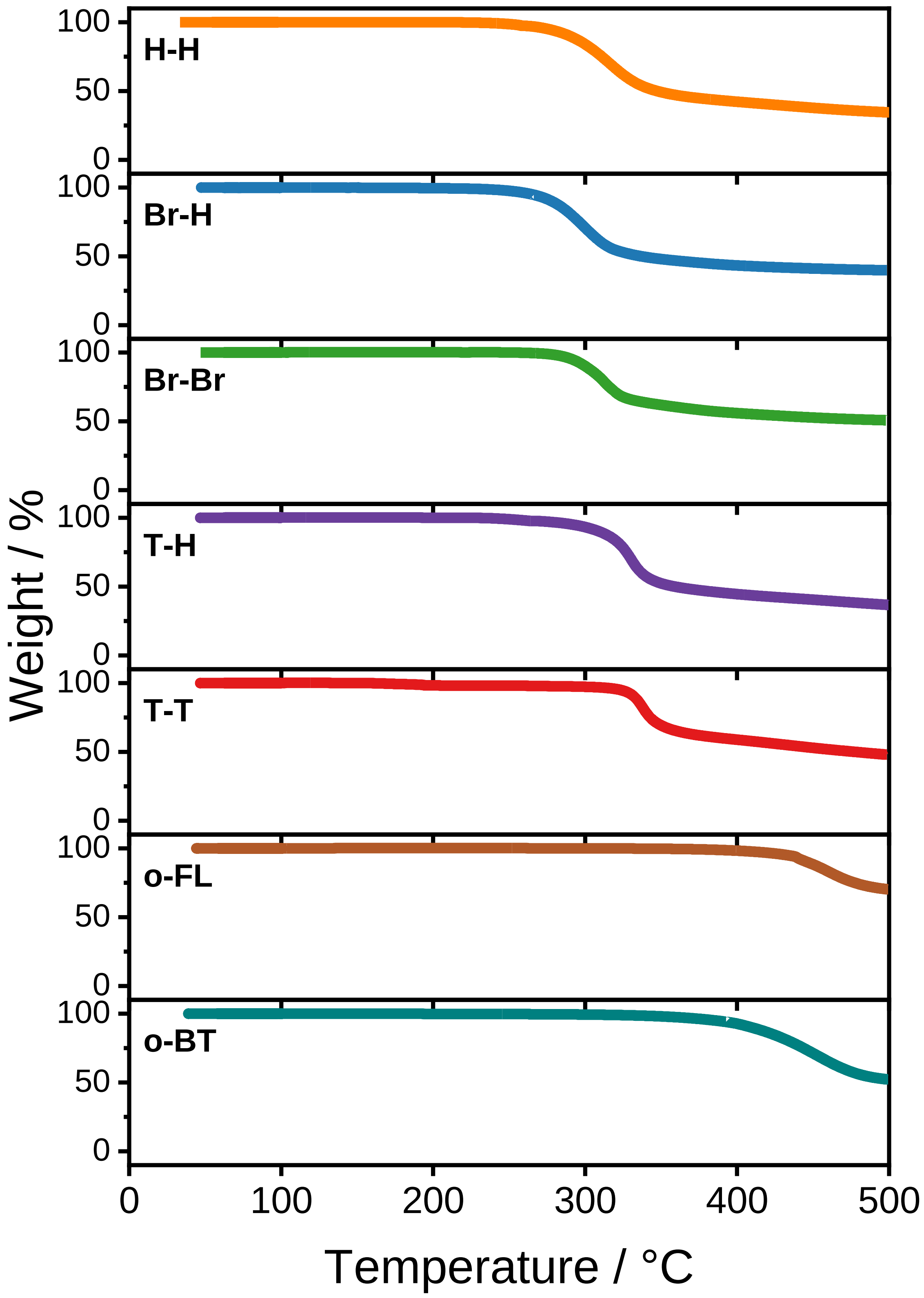

Figure S20. TGA thermograms of *C*,*C*′-diaryl-*o*-carborane derivatives.

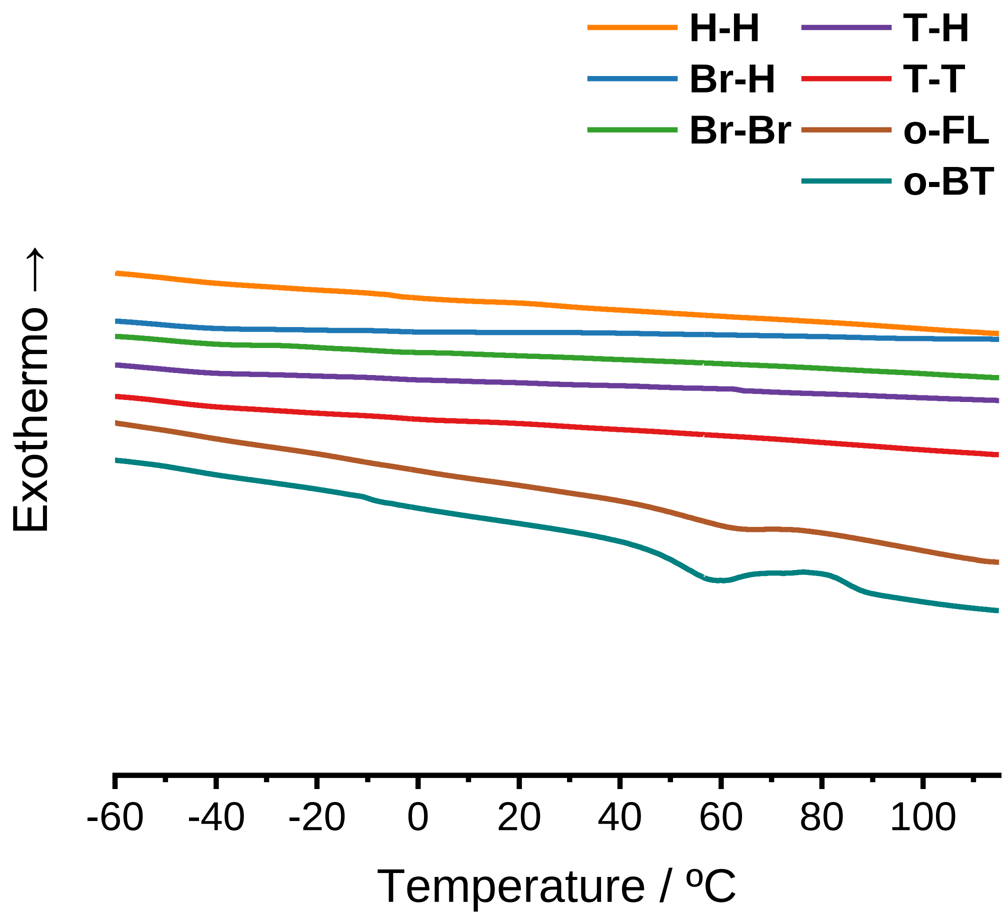

Figure S21. DSC thermograms *C*,*C*′-diaryl-*o*-carborane derivatives.

Theoretical Calculation

General

The Gaussian 16 program Revision C.01 package[12] was used for density functional theory (DFT) and time-dependent DFT (TD-DFT) calculations. Several pairs of functional and basis sets were tested on **H-H**, **Br-H**, and **Br-Br** to find appropriate one, which reproduce single-crystal X-ray structure at best. CAM-B3LYP functional with 6-31+G(d,p) (for H, B, and C) and LanL2DZ (for Br) basis sets were selected for further calculation. Effective core potential was calculated with LanL2DZ level. Geometry optimization was conducted for each compound in ground singlet (S_0) and excited singlet (S_1) states. Optimized structures at S_0 states were obtained for all compounds and confirmed as local minimum on each potential energy surface using frequency calculations. The polarized continuum model (PCM)[13–15] of $CHCl_3$ solvated state was selected to simulate the effect of solvent molecules. Kohn-Sham orbitals of HOMOs and LUMOs were generated from the optimized structure using GaussView 6 (isovalue: 0.02). The optimized geometries and calculated electronic transitions are tabulated in Tables S9–S38.

QM/MM calculation

The molecular structures in crystalline state were optimized by the quantum mechanics / molecular mechanics (QM/MM) method. The molecular coordinates for QM/MM analyses were extracted from single-crystal structures. The calculation models were constructed by adding molecules until fully covering central one molecule with surrounding molecules in ball and stick drawing mode. The central one molecule in the high layer was calculated at CAM-B3LYP/6-31+G(d,p) (for H, B, and C) and LanL2DZ (for Br) level and the surround molecules in the low layer were dealt in the universal force field. The QM/MM model was constructed from the cut-out cluster consisting of 24–72 molecules from crystal packing structure (Figure S23).

Scan calculation

Scan The S_0 and S_1 potential energy curves (PESs) were calculated through scan method with variance of C_{cage}–C_{cage} bond between 1.8–2.7 Å (0.1 Å increments). Opt=modredundant keyword was used for restricted structural optimization. It should be noted that S_1 state optimization at C_{cage}–C_{cage} bond length of 1.8 Å for **T-T** was not converged.

Geometry of T-H

The geometry of **T-H** used for calculations varied in ground and excited states. **T-H** had two geometries with rotation of the thiophene ring (Geometry **A** and **B**, Figure S22). Geometry **A** has the conformation in which the sulfur atom of the thiophene ring faces the phenyl group side, which is same conformation as observed in SCXRD analysis. Geometry **B** has the conformation in which the sulfur atom of the thiophene ring faces the opposite side to the phenyl group. Geometrical optimization to S_0 and S_1 minimum states were performed with geometry **B** because S_0 optimization was not converged in geometry **A**. Scan calculation for S_0 state was not converged with geometry **A**. Then the geometry **B** was used instead. However S_1 state scan calculation was not converged with geometry B, so we performed it with geometry **A**.

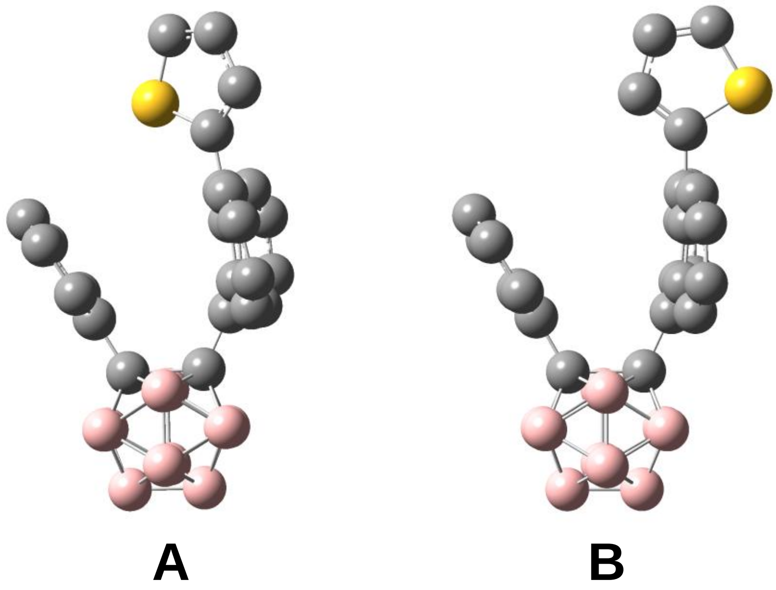

Figure S22. Geometries of **T-H** used for calculations. (Color list: boron, pink; carbon, grey; sulfur, yellow) Hydrogen atoms were omitted.

Table S8. Screening of various calculation level on S_0 state optimized geometry

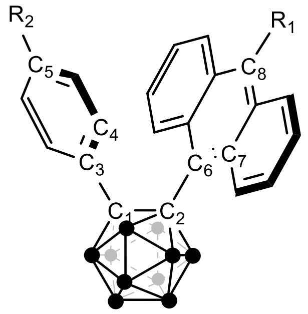

H-H ($R_1 = R_2 = H$)
Br-H (R_1 = Br, R_2 = H)
T-H (R_1 = 2-thienyl, R_2 = H)

Compound	Calculation level[a]	d(C1–C2) / Å	d(C3–C6) / Å	d(C5–C8) / Å	φ(C2–C1–C3–C4) / °	φ(C1–C2–C6–C7) / °
H-H	Crystal data[b]	1.830(5)	3.077(5)	4.318(6)	−95.2(4)	83.6(4)
	B3LYP	2.009	3.403	5.405	−91.526	87.586
	B3LYP-D3	1.879	3.166	4.599	−73.934	85.908
	B3PW91-D3	1.803	3.066	4.327	−71.813	85.877
	CAM-B3LYP	1.791	3.194	5.109	−88.423	87.280
Br-H	Crystal data[b]	1.821(3)	3.192(3)	5.109(4)	−63.0(3)	89.7(3)
	B3LYP	1.932	3.233	4.550	−90.089	85.900
	B3LYP-D3	1.857	3.082	3.976	−76.830	85.209
	B3PW91-D3	1.794	2.999	3.759	−101.10	81.390
	CAM-B3LYP	1.777	3.093	4.372	−80.616	86.106
	CAM-B3LYP LanL2DZ for Br	1.778	3.148	4.818	−98.232	86.485
T-H	Crystal data[b]	1.830(3)	3.153(3)	4.756(3)	−111.3(2)	94.2(2)
	B3LYP [c]	1.988	3.375	5.299	−91.563	87.441
	B3LYP-D3 [c]	1.865	3.134	4.399	−73.664	85.837
	B3PW91-D3 [c]	1.796	3.052	4.249	−106.007	83.733
	CAM-B3LYP [d]	1.786	3.179	5.010	−91.472	86.978

[s] 6-31G+(d,p) basis set was used for carbon, hydrogen and boron atoms. Solvent effect of chloroform was considered with polarized continuum model. [b] Structural parameters of experimentally determined crystal structures measured with *Mercury 2022.3.0* software. [c] Geometry **A** was used for structural optimization (see Figure S22). [d] Geometry **B** was used for structural optimization because S_0 optimization was not converged in geometry **A** (see Figure S22).

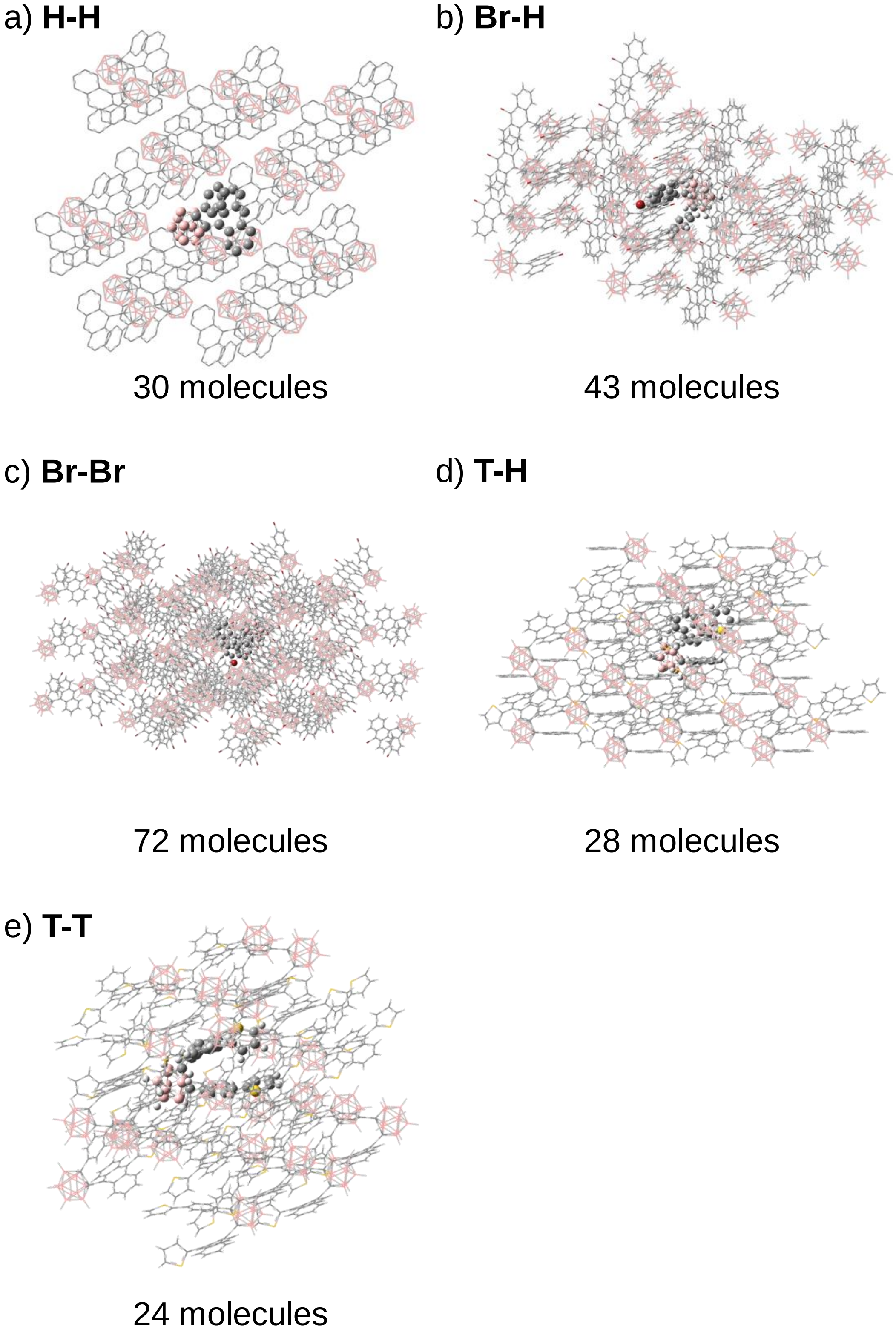

Figure S23. Setup of QM/MM model for a) **H-H**, b) **Br-H**, c) **Br-Br**, d) **T-H**, and e) **T-T**.

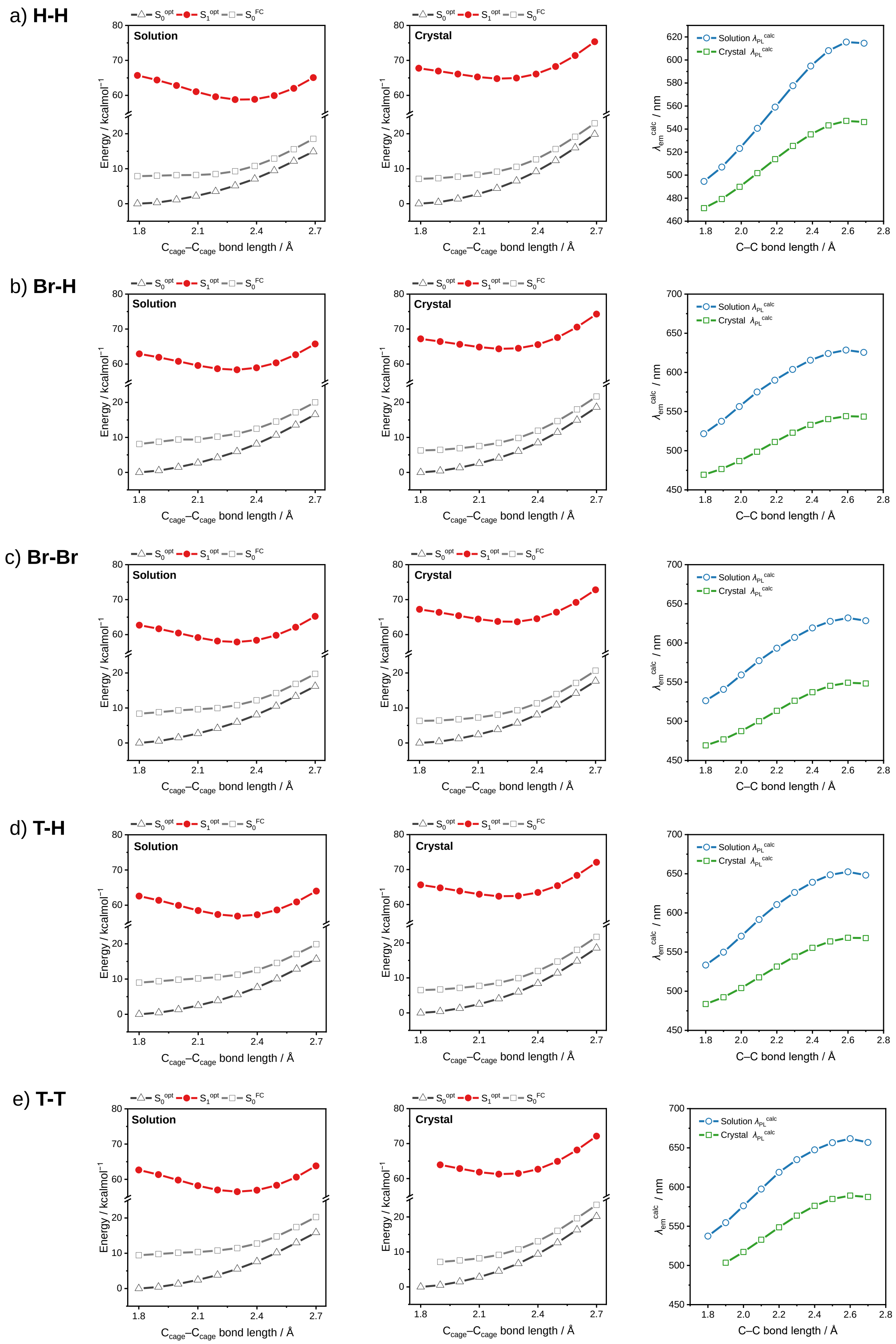

Figure S24. Energy levels of the S_0 and S_1 states modeled in solution (left) and crystal (middle) and calculated emission wavelength in both states (right) of a) **H-H**, b) **Br-H**, c) **Br-Br**, d) **T-H**, and e) **T-T** with variable C_{cage}–C_{cage} bond lengths. S_0^{opt} and S_1^{opt} denote energy levels of optimized geometries in ground state and excited state, respectively. S_0^{FC} denotes energy levels calculated with single point energy calculation using excited-state optimized geometries.

Table S9. Optimized geometry of **H-H** at the S_0 state calculated at B3LYP 6-31G+(d,p) level

Center Number	Atomic Number	Coordinates (Angstroms) x	y	z
1	5	4.290177	-0.001214	-0.588355
2	5	3.261515	-0.886303	0.568302
3	6	-0.835701	2.51036	-1.396339
4	6	-3.434402	2.43343	-0.36485
5	5	3.366421	1.4349	-1.115855
6	6	-2.696219	-1.216675	-0.502426
7	6	-3.434623	-2.434756	-0.357187
8	5	3.261347	0.887931	0.565158
9	5	1.957914	0.882956	-2.042256
10	6	-1.589462	3.65615	-1.295468
11	6	1.015532	0.003525	1.972328
12	6	-2.897036	3.635166	-0.740503
13	6	-0.835731	-2.515264	-1.38793
14	6	-1.589581	-3.660665	-1.283396
15	6	0.924609	-0.001839	-1.054718
16	5	1.777016	1.353526	-0.31654
17	6	1.849465	0.00114	0.729114
18	1	-3.467488	4.554074	-0.648861
19	1	-1.177346	4.591967	-1.661608
20	5	1.777046	-1.354933	-0.311467
21	5	1.957641	-0.890369	-2.038889
22	5	3.497503	-0.004099	-2.162518
23	6	-1.324393	1.231839	-0.970973
24	6	-2.696132	1.214825	-0.506274
25	6	-3.317638	-0.000449	-0.21895
26	6	-1.324437	-1.235301	-0.966941
27	6	-2.897279	-3.637753	-0.7288
28	1	-4.448985	-2.372034	0.026965
29	1	-4.331312	0.000213	0.173739
30	1	-1.177449	-4.597728	-1.646316
31	1	-3.467806	-4.556321	-0.634251
32	1	0.13067	-2.594736	-1.856034
33	1	0.130603	2.588216	-1.86492
34	1	-4.448679	2.372037	0.019732
35	6	-0.581927	-0.00184	-1.032085
36	1	1.172892	-2.295371	0.041112
37	1	3.58653	-1.538791	1.500576
38	1	4.097511	-0.006123	-3.187276

39	1	1.173155	2.295333	0.03286
40	1	3.871438	-2.48193	-1.368159
41	1	5.470883	-0.000989	-0.462866
42	1	3.871659	2.476736	-1.376765
43	1	3.586601	1.54398	1.494842
44	1	1.466019	1.518777	-2.907942
45	1	1.466115	-1.529283	-2.902498
46	5	3.366283	-1.439204	-1.110659
47	6	0.642023	1.213011	2.585146
48	6	0.641447	-1.203554	2.589526
49	6	-0.090837	-1.200178	3.776995
50	6	-0.090287	1.214311	3.772601
51	6	-0.463731	0.008238	4.371597
52	1	0.928141	-2.150537	2.148902
53	1	-0.367487	-2.144221	4.2364
54	1	0.929191	2.158247	2.141088
55	1	-0.366503	2.160148	4.228562
56	1	-1.034639	0.010047	5.295298

Table S10. Optimized geometry of **H-H** at the S_0 state calculated at B3LYP-D3 6-31G+(d,p) level

Center Number	Atomic Number	Coordinates (Angstroms) x	y	z
1	5	4.352274	0.085455	0.140322
2	5	3.141085	-0.9608	0.915566
3	6	-0.617282	2.723192	-1.076863
4	6	-3.273972	2.476478	-0.230523
5	5	3.524153	1.604105	-0.309742
6	6	-2.472205	-1.102767	-0.901927
7	6	-3.184921	-2.340444	-1.003329
8	5	3.107241	0.782337	1.209836
9	5	2.304645	1.22149	-1.549825
10	6	-1.386571	3.83683	-0.839079
11	6	0.590887	-0.326632	1.905735
12	6	-2.7246	3.722864	-0.37155
13	6	-0.528613	-2.210369	-1.877374
14	6	-1.257812	-3.36713	-2.011712
15	6	1.143864	0.187875	-0.870156
16	5	1.830235	1.435251	0.162738
17	6	1.685494	-0.092689	0.906586
18	1	-3.308576	4.614488	-0.166041
19	1	-0.96627	4.820282	-1.027656
20	5	1.882372	-1.29652	-0.295733
21	5	2.342104	-0.524852	-1.843225
22	5	3.859578	0.355011	-1.540793
23	6	-1.11922	1.395016	-0.884237
24	6	-2.517346	1.296354	-0.520729
25	6	-3.132558	0.045505	-0.463314
26	6	-1.074414	-1.031693	-1.272363
27	6	-2.594444	-3.455773	-1.534596
28	1	-4.221247	-2.360955	-0.677569
29	1	-4.165171	-0.026758	-0.131301
30	1	-0.806535	-4.223053	-2.504829
31	1	-3.145613	-4.386412	-1.626154
32	1	0.464325	-2.186021	-2.29593
33	1	0.374659	2.86831	-1.472186
34	1	-4.309546	2.356426	0.075578
35	6	-0.355798	0.19401	-1.070568
36	1	1.229786	-2.264889	-0.198007
37	1	3.293556	-1.745969	1.787703
38	1	4.637834	0.519665	-2.423473

39	1	1.161164	2.317455	0.542585
40	1	4.148842	-2.228116	-1.109863
41	1	5.489753	0.049121	0.481564
42	1	4.048767	2.669492	-0.300124
43	1	3.221215	1.248495	2.292169
44	1	1.939475	1.980587	-2.378931
45	1	1.998865	-0.985647	-2.876379
46	5	3.57952	-1.238286	-0.783377
47	6	-0.232846	0.717828	2.353278
48	6	0.36334	-1.622736	2.399042
49	6	-0.661733	-1.866818	3.312315
50	6	-1.264254	0.470401	3.260418
51	6	-1.48489	-0.821773	3.742346
52	1	0.986505	-2.445657	2.07053
53	1	-0.819639	-2.875465	3.681548
54	1	-0.083892	1.72523	1.988517
55	1	-1.895922	1.291723	3.584556
56	1	-2.289013	-1.013452	4.446453

Table S11. Optimized geometry of **H-H** at the S_0 state calculated at B3PW91-D3 6-31G+(d,p) level

Center Number	Atomic Number	Coordinates (Angstroms)		
		x	y	z
1	5	4.335299	0.036101	0.316513
2	5	3.075491	-1.007295	1.003942
3	6	-0.524911	2.743001	-1.048335
4	6	-3.190581	2.517703	-0.239045
5	5	3.554633	1.571883	-0.143717
6	6	-2.415492	-1.057614	-0.929003
7	6	-3.129697	-2.289507	-1.045359
8	5	3.045797	0.724467	1.332191
9	5	2.385741	1.226555	-1.439399
10	6	-1.281181	3.861417	-0.803704
11	6	0.476743	-0.366287	1.84604
12	6	-2.623575	3.757064	-0.354468
13	6	-0.472197	-2.160333	-1.903067
14	6	-1.203279	-3.311196	-2.054503
15	6	1.192786	0.191562	-0.805074
16	5	1.843575	1.42749	0.245161
17	6	1.626584	-0.120368	0.916558
18	1	-3.199042	4.653073	-0.142221
19	1	-0.846358	4.842379	-0.973281
20	5	1.888437	-1.317138	-0.271138
21	5	2.416553	-0.508704	-1.766064
22	5	3.92709	0.345242	-1.381375
23	6	-1.04741	1.423247	-0.880079
24	6	-2.446881	1.334778	-0.534815
25	6	-3.070769	0.089871	-0.486465
26	6	-1.018497	-0.991974	-1.286933
27	6	-2.539373	-3.399845	-1.583139
28	1	-4.168684	-2.310697	-0.726891
29	1	-4.105093	0.022127	-0.15749
30	1	-0.753955	-4.162382	-2.558203
31	1	-3.093433	-4.327948	-1.686539
32	1	0.523707	-2.127854	-2.319349
33	1	0.475622	2.876479	-1.430974
34	1	-4.231581	2.40747	0.05358
35	6	-0.296253	0.220782	-1.062695
36	1	1.216409	-2.28035	-0.219352
37	1	3.169771	-1.804295	1.877569
38	1	4.746891	0.519815	-2.227012

39	1	1.162687	2.310262	0.615834
40	1	4.17523	-2.249184	-0.992693
41	1	5.45531	-0.021889	0.716114
42	1	4.090468	2.632822	-0.086111
43	1	3.102379	1.155737	2.436265
44	1	2.055826	1.996004	-2.27823
45	1	2.101167	-0.93294	-2.827265
46	5	3.601453	-1.256891	-0.672813
47	6	-0.385053	0.666698	2.233542
48	6	0.227041	-1.664624	2.311724
49	6	-0.861862	-1.923284	3.139702
50	6	-1.481187	0.404311	3.052265
51	6	-1.725707	-0.890683	3.507082
52	1	0.881938	-2.479795	2.025282
53	1	-1.038638	-2.936027	3.489646
54	1	-0.218241	1.677399	1.882907
55	1	-2.145949	1.217711	3.327402
56	1	-2.582287	-1.094781	4.143129

Table S12. Optimized geometry of **H-H** at the S_0 state calculated at CAM-B3LYP 6-31G+(d,p) level

Center Number	Atomic Number	Coordinates (Angstroms)		
		x	y	z
1	5	4.309103	0.043184	-0.260184
2	5	3.188354	-0.883959	0.744013
3	6	-0.725166	2.557486	-1.307442
4	6	-3.36272	2.428738	-0.417563
5	5	3.445025	1.494486	-0.809725
6	6	-2.59446	-1.194648	-0.664337
7	6	-3.329685	-2.421329	-0.614847
8	5	3.176997	0.869581	0.818188
9	5	2.114612	0.973679	-1.852282
10	6	-1.4868	3.685642	-1.20864
11	6	0.789821	-0.079243	1.92248
12	6	-2.819263	3.638055	-0.718392
13	6	-0.69236	-2.440926	-1.514135
14	6	-1.438847	-3.583365	-1.508716
15	6	1.043667	0.0486	-0.906456
16	5	1.815183	1.415134	-0.159351
17	6	1.728209	-0.015429	0.746782
18	1	-3.398838	4.549912	-0.622665
19	1	-1.067906	4.634602	-1.527958
20	5	1.83286	-1.365007	-0.275916
21	5	2.126489	-0.780509	-1.926119
22	5	3.653872	0.107043	-1.895277
23	6	-1.223998	1.260845	-0.94674
24	6	-2.610892	1.220239	-0.566165
25	6	-3.237622	-0.001821	-0.362288
26	6	-1.207715	-1.185361	-1.047109
27	6	-2.77076	-3.594279	-1.014807
28	1	-4.360888	-2.380297	-0.277557
29	1	-4.270664	-0.022605	-0.027016
30	1	-1.008085	-4.496979	-1.905825
31	1	-3.337917	-4.518644	-0.993959
32	1	0.291701	-2.489084	-1.946791
33	1	0.258383	2.654427	-1.733016
34	1	-4.393719	2.34649	-0.087006
35	6	-0.477842	0.043025	-1.006848
36	1	1.201639	-2.311214	-0.00603
37	1	3.414796	-1.544004	1.697766
38	1	4.333305	0.152412	-2.866518

39	1	1.1757	2.33161	0.182423
40	1	3.998067	-2.395201	-1.187324
41	1	5.471925	0.040683	-0.026518
42	1	3.965368	2.545869	-0.981524
43	1	3.393135	1.450938	1.824292
44	1	1.656168	1.61213	-2.73212
45	1	1.675923	-1.348834	-2.856658
46	5	3.463549	-1.368785	-0.929532
47	6	0.300769	1.088028	2.515796
48	6	0.438407	-1.311649	2.481514
49	6	-0.393316	-1.375272	3.593566
50	6	-0.531876	1.023432	3.627507
51	6	-0.885895	-0.208133	4.168718
52	1	0.818982	-2.231639	2.056867
53	1	-0.652778	-2.342662	4.010556
54	1	0.571489	2.057541	2.118739
55	1	-0.900601	1.942402	4.070901
56	1	-1.535339	-0.257893	5.036598

Table S13. Optimized geometry of **Br-H** at the S_0 state calculated at B3LYP 6-31G+(d,p) level

Center Number	Atomic Number	Coordinates (Angstroms)		
		x	y	z
1	5	-5.025327	0	0.312372
2	5	-3.754241	0.885983	1.191663
3	6	-0.182642	-2.475946	-1.612131
4	6	2.489082	-2.468906	-0.80171
5	5	-4.256156	-1.438245	-0.417188
6	6	1.778827	1.226783	-0.843482
7	6	2.489081	2.468896	-0.801739
8	5	-3.754241	-0.885972	1.191674
9	5	-3.09338	-0.884899	-1.641355
10	6	0.550524	-3.636249	-1.625741
11	6	-1.202481	0.000013	1.980987
12	6	1.897862	-3.644071	-1.181489
13	6	-0.182643	2.475925	-1.612161
14	6	0.550522	3.636228	-1.625784
15	6	-1.866483	-0.000006	-0.879419
16	5	-2.533062	-1.373449	-0.011647
17	6	-2.333874	0.000005	0.995484
18	1	2.464992	-4.56952	-1.171153
19	1	0.094886	-4.551656	-1.990876
20	5	-2.533063	1.373446	-0.011664
21	5	-3.09338	0.884876	-1.641366
22	5	-4.619119	-0.000011	-1.407923
23	6	0.369036	-1.223852	-1.188906
24	6	1.778827	-1.226794	-0.843468
25	6	2.398422	-0.000004	-0.559875
26	6	0.369035	1.223836	-1.18892
27	6	1.89786	3.644056	-1.181532
28	1	3.52888	2.456592	-0.501815
29	1	0.094883	4.551631	-1.99093
30	1	2.464989	4.569506	-1.171208
31	1	-1.191997	2.506188	-1.989219
32	1	-1.191996	-2.506214	-1.989189
33	1	3.528881	-2.456598	-0.501786
34	6	-0.376455	-0.000008	-1.145105
35	1	-1.862969	2.314761	0.180592
36	1	-3.845727	1.529508	2.18037
37	1	-5.439946	-0.000016	-2.26568
38	1	-1.862968	-2.314762	0.18062

39	1	-4.809004	2.479522	-0.55217
40	1	-6.144227	0.000002	0.708895
41	1	-4.809002	-2.479533	-0.552139
42	1	-3.845725	-1.529485	2.180389
43	1	-2.802466	-1.512471	-2.598783
44	1	-2.802467	1.512436	-2.598801
45	5	-4.256157	1.438236	-0.417206
46	6	-0.661189	-1.207889	2.454973
47	6	-0.661204	1.207922	2.454968
48	6	0.418657	1.207202	3.338309
49	6	0.418672	-1.207152	3.338313
50	6	0.979367	0.000029	3.762922
51	1	-1.075812	2.154316	2.130651
52	1	0.828688	2.152167	3.681166
53	1	-1.075786	-2.154289	2.130659
54	1	0.828715	-2.15211	3.681173
55	35	4.176127	0.000001	0.149953
56	1	1.838559	0.000036	4.427123

Table S14. Optimized geometry of **Br-H** at the S_0 state calculated at B3LYP-D3 6-31G+(d,p) level

Center Number	Atomic Number	Coordinates (Angstroms)		
		x	y	z
1	5	-4.960095	0.045491	0.682792
2	5	-3.613484	1.052824	1.264
3	6	-0.292297	-2.716245	-1.272362
4	6	2.382334	-2.594065	-0.476328
5	5	-4.259757	-1.498558	0.117995
6	6	1.663731	1.058159	-1.042371
7	6	2.357378	2.302825	-1.177857
8	5	-3.590991	-0.692396	1.555534
9	5	-3.22528	-1.152441	-1.290978
10	6	0.435235	-3.86803	-1.109771
11	6	-0.952717	0.332078	1.844749
12	6	1.784745	-3.810727	-0.673358
13	6	-0.310608	2.159507	-1.99612
14	6	0.407382	3.314929	-2.173372
15	6	-1.945841	-0.156075	-0.779349
16	5	-2.51262	-1.391411	0.331246
17	6	-2.203545	0.137372	1.035612
18	1	2.349405	-4.725698	-0.524484
19	1	-0.02367	-4.827207	-1.328933
20	5	-2.548362	1.354453	-0.125796
21	5	-3.248394	0.594019	-1.581094
22	5	-4.732589	-0.237481	-1.054373
23	6	0.267809	-1.420088	-1.039815
24	6	1.677284	-1.369199	-0.700634
25	6	2.285501	-0.110029	-0.572539
26	6	0.256485	0.995613	-1.386293
27	6	1.75151	3.402719	-1.724765
28	1	3.396009	2.351248	-0.876978
29	1	-0.054031	4.161791	-2.67193
30	1	2.307028	4.327435	-1.844963
31	1	-1.318467	2.113008	-2.378568
32	1	-1.305385	-2.792851	-1.634132
33	1	3.423565	-2.545226	-0.184696
34	6	-0.47857	-0.20677	-1.152362
35	1	-1.861371	2.302732	-0.142755
36	1	-3.602072	1.839266	2.148363
37	1	-5.638371	-0.376421	-1.81053
38	1	-1.817749	-2.29514	0.598429

39	1	-4.875854	2.352196	-0.59401
40	1	-6.032504	0.116811	1.188811
41	1	-4.811513	-2.546008	0.209452
42	1	-3.55621	-1.152673	2.645675
43	1	-3.010989	-1.919662	-2.16378
44	1	-3.041853	1.045503	-2.654141
45	5	-4.295808	1.344652	-0.352161
46	6	-0.137684	-0.751584	2.207845
47	6	-0.552886	1.627492	2.214098
48	6	0.643915	1.834847	2.899348
49	6	1.064939	-0.541477	2.883391
50	6	1.46693	0.752144	3.221417
51	1	-1.171076	2.479761	1.959803
52	1	0.937547	2.845107	3.167086
53	1	-0.423382	-1.76165	1.94587
54	1	1.690097	-1.392678	3.133883
55	35	4.044153	0.004273	0.17602
56	1	2.406218	0.914659	3.741014

Table S15. Optimized geometry of **Br-H** at the S_0 state calculated at B3PW91-D3 6-31G+(d,p) level

Center Number	Atomic Number	Coordinates (Angstroms)		
		x	y	z
1	5	-4.924868	-0.066528	0.776265
2	5	-3.527811	0.637479	1.626811
3	6	-0.340505	-2.100542	-2.01718
4	6	2.317538	-2.264598	-1.18489
5	5	-4.301254	-1.327666	-0.322477
6	6	1.64507	1.396342	-0.675105
7	6	2.34713	2.614536	-0.430668
8	5	-3.564427	-1.091704	1.277133
9	5	-3.280247	-0.538461	-1.547602
10	6	0.372703	-3.255254	-2.204191
11	6	-0.883264	-0.399227	1.771615
12	6	1.709976	-3.3547	-1.745253
13	6	-0.330019	2.746082	-1.199235
14	6	0.393033	3.894997	-1.013745
15	6	-1.96053	0.175872	-0.732182
16	5	-2.553224	-1.357029	-0.1493
17	6	-2.159345	-0.17009	1.016733
18	1	2.262064	-4.281097	-1.871326
19	1	-0.087726	-4.092999	-2.719488
20	5	-2.496033	1.386679	0.40354
21	5	-3.24643	1.191964	-1.198985
22	5	-4.747499	0.275245	-0.956623
23	6	0.228153	-0.952553	-1.387123
24	6	1.629507	-1.022044	-1.040962
25	6	2.252583	0.137536	-0.557506
26	6	0.237669	1.450861	-1.003993
27	6	1.744219	3.83198	-0.591999
28	1	3.391944	2.561055	-0.148324
29	1	-0.072013	4.857702	-1.204292
30	1	2.307426	4.745248	-0.425674
31	1	-1.348344	2.824389	-1.550415
32	1	-1.345885	-2.038671	-2.40927
33	1	3.355493	-2.319472	-0.878492
34	6	-0.503928	0.241787	-1.132945
35	1	-1.786169	2.280693	0.682964
36	1	-3.450015	1.051134	2.736284
37	1	-5.673653	0.443131	-1.685585
38	1	-1.86595	-2.307528	-0.215241

39	1	-4.790836	2.540053	0.387387
40	1	-5.982728	-0.154598	1.315044
41	1	-4.890216	-2.328423	-0.582263
42	1	-3.520287	-1.902813	2.141977
43	1	-3.09018	-0.944776	-2.645337
44	1	-3.047437	1.980319	-2.060748
45	5	-4.24436	1.493001	0.243301
46	6	-0.481864	-1.706209	2.080191
47	6	-0.042691	0.663955	2.123678
48	6	1.190877	0.422573	2.723469
49	6	0.745666	-1.944938	2.692162
50	6	1.59499	-0.882245	3.000615
51	1	-0.331383	1.683978	1.902284
52	1	1.84209	1.259391	2.956611
53	1	-1.122598	-2.544395	1.831289
54	1	1.042557	-2.96601	2.912385
55	35	3.99517	0.016096	0.181798
56	1	2.56185	-1.069299	3.458058

Table S16. Optimized geometry of **Br-H** at the S_0 state calculated at CAM-B3LYP 6-31G+(d,p) level

Center Number	Atomic Number	Coordinates (Angstroms) x	y	z
1	5	-4.987507	0.003276	0.42243
2	5	-3.700943	0.995064	1.117294
3	6	-0.209112	-2.669678	-1.260967
4	6	2.464307	-2.55064	-0.500313
5	5	-4.244534	-1.510596	-0.132413
6	6	1.731447	1.092551	-0.983173
7	6	2.433805	2.333324	-1.103063
8	5	-3.683972	-0.744608	1.357061
9	5	-3.117682	-1.116527	-1.439424
10	6	0.525589	-3.811307	-1.142624
11	6	-1.106592	0.27118	1.885036
12	6	1.878622	-3.758246	-0.720844
13	6	-0.234881	2.224197	-1.884078
14	6	0.486808	3.367664	-2.052556
15	6	-1.894299	-0.130002	-0.781439
16	5	-2.527409	-1.411647	0.207396
17	6	-2.267926	0.099711	0.940522
18	1	2.450056	-4.672828	-0.604403
19	1	0.072251	-4.766435	-1.386401
20	5	-2.55424	1.356315	-0.172143
21	5	-3.135096	0.623254	-1.677969
22	5	-4.636082	-0.226055	-1.291247
23	6	0.342049	-1.372131	-1.003778
24	6	1.74659	-1.326997	-0.685846
25	6	2.360604	-0.079153	-0.556552
26	6	0.328218	1.040525	-1.304885
27	6	1.83584	3.439961	-1.620311
28	1	3.474422	2.36497	-0.810287
29	1	0.026415	4.22474	-2.532812
30	1	2.395416	4.362449	-1.731743
31	1	-1.244289	2.196633	-2.259537
32	1	-1.22143	-2.749452	-1.619809
33	1	3.507243	-2.49702	-0.219204
34	6	-0.402504	-0.1625	-1.095156
35	1	-1.876057	2.306999	-0.11198
36	1	-3.753714	1.744105	2.029609
37	1	-5.478663	-0.348544	-2.116871

38	1	-1.843061	-2.311917	0.503207
39	1	-4.840819	2.337258	-0.774061
40	1	-6.090034	0.052925	0.856453
41	1	-4.79177	-2.561911	-0.109556
42	1	-3.71787	-1.223207	2.437235
43	1	-2.828445	-1.842811	-2.322751
44	1	-2.852626	1.09226	-2.723307
45	5	-4.271954	1.328706	-0.520005
46	6	-0.382792	-0.827372	2.356262
47	6	-0.729137	1.550821	2.304706
48	6	0.366046	1.729224	3.141668
49	6	0.716672	-0.647527	3.188543
50	6	1.105823	0.631524	3.570594
51	1	-1.286705	2.418674	1.975944
52	1	0.64607	2.731766	3.447425
53	1	-0.663315	-1.831912	2.069001
54	1	1.274587	-1.51349	3.528899
55	35	4.125539	0.015974	0.136106
56	1	1.974489	0.770981	4.205873

Table S17. Optimized geometry of **Br-H** at the S_0 state calculated at CAM-B3LYP functional with 6-31G+(d,p) basis set for C, H, O atoms and LanL2DZ basis set for Br atom

Center	Atomic	Coordinates (Angstroms)		
Number	Number	x	y	z
1	5	-5.015234	0.023466	0.157892
2	5	-3.774748	0.792923	1.156557
3	6	-0.163519	-2.288809	-1.784968
4	6	2.501799	-2.380709	-0.999179
5	5	-4.244014	-1.333141	-0.691274
6	6	1.817941	1.298007	-0.671615
7	6	2.532006	2.529053	-0.508924
8	5	-3.786745	-0.952382	0.969277
9	5	-3.027106	-0.667225	-1.78764
10	6	0.553353	-3.440092	-1.914532
11	6	-1.268524	-0.209326	1.917281
12	6	1.900918	-3.503115	-1.47742
13	6	-0.136944	2.628071	-1.280622
14	6	0.593326	3.773797	-1.178044
15	6	-1.842986	0.106455	-0.833067
16	5	-2.552882	-1.3564	-0.223244
17	6	-2.338016	-0.069335	0.865722
18	1	2.458495	-4.43021	-1.557039
19	1	0.09045	-4.309659	-2.369545
20	5	-2.534664	1.418353	0.072513
21	5	-3.014746	1.077772	-1.601536
22	5	-4.544864	0.199208	-1.531937
23	6	0.397599	-1.087165	-1.239028
24	6	1.803177	-1.133003	-0.914119
25	6	2.436419	0.053487	-0.540247
26	6	0.411293	1.334261	-0.993682
27	6	1.943606	3.73188	-0.747064
28	1	3.574557	2.487819	-0.225495
29	1	0.138891	4.722677	-1.443771
30	1	2.512689	4.649421	-0.642105
31	1	-1.143218	2.701929	-1.654747
32	1	-1.168193	-2.272259	-2.170629
33	1	3.542858	-2.410568	-0.708935
34	6	-0.333882	0.123032	-1.070794
35	1	-1.866069	2.32181	0.393825
36	1	-3.879059	1.304245	2.217112
37	1	-5.326168	0.299642	-2.418741
38	1	-1.887728	-2.308613	-0.085905

39	1	-4.76511	2.571115	-0.434589
40	1	-6.145195	-0.007891	0.516995
41	1	-4.799688	-2.346849	-0.954487
42	1	-3.905788	-1.672846	1.898281
43	1	-2.680601	-1.166563	-2.798841
44	1	-2.661983	1.774072	-2.48603
45	5	-4.22509	1.516678	-0.388469
46	6	-0.919626	-1.475418	2.398359
47	6	-0.638228	0.911908	2.464303
48	6	0.331488	0.768797	3.45114
49	6	0.04692	-1.617109	3.38756
50	6	0.681928	-0.495772	3.913216
51	1	-0.900184	1.906207	2.127176
52	1	0.811948	1.652563	3.85785
53	1	-1.405684	-2.360485	2.007631
54	1	0.30248	-2.608986	3.74555
55	35	4.268634	-0.023991	0.125102
56	1	1.440273	-0.606529	4.681509

Table S18. Optimized geometry of **T-H** at the S_0 state calculated at B3LYP 6-31G+(d,p) level

Center Number	Atomic Number	Coordinates (Angstroms) x	y	z
1	5	5.313286	-0.000024	0.093854
2	5	4.09634	-0.886952	1.047761
3	6	0.410355	2.493077	-1.602119
4	6	-2.300387	2.458249	-0.94505
5	5	4.497931	1.437687	-0.586368
6	6	-1.579909	-1.21888	-0.972601
7	6	-2.300543	-2.458036	-0.945437
8	5	4.096322	0.886826	1.047803
9	5	3.273609	0.885635	-1.746076
10	6	-0.326911	3.651497	-1.623995
11	6	1.636123	-0.00009	2.031685
12	6	-1.696451	3.647604	-1.254083
13	6	0.410251	-2.492964	-1.602299
14	6	-0.327084	-3.651338	-1.624342
15	6	2.083784	-0.000005	-0.945874
16	5	2.793797	1.359435	-0.080515
17	6	2.674709	-0.000073	0.952649
18	1	-2.265185	4.57226	-1.248618
19	1	0.14591	4.576534	-1.940517
20	5	2.793802	-1.359507	-0.080583
21	5	3.273611	-0.885626	-1.74611
22	5	4.809776	0.000007	-1.595868
23	6	-0.154278	1.227347	-1.236562
24	6	-1.579842	1.219044	-0.972445
25	6	-2.258642	0.000087	-0.760487
26	6	-0.154336	-1.227238	-1.236665
27	6	-1.69666	-3.647394	-1.254561
28	1	-3.357235	-2.430086	-0.708632
29	1	0.145703	-4.576373	-1.940924
30	1	-2.265462	-4.57201	-1.249274
31	1	1.434598	-2.5441	-1.929564
32	1	1.434683	2.544195	-1.929447
33	1	-3.357054	2.430344	-0.708133
34	6	0.590737	0.000033	-1.176846
35	1	2.136109	-2.300162	0.156485
36	1	4.249926	-1.53793	2.023886
37	1	5.580026	0.000029	-2.49958
38	1	2.136097	2.300065	0.156631

39	1	5.041167	-2.479704	-0.752767
40	1	6.453117	-0.000029	0.426038
41	1	5.041152	2.479685	-0.752634
42	1	4.24991	1.537754	2.023961
43	1	2.941828	1.518632	-2.686349
44	1	2.941835	-1.518589	-2.686409
45	5	4.497942	-1.437718	-0.586439
46	6	1.161585	1.208282	2.572298
47	6	1.161254	-1.208491	2.571943
48	6	0.234181	-1.207423	3.614445
49	6	0.234513	1.207155	3.614802
50	6	-0.236279	-0.000147	4.137813
51	1	1.520133	-2.154576	2.185665
52	1	-0.11821	-2.152302	4.016656
53	1	1.520725	2.154385	2.186302
54	1	-0.11762	2.152008	4.017302
55	1	-0.959135	-0.000169	4.948122
56	6	-3.694925	0.000101	-0.382135
57	6	-4.797799	0.000517	-1.201185
58	16	-4.184637	-0.000447	1.300829
59	6	-6.037503	0.000396	-0.488255
60	1	-4.721131	0.000894	-2.283048
61	6	-5.865776	-0.000111	0.870572
62	1	-7.009579	0.000671	-0.968199
63	1	-6.62117	-0.000305	1.644893

Table S19. Optimized geometry of **T-H** at the S_0 state calculated at B3LYP-D3 6-31G+(d,p) level

Center Number	Atomic Number	Coordinates (Angstroms) x	y	z
1	5	5.250817	-0.082171	0.633817
2	5	3.91651	-1.13571	1.154623
3	6	0.567911	2.823548	-1.016725
4	6	-2.153657	2.634448	-0.413452
5	5	4.536977	1.498871	0.204414
6	6	-1.407177	-0.937731	-1.260773
7	6	-2.109801	-2.161419	-1.511527
8	5	3.894639	0.579627	1.583543
9	5	3.482561	1.26116	-1.211086
10	6	-0.172274	3.9543	-0.775455
11	6	1.272568	-0.479226	1.843415
12	6	-1.546696	3.86224	-0.42951
13	6	0.603404	-2.005817	-2.162617
14	6	-0.11779	-3.137743	-2.449918
15	6	2.211349	0.224409	-0.767858
16	5	2.791885	1.365969	0.436178
17	6	2.500103	-0.211229	1.022264
18	1	-2.116864	4.760661	-0.214509
19	1	0.298898	4.928638	-0.864147
20	5	2.825226	-1.330214	-0.235515
21	5	3.506404	-0.456783	-1.638696
22	5	4.995519	0.335674	-1.07035
23	6	-0.001092	1.510353	-0.954521
24	6	-1.428186	1.437153	-0.718483
25	6	-2.093882	0.196646	-0.783139
26	6	0.01774	-0.872959	-1.509897
27	6	-1.485914	-3.239226	-2.081546
28	1	-3.166127	-2.204167	-1.273532
29	1	0.363164	-3.957927	-2.974494
30	1	-2.039166	-4.151066	-2.283934
31	1	1.628603	-1.955625	-2.492576
32	1	1.597149	2.941816	-1.313706
33	1	-3.213038	2.551581	-0.200762
34	6	0.74599	0.304028	-1.145093
35	1	2.137471	-2.276074	-0.30575
36	1	3.926326	-1.989514	1.973829
37	1	5.888646	0.537096	-1.827658
38	1	2.102784	2.242616	0.793006

39	1	5.150369	-2.282089	-0.817905
40	1	6.330831	-0.19029	1.116863
41	1	5.087189	2.538199	0.36943
42	1	3.875553	0.953477	2.706679
43	1	3.254795	2.093805	-2.018095
44	1	3.289016	-0.820335	-2.742322
45	5	4.57155	-1.298683	-0.488935
46	6	0.422333	0.558428	2.256104
47	6	0.940669	-1.800058	2.189538
48	6	-0.213583	-2.074904	2.922212
49	6	-0.73834	0.280609	2.979027
50	6	-1.063063	-1.035965	3.312415
51	1	1.581425	-2.618571	1.884818
52	1	-0.452862	-3.102661	3.177092
53	1	0.649772	1.584875	2.001734
54	1	-1.392441	1.096378	3.270199
55	1	-1.971423	-1.250883	3.866448
56	6	-3.524561	0.09975	-0.411166
57	6	-4.626223	0.255414	-1.215469
58	16	-4.006846	-0.251345	1.234997
59	6	-5.865019	0.095149	-0.518737
60	1	-4.545508	0.478409	-2.273507
61	6	-5.690002	-0.181495	0.811608
62	1	-6.838149	0.182072	-0.98836
63	1	-6.446148	-0.349821	1.56705

Table S20. Optimized geometry of **T-H** at the S_0 state calculated at B3PW91-D3 6-31G+(d,p) level

Center Number	Atomic Number	Coordinates (Angstroms) x	y	z
1	5	-5.235201	-0.07788	0.668467
2	5	-3.866487	0.583726	1.594407
3	6	-0.620184	-2.015893	-2.113146
4	6	2.086141	-2.169903	-1.449555
5	5	-4.576558	-1.294543	-0.460592
6	6	1.407113	1.42986	-0.700868
7	6	2.130662	2.624634	-0.399083
8	5	-3.895457	-1.12716	1.169839
9	5	-3.516522	-0.456933	-1.615677
10	6	0.098695	-3.151044	-2.383909
11	6	-1.239722	-0.470879	1.795176
12	6	1.462093	-3.252045	-2.006852
13	6	-0.5864	2.809332	-1.005214
14	6	0.150712	3.939575	-0.7631
15	6	-2.219524	0.217062	-0.732597
16	5	-2.832704	-1.337046	-0.228903
17	6	-2.47814	-0.200981	0.994988
18	1	2.014005	-4.167936	-2.196026
19	1	-0.380971	-3.974717	-2.904878
20	5	-2.79014	1.378143	0.441022
21	5	-3.48845	1.256936	-1.192791
22	5	-4.99913	0.33637	-1.039891
23	6	-0.034747	-0.882191	-1.46891
24	6	1.385189	-0.946049	-1.216334
25	6	2.071157	0.191346	-0.754011
26	6	-0.0158	1.500665	-0.938267
27	6	1.522211	3.84976	-0.414723
28	1	3.191109	2.540475	-0.186282
29	1	-0.321645	4.913455	-0.854636
30	1	2.090769	4.749367	-0.198679
31	1	-1.616218	2.923488	-1.307754
32	1	-1.643665	-1.961487	-2.453404
33	1	3.143055	-2.208543	-1.208145
34	6	-0.758927	0.296207	-1.119831
35	1	-2.092376	2.255199	0.793322
36	1	-3.823621	0.949478	2.72242
37	1	-5.899442	0.538291	-1.792325
38	1	-2.140424	-2.284437	-0.299262

39	1	-5.080921	2.542708	0.39657
40	1	-6.310013	-0.185839	1.168868
41	1	-5.159509	-2.280962	-0.781843
42	1	-3.888725	-1.973369	2.001134
43	1	-3.29696	-0.811719	-2.725333
44	1	-3.257877	2.079274	-2.014181
45	5	-4.532976	1.500286	0.226315
46	6	-0.919626	-1.787667	2.153029
47	6	-0.366097	0.559844	2.162418
48	6	0.809767	0.277469	2.853343
49	6	0.249325	-2.066699	2.855792
50	6	1.123035	-1.035663	3.201425
51	1	-0.586458	1.585262	1.893424
52	1	1.484993	1.088391	3.108822
53	1	-1.581773	-2.601303	1.879358
54	1	0.481055	-3.093601	3.122214
55	1	2.043749	-1.254624	3.733629
56	6	3.503848	0.103024	-0.405616
57	6	4.584602	0.262309	-1.237145
58	16	4.022783	-0.235359	1.219259
59	6	5.83492	0.11329	-0.568369
60	1	4.474648	0.479839	-2.293864
61	6	5.686868	-0.157915	0.765789
62	1	6.79892	0.203298	-1.056428
63	1	6.458859	-0.318438	1.507567

Table S21. Optimized geometry of **T-H** at the S_0 state calculated at CAM-B3LYP 6-31G+(d,p) level

Center Number	Atomic Number	Coordinates (Angstroms) x	y	z
1	5	5.321947	0.000089	-0.032067
2	5	4.13301	-0.878164	0.937831
3	6	0.385423	2.483744	-1.489801
4	6	-2.26589	2.451838	-0.655138
5	5	4.506893	1.433411	-0.693142
6	6	-1.551444	-1.211194	-0.73503
7	6	-2.265834	-2.451254	-0.657354
8	5	4.132998	0.877449	0.938632
9	5	3.23879	0.878457	-1.794116
10	6	-0.346815	3.633178	-1.468804
11	6	1.674261	-0.000884	1.931252
12	6	-1.686437	3.632115	-1.001812
13	6	0.385478	-2.482344	-1.492046
14	6	-0.346734	-3.631811	-1.472097
15	6	2.102495	0.00044	-0.876026
16	5	2.839635	1.393165	-0.142931
17	6	2.683091	-0.000314	0.813227
18	1	-2.249928	4.5579	-0.955539
19	1	0.099921	4.55547	-1.825856
20	5	2.839658	-1.392932	-0.144199
21	5	3.238809	-0.87672	-1.794918
22	5	4.769144	0.000843	-1.705763
23	6	-0.153473	1.219186	-1.077849
24	6	-1.551473	1.211865	-0.73394
25	6	-2.213106	0.000215	-0.484593
26	6	-0.153444	-1.218172	-1.078945
27	6	-1.686356	-3.631202	-1.005104
28	1	-3.30014	-2.426736	-0.338395
29	1	0.100021	-4.553768	-1.829989
30	1	-2.249827	-4.557041	-0.959674
31	1	1.381918	-2.528001	-1.895361
32	1	1.381861	2.529791	-1.893075
33	1	-3.300194	2.427008	-0.336198
34	6	0.586235	0.000506	-1.055583
35	1	2.18567	-2.325242	0.119241
36	1	4.292361	-1.499062	1.930677
37	1	5.506705	0.001274	-2.634663
38	1	2.185655	2.325249	0.121316

39	1	5.046621	-2.472277	-0.877144
40	1	6.468053	-0.000042	0.272957
41	1	5.046573	2.473216	-0.874905
42	1	4.292323	1.497449	1.932045
43	1	2.843663	1.48118	-2.727922
44	1	2.843693	-1.478597	-2.729274
45	5	4.506918	-1.432649	-0.694444
46	6	1.219425	1.200836	2.481909
47	6	1.220169	-1.203181	2.481266
48	6	0.321345	-1.203329	3.541963
49	6	0.320594	1.199854	3.542602
50	6	-0.135713	-0.002021	4.074391
51	1	1.570997	-2.149364	2.090297
52	1	-0.017867	-2.148413	3.952799
53	1	1.569655	2.147448	2.091447
54	1	-0.01921	2.144507	3.953939
55	1	-0.836306	-0.002461	4.903117
56	6	-3.622412	-0.000011	-0.020789
57	6	-4.07582	-0.000614	1.267205
58	16	-4.954742	0.000495	-1.13934
59	6	-5.500906	-0.000671	1.363905
60	1	-3.408351	-0.001005	2.121067
61	6	-6.107388	-0.000111	0.143906
62	1	-6.043016	-0.001112	2.301725
63	1	-7.165607	-0.000018	-0.077883

Table S22. Optimized geometry of **H-H** at the S_1 state calculated at CAM-B3LYP 6-31G+(d,p) level

Center Number	Atomic Number	Coordinates (Angstroms) x	y	z
1	5	4.061469	-1.310395	0.003639
2	5	3.303574	0.031015	0.891741
3	6	-1.15576	-1.366674	-2.481622
4	6	-3.481904	0.151149	-2.425848
5	5	3.036936	-1.630808	-1.419707
6	6	-2.80115	-0.116716	1.218834
7	6	-3.481891	0.165576	2.425352
8	5	3.3035	0.025442	-0.892828
9	5	1.511466	-2.329959	-0.886062
10	6	-1.867344	-1.122247	-3.652848
11	6	1.523007	1.92565	-0.006157
12	6	-3.023267	-0.340166	-3.633483
13	6	-1.155463	-1.351573	2.490031
14	6	-1.866845	-1.100024	3.659874
15	6	0.605062	-1.298227	0.00401
16	5	1.610846	-0.540143	-1.251149
17	6	2.041301	0.542234	-0.002057
18	1	-3.563106	-0.131834	-4.550602
19	1	-1.508367	-1.542547	-4.585988
20	5	1.61101	-0.532336	1.254004
21	5	1.511709	-2.324495	0.900324
22	5	2.997993	-2.693891	0.008106
23	6	-1.571527	-0.863221	-1.237255
24	6	-2.801163	-0.124071	-1.217739
25	6	-3.353933	0.292614	-0.000684
26	6	-1.57146	-0.855754	1.242726
27	6	-3.022927	-0.318255	3.635913
28	1	-4.388721	0.76071	2.380647
29	1	-4.27604	0.866163	-0.002518
30	1	-1.507573	-1.514696	4.595416
31	1	-3.562697	-0.104394	4.551802
32	1	-0.273918	-1.967197	2.557764
33	1	-0.274364	-1.98286	-2.54578
34	1	-4.388549	0.746785	-2.384468
35	6	-0.831478	-1.05501	0.003299
36	1	1.054411	-0.081227	2.190271
37	1	3.839173	0.8337	1.580501
38	1	3.417307	-3.80604	0.011433

39	1	1.053768	-0.095244	-2.190074
40	1	3.478319	-1.969087	2.476298
41	1	5.243356	-1.434663	0.003859
42	1	3.477608	-1.984902	-2.464675
43	1	3.839007	0.823704	-1.586735
44	1	0.947066	-3.125606	-1.555745
45	1	0.947417	-3.115965	1.575027
46	5	3.037234	-1.621887	1.429199
47	6	1.283686	2.602922	-1.211778
48	6	1.285957	2.610535	1.195606
49	6	0.829769	3.922686	1.191144
50	6	0.827406	3.915051	-1.214713
51	6	0.595094	4.5819	-0.013667
52	1	1.46921	2.113383	2.140905
53	1	0.658989	4.432911	2.133781
54	1	1.465204	2.099896	-2.154283
55	1	0.654753	4.419292	-2.160224
56	1	0.238057	5.606716	-0.01656

Table S23. Optimized geometry of **Br-H** at the S_1 state calculated at CAM-B3LYP 6-31G+(d,p) level

Center Number	Atomic Number	Coordinates (Angstroms)		
		x	y	z
1	5	-4.96026	0.000329	0.002149
2	5	-3.789806	0.838186	1.046953
3	6	-0.019187	-2.347156	-1.944306
4	6	2.545726	-2.420698	-0.896984
5	5	-4.109168	-1.389164	-0.717879
6	6	1.854081	1.2776	-0.787612
7	6	2.545915	2.500896	-0.639574
8	5	-3.789961	-0.941827	0.954096
9	5	-2.901717	-0.797134	-1.855765
10	6	0.706635	-3.534167	-1.966072
11	6	-1.441761	-0.111957	2.141755
12	6	1.9854	-3.575186	-1.416509
13	6	-0.019112	2.537282	-1.688558
14	6	0.70678	3.720044	-1.586332
15	6	-1.703639	0.059415	-1.133975
16	5	-2.404941	-1.264511	-0.170057
17	6	-2.423264	-0.053848	1.037154
18	1	2.55078	-4.500574	-1.402087
19	1	0.263732	-4.4237	-2.400438
20	5	-2.404802	1.275929	-0.037374
21	5	-2.901593	0.986528	-1.762635
22	5	-4.426164	0.086894	-1.658127
23	6	0.503737	-1.162123	-1.40867
24	6	1.853991	-1.188566	-0.916606
25	6	2.445448	0.026185	-0.501818
26	6	0.503802	1.302753	-1.279689
27	6	1.985608	3.703354	-1.035669
28	1	3.545376	2.494861	-0.225668
29	1	0.26389	4.650133	-1.925303
30	1	2.551047	4.622144	-0.924713
31	1	-1.010529	2.57774	-2.110939
32	1	-1.01051	-2.34317	-2.368823
33	1	3.5452	-2.457823	-0.484705
34	6	-0.266289	0.069445	-1.327086
35	1	-1.730219	2.20243	0.236573
36	1	-4.014353	1.474372	2.021491
37	1	-5.19267	0.134256	-2.564892

38	1	-1.730423	-2.214555	0.006037
39	1	-4.644247	2.509703	-0.697216
40	1	-6.113521	-0.014554	0.287314
41	1	-4.644563	-2.422657	-0.954406
42	1	-4.014674	-1.675917	1.857142
43	1	-2.633484	-1.417168	-2.826491
44	1	-2.633212	1.704225	-2.663514
45	5	-4.109077	1.457119	-0.569399
46	6	-0.974858	-1.343329	2.626824
47	6	-0.971539	1.061698	2.750792
48	6	-0.066722	1.005443	3.803682
49	6	-0.070139	-1.398108	3.679839
50	6	0.392618	-0.224259	4.271196
51	1	-1.322371	2.025603	2.401496
52	1	0.280407	1.92668	4.260808
53	1	-1.328256	-2.265258	2.180324
54	1	0.274359	-2.362404	4.039848
55	35	4.176981	-0.018482	0.35189
56	1	1.101956	-0.267551	5.09151

Table S24. Optimized geometry of **Br-Br** at the S_0 state calculated at CAM-B3LYP 6-31G+(d,p) level

Center Number	Atomic Number	Coordinates (Angstroms) x	y	z
1	5	4.9567	1.877769	0.000051
2	5	3.446339	2.147172	0.878202
3	6	1.339495	-1.796917	-2.470222
4	6	-1.405443	-2.241224	-2.467055
5	5	4.567851	0.902727	-1.432974
6	6	-0.752165	-1.970434	1.221503
7	6	-1.405551	-2.241058	2.467152
8	5	3.446377	2.147114	-0.878183
9	5	3.993783	-0.675879	-0.877457
10	6	0.693184	-2.123184	-3.624494
11	6	0.813341	1.801792	-0.000041
12	6	-0.712294	-2.311631	-3.635159
13	6	1.339386	-1.796753	2.470409
14	6	0.693024	-2.122942	3.624676
15	6	2.553645	-0.420966	0.000075
16	5	2.845545	0.572529	-1.395445
17	6	2.242804	1.329705	0.000011
18	1	-1.225267	-2.544819	-4.56208
19	1	1.26387	-2.253507	-4.538153
20	5	2.845484	0.572621	1.395542
21	5	3.993745	-0.675821	0.877686
22	5	5.28785	0.145862	0.000115
23	6	0.656948	-1.657955	-1.216774
24	6	-0.752112	-1.970515	-1.221396
25	6	-1.427376	-2.008768	0.00004
26	6	0.656894	-1.657875	1.216923
27	6	-0.712454	-2.311387	3.635292
28	1	-2.470071	-2.430183	2.461679
29	1	1.26367	-2.253204	4.538369
30	1	-1.225468	-2.544512	4.562206
31	1	2.411648	-1.706565	2.498263
32	1	2.411757	-1.706729	-2.498034
33	1	-2.469962	-2.430349	-2.461616
34	6	1.302317	-1.296531	0.000077
35	1	2.145386	0.482222	2.327667
36	1	3.099727	3.092268	1.497608
37	1	6.383851	-0.307261	0.000154

38	1	2.145484	0.482069	-2.327593
39	1	5.127797	1.005926	2.472817
40	1	5.809973	2.701325	0.000042
41	1	5.127905	1.005764	-2.47265
42	1	3.099794	3.092168	-1.497666
43	1	4.101977	-1.684565	-1.479459
44	1	4.101913	-1.684467	1.47976
45	5	4.567789	0.902822	1.433124
46	6	0.141464	2.045661	-1.200553
47	6	0.141379	2.045682	1.20042
48	6	-1.174784	2.492615	1.208021
49	6	-1.174698	2.492594	-1.208256
50	6	-1.821906	2.702197	-0.000142
51	1	0.638252	1.891995	2.149433
52	1	-1.682361	2.67085	2.148498
53	1	0.638405	1.891959	-2.149528
54	1	-1.682208	2.670814	-2.148772
55	35	-3.368516	-2.188641	0.000004
56	35	-3.665312	3.305258	-0.000212

Table S25. Optimized geometry of **Br-Br** at the S_1 state calculated at CAM-B3LYP 6-31G+(d,p) level

Center Number	Atomic Number	Coordinates (Angstroms) x	y	z
1	5	4.554861	2.55894	0.000005
2	5	3.018719	2.65073	0.891473
3	6	1.708596	-1.874083	-2.444969
4	6	-0.97456	-2.569829	-2.463818
5	5	4.266223	1.52937	-1.425029
6	6	-0.370528	-2.222338	1.234469
7	6	-0.974721	-2.56955	2.464054
8	5	3.01878	2.650625	-0.89158
9	5	4.007998	-0.130782	-0.8932
10	6	1.103523	-2.277509	-3.63098
11	6	0.458115	2.139258	-0.000111
12	6	-0.250748	-2.602342	-3.643318
13	6	1.708436	-1.873802	2.445302
14	6	1.103286	-2.277095	3.631319
15	6	2.646058	-0.316292	0.000108
16	5	2.581288	0.931925	-1.270906
17	6	1.908042	1.854522	-0.000044
18	1	-0.740619	-2.891514	-4.566666
19	1	1.690362	-2.323413	-4.541787
20	5	2.581201	0.932075	1.270971
21	5	4.007937	-0.130677	0.893487
22	5	5.132149	0.910656	0.000121
23	6	1.005959	-1.808602	-1.233597
24	6	-0.370447	-2.222479	-1.234232
25	6	-1.055017	-2.295136	0.0001
26	6	1.005877	-1.808459	1.233877
27	6	-0.250986	-2.601928	3.643606
28	1	-2.022911	-2.836655	2.479895
29	1	1.690065	-2.322895	4.54217
30	1	-0.740917	-2.890997	4.566955
31	1	2.756327	-1.61938	2.463268
32	1	2.756489	-1.619664	-2.462896
33	1	-2.02275	-2.836934	-2.479696
34	6	1.612351	-1.33402	0.000133
35	1	1.906197	0.705499	2.210058
36	1	2.62943	3.535188	1.577854
37	1	6.29123	0.649658	0.000176

38	1	1.906348	0.705241	-2.210012
39	1	4.802517	1.706684	2.469754
40	1	5.302554	3.482094	-0.000024
41	1	4.802686	1.706395	-2.469628
42	1	2.629538	3.535002	-1.578092
43	1	4.359498	-1.038819	-1.564403
44	1	4.359392	-1.038634	1.564821
45	5	4.266125	1.529537	1.425139
46	6	-0.248976	2.285325	-1.20242
47	6	-0.249058	2.285467	1.202134
48	6	-1.610642	2.559697	1.209552
49	6	-1.61056	2.559555	-1.209963
50	6	-2.279086	2.687157	-0.000236
51	1	0.268624	2.188573	2.148828
52	1	-2.139649	2.66988	2.148975
53	1	0.26877	2.188319	-2.149068
54	1	-2.139503	2.669626	-2.149435
55	35	-2.953164	-2.645477	0.000059
56	35	-4.186252	3.051467	-0.000322

Table S26. Optimized geometry of **T-H** at the S_1 state calculated at CAM-B3LYP 6-31G+(d,p) level

Center Number	Atomic Number	Coordinates (Angstroms)		
		x	y	z
1	5	5.256337	-0.011529	0.022743
2	5	4.092469	-1.183909	-0.63456
3	6	0.322278	2.299661	1.988771
4	6	-2.221551	1.245146	2.242292
5	5	4.395107	0.930019	1.266552
6	6	-1.576139	0.653955	-1.413767
7	6	-2.299023	0.417874	-2.605465
8	5	4.081045	-0.793609	1.104304
9	5	3.193815	1.954063	0.484965
10	6	-0.385585	2.481865	3.169684
11	6	1.749724	-2.118849	0.473805
12	6	-1.650079	1.914647	3.310502
13	6	0.339394	1.229674	-2.793759
14	6	-0.39812	0.999295	-3.94833
15	6	1.996893	1.10638	-0.246275
16	5	2.688863	0.366266	1.220819
17	6	2.720177	-1.028634	0.235381
18	1	-2.190708	1.995226	4.247289
19	1	0.065331	3.037206	3.984719
20	5	2.704357	-0.189924	-1.250486
21	5	3.202923	1.562239	-1.257563
22	5	4.722701	1.60952	-0.344507
23	6	-0.215839	1.605901	0.892698
24	6	-1.571138	1.142641	0.992037
25	6	-2.22182	0.570106	-0.140832
26	6	-0.205512	1.058448	-1.510658
27	6	-1.722148	0.578702	-3.853412
28	1	-3.340534	0.133543	-2.539189
29	1	0.063264	1.155996	-4.917248
30	1	-2.30962	0.397788	-4.746986
31	1	1.354336	1.577032	-2.897209
32	1	1.314499	2.714789	1.916167
33	1	-3.194731	0.792554	2.371546
34	6	0.559979	1.304644	-0.299327
35	1	2.034545	-0.617808	-2.120641
36	1	4.323058	-2.25076	-1.096917
37	1	5.490368	2.49558	-0.539115
38	1	2.008741	0.350036	2.183097

39	1	4.951758	0.256646	-2.570811
40	1	6.409919	-0.287634	0.091979
41	1	4.924139	1.337228	2.249036
42	1	4.303292	-1.559409	1.981392
43	1	2.929493	3.016603	0.931728
44	1	2.943498	2.32976	-2.119214
45	5	4.411277	0.305696	-1.514193
46	6	1.278281	-2.395194	1.766029
47	6	1.297587	-2.924922	-0.581863
48	6	0.410027	-3.969016	-0.352943
49	6	0.390193	-3.438929	1.993565
50	6	-0.051673	-4.229982	0.935316
51	1	1.6515	-2.738321	-1.588838
52	1	0.079965	-4.582534	-1.185273
53	1	1.616242	-1.792592	2.60069
54	1	0.04308	-3.635543	3.002914
55	1	-0.745542	-5.045143	1.113832
56	6	-3.550892	-0.031732	-0.062858
57	6	-3.890507	-1.302882	-0.469496
58	16	-4.979336	0.817237	0.484777
59	6	-5.27044	-1.599841	-0.32108
60	1	-3.156156	-2.006409	-0.84334
61	6	-5.981951	-0.543736	0.173529
62	1	-5.714205	-2.555419	-0.571482
63	1	-7.043308	-0.489711	0.373825

Table S27. Optimized geometry of **T-T** at the S_0 state calculated at CAM-B3LYP 6-31G+(d,p) level

Center Number	Atomic Number	Coordinates (Angstroms) x	y	z
1	5	-5.133546	-2.396621	-0.056552
2	5	-3.587975	-2.529849	0.792333
3	6	-2.00468	1.77679	-2.401821
4	6	0.649323	2.605999	-2.372312
5	5	-4.880848	-1.319595	-1.446846
6	6	0.06949	2.101074	1.279613
7	6	0.713477	2.402881	2.523555
8	5	-3.616152	-2.449635	-0.961425
9	5	-4.485328	0.288244	-0.824924
10	6	-1.409312	2.231272	-3.540735
11	6	-1.027268	-1.851501	-0.106959
12	6	-0.043568	2.615414	-3.542531
13	6	-1.936099	1.559852	2.555294
14	6	-1.310215	1.918349	3.71205
15	6	-3.013122	0.166949	0.025078
16	5	-3.205849	-0.794021	-1.409525
17	6	-2.497764	-1.542917	-0.059644
18	1	0.429636	2.945945	-4.461031
19	1	-1.993985	2.31166	-4.451436
20	5	-3.161182	-0.920714	1.373089
21	5	-4.45654	0.208658	0.928479
22	5	-5.661669	-0.716912	0.02765
23	6	-1.307128	1.688809	-1.151214
24	6	0.037704	2.20279	-1.140744
25	6	0.741754	2.317727	0.067343
26	6	-1.27415	1.583831	1.282712
27	6	0.053403	2.309642	3.708939
28	1	1.739746	2.746954	2.496689
29	1	-1.869231	1.91655	4.642205
30	1	0.550837	2.564247	4.638726
31	1	-2.982565	1.313797	2.604475
32	1	-3.05371	1.539643	-2.441741
33	1	1.677809	2.943391	-2.344824
34	6	-1.882446	1.1915	0.054515
35	1	-2.464819	-0.793288	2.303231
36	1	-3.127055	-3.455529	1.364627
37	1	-6.802675	-0.394714	0.060982
38	1	-2.531919	-0.585401	-2.34186
39	1	-5.363459	-1.66275	2.455513

40	1	-5.886344	-3.312602	-0.086396
41	1	-5.442069	-1.440827	-2.484056
42	1	-3.177454	-3.32049	-1.629013
43	1	-4.718439	1.303291	-1.378975
44	1	-4.671671	1.168757	1.579094
45	5	-4.83525	-1.449219	1.415881
46	6	-0.376671	-2.040294	-1.330084
47	6	-0.282611	-2.012902	1.063661
48	6	1.06918	-2.321537	1.013168
49	6	0.971133	-2.360805	-1.380721
50	6	1.726047	-2.49529	-0.209483
51	1	-0.750949	-1.89351	2.031785
52	1	1.619597	-2.412805	1.94372
53	1	-0.924788	-1.954305	-2.259518
54	1	1.437377	-2.524918	-2.345781
55	6	2.167523	2.726146	0.06629
56	6	2.692533	3.986599	0.10188
57	16	3.432488	1.535131	0.016825
58	6	4.120386	4.002291	0.089737
59	1	2.075653	4.877078	0.136307
60	6	4.656057	2.74997	0.044909
61	1	4.71495	4.907451	0.113913
62	1	5.699905	2.468758	0.027329
63	6	3.159544	-2.810067	-0.280161
64	6	4.035694	-2.526269	-1.295128
65	16	3.978017	-3.640642	1.011244
66	6	5.363612	-2.972397	-1.036774
67	1	3.747799	-1.991547	-2.192135
68	6	5.482133	-3.590796	0.172719
69	1	6.192132	-2.832062	-1.720277
70	1	6.365566	-4.024945	0.619606

Table S28. Optimized geometry of **T-T** at the S_1 state calculated at CAM-B3LYP 6-31G+(d,p) level

Center Number	Atomic Number	Coordinates (Angstroms) x	y	z
1	5	4.679767	3.03604	-0.008716
2	5	3.112696	2.992141	0.829004
3	6	2.447854	-1.773537	-2.35829
4	6	-0.156278	-2.707877	-2.447774
5	5	4.557516	1.925518	-1.397224
6	6	0.312431	-2.282276	1.255311
7	6	-0.252938	-2.752609	2.462549
8	5	3.177256	2.921813	-0.952201
9	5	4.469107	0.269496	-0.803499
10	6	1.924034	-2.247703	-3.553968
11	6	0.658842	2.177763	-0.123567
12	6	0.600456	-2.681788	-3.605856
13	6	2.25902	-1.589515	2.533082
14	6	1.684211	-2.070581	3.702475
15	6	3.104183	-0.037407	0.051368
16	5	2.943314	1.148815	-1.268675
17	6	2.124247	2.047482	-0.063675
18	1	0.160525	-2.999197	-4.545112
19	1	2.540302	-2.247346	-4.44633
20	5	2.84943	1.249111	1.262422
21	5	4.401887	0.33848	0.979871
22	5	5.434925	1.464141	0.080547
23	6	1.703825	-1.766701	-1.167304
24	6	0.386153	-2.335249	-1.19674
25	6	-0.35415	-2.496097	0.011004
26	6	1.603904	-1.665512	1.293297
27	6	0.415346	-2.645275	3.669206
28	1	-1.219099	-3.239137	2.43693
29	1	2.232749	-2.000265	4.635439
30	1	-0.042058	-3.025735	4.576003
31	1	3.250798	-1.170163	2.584633
32	1	3.462523	-1.408718	-2.350129
33	1	-1.189155	-3.024853	-2.497966
34	6	2.198869	-1.169501	0.062481
35	1	2.169017	0.985182	2.187747
36	1	2.607133	3.857452	1.462129
37	1	6.615419	1.336166	0.129398
38	1	2.331013	0.812609	-2.217979
39	1	4.928036	2.312252	2.502229

40	1	5.321419	4.035982	-0.024377
41	1	5.109698	2.12213	-2.430425
42	1	2.72261	3.733411	-1.686963
43	1	4.949238	-0.617402	-1.421198
44	1	4.82973	-0.497505	1.698995
45	5	4.452141	2.036134	1.449461
46	6	-0.019498	2.214004	-1.352822
47	6	-0.11082	2.2917	1.044421
48	6	-1.488219	2.424887	0.986779
49	6	-1.395084	2.355316	-1.410526
50	6	-2.163947	2.452493	-0.241051
51	1	0.37545	2.272991	2.01233
52	1	-2.047189	2.491551	1.91475
53	1	0.541427	2.14636	-2.277337
54	1	-1.8795	2.407342	-2.379413
55	6	-1.742632	-2.952651	-0.012436
56	6	-2.270882	-4.106045	-0.544003
57	16	-3.016753	-1.973644	0.679149
58	6	-3.679157	-4.20919	-0.387878
59	1	-1.65729	-4.873516	-1.000361
60	6	-4.216366	-3.125259	0.247188
61	1	-4.265043	-5.052801	-0.731323
62	1	-5.255714	-2.937028	0.4793
63	6	-3.623183	2.57386	-0.317393
64	6	-4.453135	2.186658	-1.339515
65	16	-4.552159	3.276465	0.977676
66	6	-5.828531	2.450187	-1.083812
67	1	-4.095413	1.704817	-2.241233
68	6	-6.033164	3.035318	0.131125
69	1	-6.628339	2.208481	-1.773205
70	1	-6.968241	3.343969	0.577243

Table S29. Calculated electronic transitions for the optimized structure of **H-H** at S_0 state

Excited State	Spin Multiplicity	Energy / eV	Wavelength / nm	*f*	Composition	Coefficient
1	Singlet-A	3.2148	385.67	0.2035		
					HOMO -> LUMO	0.70114
2	Singlet-A	3.8966	318.19	0.0327		
					HOMO-1 -> LUMO	0.56134
					HOMO -> LUMO+2	0.38538
					HOMO -> LUMO+4	-0.11665
3	Singlet-A	4.6432	267.02	0.0192		
					HOMO -> LUMO+1	0.67499
					HOMO -> LUMO+6	0.12934
4	Singlet-A	4.6959	264.03	0.0318		
					HOMO-3 -> LUMO	0.6854
5	Singlet-A	4.8696	254.61	1.3701		
					HOMO-1 -> LUMO	-0.40355
					HOMO -> LUMO+2	0.55555
					HOMO -> LUMO+4	-0.11516

Table S30. Calculated electronic transitions for the optimized structure of **H-H** at S_1 state

Excited State	Spin Multiplicity	Energy / eV	Wavelength / nm	*f*	Composition	Coefficient
1	Singlet-A	2.1172	585.6	0.4296		
					HOMO -> LUMO	0.70197

Table S31. Calculated electronic transitions for the optimized structure of **Br-H** at S_0 state

Excited State	Spin Multiplicity	Energy / eV	Wavelength / nm	*f*	Composition	Coefficient
1	Singlet-A	3.1075	398.98	0.2325		
					HOMO -> LUMO	0.70193
2	Singlet-A	3.828	323.89	0.0373		
					HOMO-3 -> LUMO	0.10871
					HOMO-1 -> LUMO	0.56331
					HOMO -> LUMO+2	0.38356
3	Singlet-A	4.5497	272.51	0.0039		
					HOMO-4 -> LUMO	0.59067
					HOMO-3 -> LUMO	0.35728
4	Singlet-A	4.751	260.96	0.0456		
					HOMO -> LUMO+1	0.66608
					HOMO -> LUMO+6	0.14691
5	Singlet-A	4.8041	258.08	1.2191		
					HOMO-1 -> LUMO	-0.39447
					HOMO -> LUMO+2	0.56098

Table S32. Calculated electronic transitions for the optimized structure of **Br-H** at S_1 state

Excited State	Spin Multiplicity	Energy / eV	Wavelength / nm	*f*	Composition	Coefficient
1	Singlet-A	2.0593	602.06	0.4157		
					HOMO -> LUMO	0.70313

Table S33. Calculated electronic transitions for the optimized structure of **Br-Br** at S_0 state

Excited State	Spin Multiplicity	Energy / eV	Wavelength / nm	*f*	Composition	Coefficient
1	Singlet-A	3.0997	399.99	0.2243		
					HOMO -> LUMO	0.70186
2	Singlet-A	3.8242	324.21	0.0377		
					HOMO-1 -> LUMO	0.57234
					HOMO -> LUMO+2	-0.36206
					HOMO -> LUMO+3	0.15266
3	Singlet-A	4.5404	273.07	0.0039		
					HOMO-3 -> LUMO	0.69056
4	Singlet-A	4.6358	267.45	0.0169		
					HOMO -> LUMO+1	0.68222
					HOMO -> LUMO+6	0.13535
5	Singlet-A	4.7945	258.6	1.2311		
					HOMO-1 -> LUMO	0.39202
					HOMO -> LUMO+2	0.55225
					HOMO -> LUMO+3	-0.14818

Table S34. Calculated electronic transitions for the optimized structure of **Br-Br** at S_1 state

Excited State	Spin Multiplicity	Energy / eV	Wavelength / nm	*f*	Composition	Coefficient
1	Singlet-A	2.0456	606.1	0.409		
					HOMO -> LUMO	0.70301

Table S35. Calculated electronic transitions for the optimized structure of **T-H** at S_0 state

Excited State	Spin Multiplicity	Energy / eV	Wavelength / nm	*f*	Composition	Coefficient
1	Singlet-A	3.1147	398.06	0.2783		
					HOMO -> LUMO	0.70146
2	Singlet-A	3.8256	324.09	0.0473		
					HOMO-2 -> LUMO	0.49567
					HOMO-1 -> LUMO	0.29359
					HOMO -> LUMO+2	0.35799
					HOMO -> LUMO+5	-0.10903
3	Singlet-A	4.2739	290.1	0.0035		
					HOMO-3 -> LUMO	0.16693
					HOMO-2 -> LUMO	-0.26863
					HOMO-1 -> LUMO	0.61001
4	Singlet-A	4.51	274.91	0.0112		
					HOMO-6 -> LUMO	0.35143
					HOMO-5 -> LUMO	-0.13872
					HOMO-3 -> LUMO	0.55857
					HOMO-2 -> LUMO	0.14906
5	Singlet-A	4.6571	266.23	0.018		
					HOMO -> LUMO+1	0.67806
					HOMO -> LUMO+8	-0.12414

Table S36. Calculated electronic transitions for the optimized structure of **T-H** at S_1 state

Excited State	Spin Multiplicity	Energy / eV	Wavelength / nm	*f*	Composition	Coefficient
1	Singlet-A	1.9647	631.05	0.5172		
					HOMO -> LUMO	-0.70223

Table S37. Calculated electronic transitions for the optimized structure of **T-T** at S_0 state

Excited State	Spin Multiplicity	Energy / eV	Wavelength / nm	*f*	Composition	Coefficient
1	Singlet-A	3.1077	398.96	0.2397		
					HOMO -> LUMO	0.70045
2	Singlet-A	3.8271	323.96	0.0451		
					HOMO-4 -> LUMO	-0.10347
					HOMO-3 -> LUMO	0.53328
					HOMO-2 -> LUMO	0.20806
					HOMO -> LUMO+2	-0.34943
3	Singlet-A	4.2637	290.79	0.0003		
					HOMO-3 -> LUMO	-0.2388
					HOMO-2 -> LUMO	0.63968
4	Singlet-A	4.2848	289.36	0.538		
					HOMO-1 -> LUMO	0.46394
					HOMO-1->LUMO+1	0.49907
5	Singlet-A	4.4359	279.5	0.0873		
					HOMO-1 -> LUMO	-0.3606
					HOMO-1->LUMO+1	0.24235
					HOMO -> LUMO+1	0.51817
					HOMO -> LUMO+6	-0.11825

Table S38. Calculated electronic transitions for the optimized structure of **T-T** at S_1 state

Excited State	Spin Multiplicity	Energy / eV	Wavelength / nm	*f*	Composition	Coefficient
1	Singlet-A	1.9498	635.88	0.4324		
					HOMO -> LUMO	0.70063

References

1 H. Naito, K. Nishino, Y. Morisaki, K. Tanaka and Y. Chujo, Highly-efficient solid-state emissions of anthracene–*o*-carborane dyads with various substituents and their thermochromic luminescence properties, *J. Mater. Chem. C*, 2017, **5**, 10047–10054.

2 S. Toyota, D. Mamiya, R. Yoshida, R. Tanaka, T. Iwanaga, A. Orita and J. Otera, Efficient synthesis of 9,10-bis(phenylethynyl)anthracene derivatives by integration of sonogashira coupling and double-elimination reactions, *Synth.*, 2013, **45**, 1060–1068.

3 Z. Tian, X. Yang, B. Liu, D. Zhong, G. Zhou and W. Y. Wong, New heterobimetallic Au(i)-Pt(ii) polyynes achieving a good trade-off between transparency and optical power limiting performance, *J. Mater. Chem. C*, 2018, **6**, 11416–11426.

4 R. S. Kularatne, P. Sista, H. D. Magurudeniya, J. Hao, H. Q. Nguyen, M. C. Biewer and M. C. Stefan, Donor-Acceptor Semiconducting Polymers Based on Pyromellitic Diimide, *J. Polym. Sci., Part A Polym. Chem*, 2015, **53**, 1617–1622.

5 G. M. Sheldrick, SHELXT - Integrated space-group and crystal-structure determination, *Acta Crystallogr. Sect. A Found. Crystallogr.*, 2015, **71**, 3–8.

6 G. M. Sheldrick, Crystal structure refinement with SHELXL, *Acta Crystallogr. Sect. C Struct. Chem.*, 2015, **71**, 3–8.

7 O. V. Dolomanov, L. J. Bourhis, R. J. Gildea, J. A. K. Howard and H. Puschmann, OLEX2: A complete structure solution, refinement and analysis program, *J. Appl. Crystallogr.*, 2009, **42**, 339–341.

8 C. F. Macrae, I. J. Bruno, J. A. Chisholm, P. R. Edgington, P. McCabe, E. Pidcock, L. Rodriguez-Monge, R. Taylor, J. Van De Streek and P. A. Wood, Mercury CSD 2.0 - New features for the visualization and investigation of crystal structures, *J. Appl. Crystallogr.*, 2008, **41**, 466–470.

9 L. J. Farrugia, ORTEP-3 for windows - A version of ORTEP-III with a graphical user interface (GUI), *J. Appl. Crystallogr.*, 1997, **30**, 565.

10 P. R. Spackman, M. J. Turner, J. J. Mckinnon, S. K. Wolff, D. J. Grimwood, D. Jayatilaka and M. A. Spackman, CrystalExplorer: a program for Hirshfeld surface analysis, visualization and quantitative analysis of molecular crystals, *J. Appl. Cryst*, 2021, 54.

11 P. D. Zoon and A. M. Brouwer, A push-pull aromatic chromophore with a touch of merocyanine, *Photochem. Photobiol. Sci.*, 2009, **8**, 345–353.

12 M. J. Frisch, G. W. Trucks, H. B. Schlegel, G. E. Scuseria, M. A. Robb, J. R. Cheeseman, G. Scalmani, V. Barone, G. A. Petersson, H. Nakatsuji, X. Li, M. Caricato, A. V. Marenich, J. Bloino, B. G. Janesko, R. Gomperts, B. Mennucci, H. P. Hratchian, J. V. Ortiz, A. F. Izmaylov, J. L. Sonnenberg, D. Williams-Young, F. Ding, F. Lipparini, F. Egidi, J. Goings, B. Peng, A. Petrone, T. Henderson, D. Ranasinghe, V. G. Zakrzewski, J. Gao, N. Rega, G. Zheng, W. Liang, M. Hada, M. Ehara, K. Toyota, R. Fukuda, J. Hasegawa, M. Ishida, T. Nakajima, Y. Honda, O. Kitao, H. Nakai, T. Vreven, K. Throssell, J. A. Montgomery, Jr., J. E. Peralta, F. Ogliaro, M. J. Bearpark, J. J. Heyd, E. N. Brothers, K. N. Kudin, V. N. Staroverov, T. A. Keith, R. Kobayashi, J. Normand, K. Raghavachari, A. P. Rendell, J. C. Burant, S. S. Iyengar, J. Tomasi, M. Cossi, J. M. Millam, M. Klene, C. Adamo, R. Cammi, J. W. Ochterski, R. L. Martin, K. Morokuma, O. Farkas, J. B. Foresman and D. J. Fox, *Gaussian 16, Rev. C.*

01 Gaussian, Inc. Wallingford CT,.

13 G. Scalmani, M. J. Frisch, B. Mennucci, J. Tomasi, R. Cammi and V. Barone, Geometries and properties of excited states in the gas phase and in solution: Theory and application of a time-dependent density functional theory polarizable continuum model, *J. Chem. Phys.*, 2006, **124**, 094107.

14 R. Improta, V. Barone, G. Scalmani and M. J. Frisch, A state-specific polarizable continuum model time dependent density functional theory method for excited state calculations in solution, *J. Chem. Phys.*, 2006, **125**, 054103.

15 M. Cossi and V. Barone, Time-dependent density functional theory for molecules in liquid solutions, *J. Chem. Phys.*, 2001, **115**, 4708–4717.